Committee III.1: Ultimate Strength

Committee III.1: Ultimate Strength

J. W. Ringsberg[1(✉)], L. Brubak[2], B.-Q. Chen[3], X. Chen[4], M. Chun[5], I. Darie[6], M. I. L. de Souza[7], M. Gaiotti[8], D. Georgiadis[9], M. Kõrgesaar[10], T. Magoga[11], A. M. Mohammad Zubar[12], K. Nahshon[13], T. Okafuji[14], M. Paredes[15], J. Romanoff[16], I. Schipperen[17], Y. Wang[18], A. Zamarin[19], and Z. Zhan[20]

[1] Chalmers University of Technology, Gothenburg, Sweden
jonas.ringsberg@chalmers.se
[2] DNV, Oslo, Norway
[3] Instituto Superior Técnico, Lisbon, Portugal
[4] Technical University of Denmark (DTU), Lyngby, Denmark
[5] KRISO, Daejeon, Republic of Korea
[6] University of Rostock, Rostock, Germany
[7] Rio de Janeiro, Brazil
[8] University of Genoa, Genoa, Italy
[9] Athens, Greece
[10] Tallinn University of Technology, Tallinn, Estonia
[11] Fishermans Bend, Australia
[12] Makassar, Indonesia
[13] Naval Surface Warfare Center, Carderock, USA
[14] Tokyo, Japan
[15] Texas A&M University, College Station, USA
[16] Aalto University, Espoo, Finland
[17] TNO, Delft, The Netherlands
[18] Southampton, UK
[19] University of Rijeka, Rijeka, Croatia
[20] Shanghai, China

Committee Mandate. Concern for the collapse behaviour of ships and offshore structures and their structural components under ultimate conditions. Uncertainties in strength assessment shall be highlighted. Attention shall be given to the influence of load combinations, fabrication-induced imperfections, life-cycle effects, damage, and user approach. Consideration shall be given to the practical application of methods.

Keywords: Buckling · Collapse · Corrosion · Fabrication-induced imperfections · In-service damage and degradation · Load-carrying capacity · Offshore structures · Rules and standards · Ships · Ship structures · Ultimate limit states · Ultimate strength · Uncertainty

W. Wu and J. Ding (Eds.): ISSC 2025, LNME, pp. 452–577, 2026.
https://doi.org/10.1007/978-981-95-2668-0_5

1 Introduction

Ultimate strength analysis is one of the most fundamental and critical assessments performed for ships or offshore structures and is required to ensure safe and reliable marine structures. This analysis is initially performed in the design phase to ensure that expected load conditions do not exceed the maximum load-bearing capacity of a structure. This assessment may also be revisited post-design if structural capacity diminishes due to damage from accidents, for example, collisions or groundings, or in-service degradation, including corrosion and fatigue. There is growing interest in predicting diminished load-carrying capacity during normal to extreme operating conditions and understanding its impact on global load-bearing capacity.

This report presents a summary and discussion of an extensive literature review of work published primarily from 2021 to 2024 that was performed by members of ISSC Committee III.1. The committee's mandate, which was unchanged from that of ISSC 2022 (ISSC, 2022a), guided this work. The effort began with a careful review of the three most recent committee reports from 2015, 2018, and 2022 to identify subjects that had been unaddressed or minimally discussed and to review the former committees' recommendations for future work, as well as discussions and questions raised during ISSC 2022 congress sessions. Subject areas covered extensively in the past reports have deliberately received less attention in this report. Subjects with low or moderate levels of progress during the committee's mandate period are specifically highlighted.

The report is organized into seven sections. Section 2 presents updates to fundamental topics related to ultimate strength analysis, including recent developments in computational tools and examples of experimental procedures and investigations. Uncertainties related to material and fabrication and how they affect the ultimate strength are presented in Section 3, including in-service degradation effects, such as corrosion and mechanical damage, and life-cycle management analysis. Sections 4 and 5 focus on the ultimate strength aspects particular to ships and offshore structures, respectively. They describe relevant load cases, structural elements, structural systems, and associated rules and regulations. Section 6 presents the report from a benchmark study in which the committee and additional invited participants simulated, analysed, and predicted in "blind" the failure progression of a transversely stiffened thin-plated structure. As in the benchmark study presented in the 2022 committee report (ISSC, 2022a), the current benchmark was also divided into three phases. Finally, in Section 7, the major conclusions, trends, and recommendations of the committee are presented.

2 Fundamentals

This section collates the main definitions and assumptions, first principles and theories, and methods, tools, and approaches for the assessment of ultimate strength for both ships and offshore structures. Ultimate strength is defined as the maximum resistance that a material, structural element, or larger structure can carry when exposed to external loading with a certain loading pattern. Ultimate strength is commonly defined as an ultimate stress, ultimate force, or ultimate moment. Examples include the maximum moment a hull girder can experience, the maximum axial load of a monopile, and the maximum

pressure a subsea structure can endure before hydrostatic collapse. An excellent review of this definition for the static and dynamic situations in a maritime context is provided in a recent article by Jagite et al. (2022) who discuss the roles of the inertia and strain rate as dynamic effects that differentiate the two situations. The inertia rate primarily affects the structural response, i.e., the amplitude of the internal load, which can differ from the applied external loading, unlike in the static case. In contrast, the strain rate affects the material level responses through changes in yield strength. Nevertheless, most current analyses are conducted statically, neglecting dynamic effects (inertia, damping, and strain rate).

2.1 Definitions, Assumptions, and Uncertainties

It is often desirable for the structural analyst to not only know the ultimate strength but also the shape of the deformation-loading curve, where deformation is quantified as either strain, displacement, or curvature. This provides insight into the stiffness characteristics of the structure as well as the energy absorbed in both elastic and inelastic deformation. In most cases, monotonic loading is considered. However, in other cases, loading path dependency may be important. This issue was also highlighted by the Official Discusser of the previous committee (ISSC, 2022b) and is accounted for in this report.

Loading on ships and offshore structural systems consists of environmental loads during normal operations, such as waves, currents, wind, and ice, as well as damage events such as collisions and groundings, dropped objects, fires, and explosions. Structural systems and sub-systems experience load effects at different times and in different ways. Quite often, this modelling is simplified from dynamic to static, in which case these phase differences of load actions are lost, along with those of inertia and strain rate effects. For example, global wave-induced hull-girder bending moments typically manifest as tensile and compressive loads at the panel level, and augmented local hydrostatic and dynamic pressures. Other loads are highly localised, such as ice impact. Wave-induced loads tend to transfer to maximum tensile and compressive stresses at the extreme "fibres" of thin-walled structures, away from the neutral axis, and their application is often based on deformation (curvature) for which the internal reactions in terms of stresses are integrated to the section moments acting on the hull girder. Wave-induced loads tend to transfer to maximum tensile and compressive stresses at the extreme "fibres" of thin-walled structures, away from the neutral axis. In comparison, ice loads tend to cause the greatest load effects close to the neutral axis of the ship hull girder, generating stronger interactions with the hull girder shear loads. In contrast, offshore applications, such as windmills, may experience interactions between local ice-induced loads and the maximum tensile and compressive loads caused by primary responses of the entire structural system. These fundamentally different load-carrying mechanisms require careful consideration in ultimate strength assessments. In addition, Fig. 1 presents the ultimate strength paths of the (a) material, (b) the sub-structure (e.g., stiffened panel), and (c) the structural system (e.g., the hull girder); and in the case of ships and offshore structures these three different length scales are coupled. Moving upwards across these scales, the effects at lower scales are "smeared" (or *averaged*) over the volume of the structure. Conversely, moving downwards in the length scales concentrates or *localises* the damage.

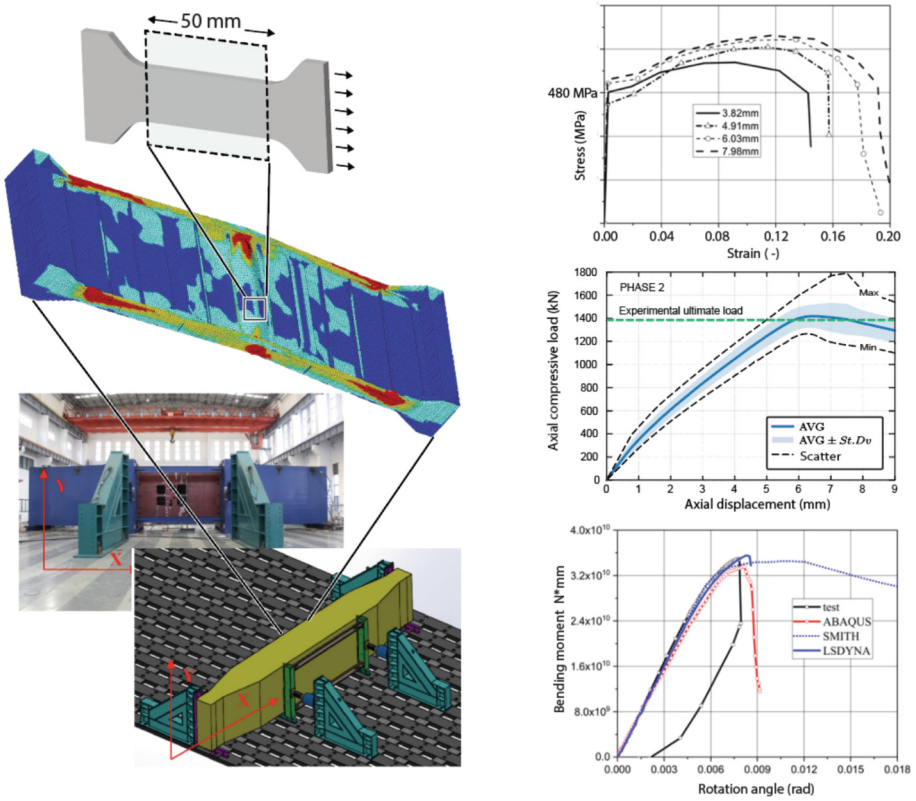

Fig. 1. Illustration of the ultimate strength progression across three hierarchical levels: (a) the material level, (b) the sub-structure level (e.g., a stiffened panel), and (c) the structural system level (e.g., the hull girder). In ships and offshore structures, these length scales are interconnected. Adopted from Ringsberg et al. (2021) and Zhao et al. (2022).

Structural elements or sub-structures are characterised by load-shortening, pressure-displacement, or other similar relationships that are analogous to the stress-strain curve at the material level. The shape and characteristics of these curves are affected by the confluence of material behaviour, structural geometry, initial imperfections, residual stresses, and flaws, such as cracks induced by manufacturing or corrosion induced by the maritime environment, and operating conditions. In the analysis, the question is whether the ultimate strength should be determined either using (a) nominal, (b) actual (which also includes life-cycle effects such as dents) or (c) anticipated values of parameters to determine the future ultimate strength or the residual strength, for example, after an accident. The use of ductile materials does not preclude quasi-brittle failure where structures fail under relatively low tensile loads. This occurs in cases of high levels of local corrosion/degradation as well as highly undermatched weld joints that appear in extruded aluminium structures. An additional feature at this level is the notable observable differences in structural behaviour when the direction of loading is changed.

Under tension, straightening leads to fracture, whereas under compression, it results in progressive buckling failure.

Larger structural systems consist of a series of interconnected structural elements. In the case of the hull girder of a ship, ultimate strength is described by the moment-curvature relationship of a cross-section. This is affected by the resistance of the structural system components, redundancy of the load-carrying mechanism, and interaction with environments, such as waves and ice, seafloor in groundings, and other structures in collisions. Therefore, in this report, attention is given to the influence of load combinations, fabrication-induced imperfections, life-cycle effects, damage from accidents, and operational practice on the estimation of resistance and ultimate strength.

The most important mathematical parameters that influence the shape of these load-deformation relationships are the initial and tangent stiffnesses of the curves (these must equate initially; for example Young's modulus in materials, and bending stiffness in beams), as well as the area below the curve, which is generally related to the energy or energy per volume of the material or structural system when loaded statically. The design point is typically much lower than the ultimate strength, and safety factors are used to create a buffer between the design values and the ultimate strength. These safety factors are usually set based on consideration of the behaviour of the material or structure beyond the ultimate strength. Due to variations in plastic behaviour, safety factors can substantially differ in ductile and brittle materials. Defining the ultimate strength of a complete structure through full-scale experimentation over its lifetime is practically infeasible; therefore, computational methods and various levels of simplification are necessary, which influence the failure sequence from the material level to the hull girder level. This issue is discussed further in Sect. 3.

2.1.1 Assumptions

All structures are fabricated based on a design that specifies materials, fabrication processes, thicknesses, dimensions, and geometrical locations for all structural elements. In the design phase, ultimate strength assessment must utilise either assumed nominal characteristics or historical ranges for deviations from nominal values, such as actual versus nominal material properties, and nominal dimensions versus dimensional tolerances. At present, the in-service condition of ships and offshore structures is minimally tracked throughout the lifecycle from the time of manufacturing to the end-of-life. There are currently efforts to accomplish this via the use of digital twins in which an analysable digital version of a structure in its existing condition is maintained allowing designers, shipbuilders, operators, and authorities to continuously monitor the real-time condition of the structural system until dismantling. However, in practice, this is a very difficult and expensive endeavour for most ships and offshore structures, as the collection and maintenance of required actual data are cumbersome within complex structural systems. Due to this, estimates are often exploited.

As a result, ultimate strength analysis of in-service structures requires assumptions about the current state of a structure, which creates uncertainties in ultimate strength predictions; these are reviewed in detail in Sect. 3. Even in instances where the current condition is described, such as the amount of wastage due to corrosion, it is rarely in the form of full-field measurements. Therefore, assumptions must be made regarding

conditions in unmeasured locations. The load history of the structure may also involve numerous assumptions. Although the instantaneous load from cargo can generally be determined with high accuracy, several assumptions are required to estimate environmental loads, such as those from waves, wind, and ice, during ultimate strength simulations. These will manifest in the ship dynamics and load distribution as local hydrodynamic pressures and hull girder loads and their phase differences; see the following sections and other committee works on direct methods for loads. If the load history has created significant fatigue damage or accumulation of plastic damage in the structure, the ultimate strength will be affected, and the way plastic damage accumulates at the material level has a substantial influence on the ultimate strength of the panel (Cui and Ding, 2022). Accidents, such as collisions, groundings and explosions, lead to sudden reduction of the capacity of the structural system. Several investigations have also focused on the dynamics of ultimate strength, i.e., where the load is not introduced quasi-statically as has been done traditionally. Load and strength may also interact dynamically.

Ultimate strength simulations require assumptions within the computational models at the material, sub-structural and structural system levels. In the context of finite element (FE) analysis, solid elements produce the most accurate mathematical descriptions of material behaviour. However, shell and beam elements are most commonly used due to the impracticality of modelling a ship or offshore structure with solid elements as a result of the number of required elements, small timesteps, and resulting computational complexity. Recent research efforts have focused on bridging beam and shell structural elements with solid elements that can capture realistic material behaviour, including multi-scale and multi-physics analyses in which the material microstructure and mechanisms are modelled and simulated explicitly and not solely from material tests. The aerospace industry has developed the NASMAT platform (Arnold et al., 2023), which aims to create an integrated framework for multi-scale and multi-physics materials and structural analyses within a seamless modelling package. This platform builds on advances in the modelling of multi-scale structures, allowing two-way coupling between material properties and structural behaviour, thereby enabling updates to material properties based on load actions at the structural level. Similar modelling approaches have been explored in maritime applications, such as multi-scale and multi-physics modelling to determine the effects of corrosion damage on ultimate strength damage (Ilman et al., 2021) by directly accounting for the interaction between corrosion and mechanical stresses. Additionally, research by Peng et al. (2022) demonstrated how the combined effects of periodic tidal movement and the harsh environment created by the tide, seawater, air temperature, and sea temperature can be incorporated into models that can analyse the degradation of marine reinforced concrete in cold regions resulting in significant stiffness reduction after only tens of load cycles. Structural elements in these models are represented by shell, plate, and beam formulations, with decreasing mathematical complexity moving from the shell towards the beams. Materials are typically considered anisotropic allowing the use of the same elements to model both composites and metals. The Carrera unified formulation (CUF) allows systematic selection of the shell, plate, and beam kinematics as a function of the thickness coordinate of the structural element, and "Best Theory Diagrams" (see Fig. 2) are used to identify the optimal kinematic assumptions for specific structural problems, such as boundary and loading conditions

or material distribution throughout the thickness (Petrolo and Carrera, 2019; Petrolo and Iannotti, 2023). Recent advancements in CUF also extend to non-classical continuum mechanics, allowing material points to possess finite sizes with defined microstructures (Carrera and Zozulya, 2020). These are important in modelling the strain fields, which may differ from those generally adopted (e.g., linear); the issue is especially important in composite structures and near the free edges. In hull girder modelling, FE models are widely used due to their flexibility and accuracy. However, due to computational costs, the application of model reduction techniques, such as the Smith method, to beam models is often preferred in practical design work, e.g., the Common Structural Rules (CSR).

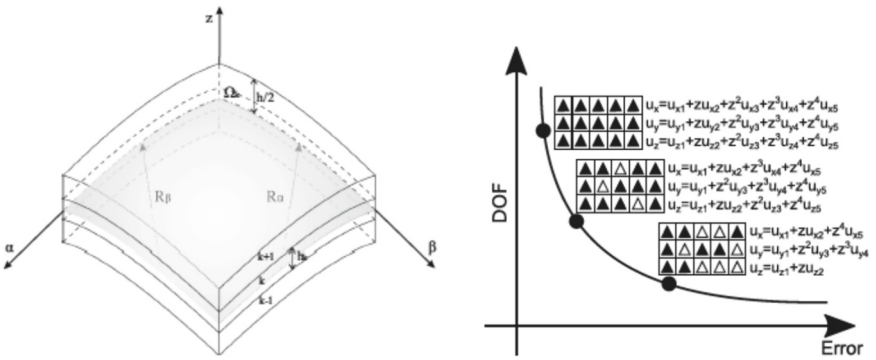

Fig. 2. Derivation of the Best Theory Diagram of a shell element based on the 4th order polynomial expansion of the in-plane displacement field throughout the thickness coordinate (Petrolo and Carrera, 2019).

2.1.2 Uncertainties

In this report, the classical definitions of uncertainty are used (epistemic and aleatoric), both individually and in combination. Section 2, which addresses the fundamentals, focuses primarily on epistemic uncertainty, while Sect. 3 considers aleatoric uncertainty. The choice is made this way as the fundamentals section focuses on the modelling aspects, while Sect. 3 on life-cycle aspects. The effects of uncertainty on hull girder and offshore structural strength are of particular interest, as demonstrated by a study on the impact of uncertainty on load-shortening curves of a panel as part of the ISSC 2022 Ultimate Strength committee's benchmark study (ISSC, 2022a). Input data accuracy, particularly in the design phase, significantly affects results, with uncertainties arising from geometry, material properties, load data, and modelling strategies. Woloszyk *et al.* (2021a) investigated the use of photogrammetry to generate meshable geometry for conducting ultimate strength calculations using the true shape of a stiffened plate of three different thicknesses. Comparisons with Smith's (1977) closed-form formulae showed similar ultimate strength values for both approaches, although the use of the measured shape moderately influenced pre- and post-ultimate load-displacement behaviour, with this effect increasing for thinner sections, as shown in Fig. 3.

In their work, Georgiadis and Samuelides (2021a) applied random field theory to describe stochastic geometric imperfections on plates and their effects on hull girder strength, modelling initial imperfections using mean values and variances, and using artificial neural networks (ANNs) to reduce the number of non-linear FE analyses. While an ANN is trained on a dataset to provide results for arbitrary input, applying Bayesian statistical interference provides an update of parameters of the probability density functions based on a number of observations. In contrast, Chen et al. (2023) showed that treating initial imperfections solely as sinusoidal distortions was insufficient, and longitudinal stiffener misalignment (LSM) due to welding must also be considered. Their work highlighted the importance of symmetric and antisymmetric modes and emphasised that LSM accelerates the reduction of load-carrying capacity.

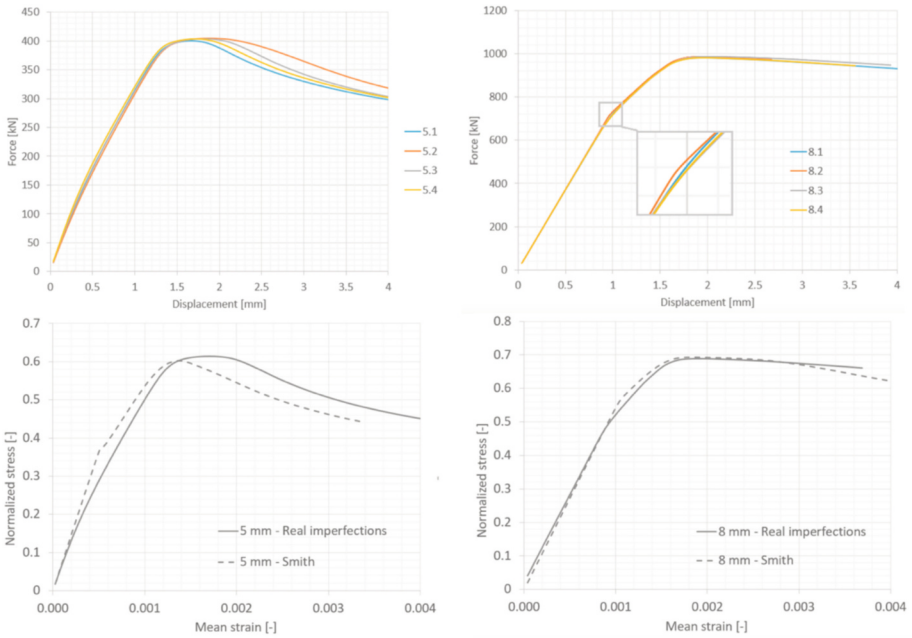

Fig. 3. Comparison of the load-displacement (upper figures), and the normalized stress average strain (lower figures) of 5 mm and 8 mm thick panels with flat bar stiffeners as predicted using the true geometry and the imperfection equations by Smith (Woloszyk *et al.*, 2021a).

The quantification of model uncertainty for hull girder ultimate strength prediction is another important aspect that has been raised in previous ISSC reports (see, e.g., ISSC, 2018a, 2022a). As prescribed by the CSR, the primary methods for assessing hull collapse are the Smith method and FE analysis. Li et al. (2021b) proposed a probabilistic approach to evaluate the uncertainty in estimates of hull girder ultimate strength resulting from variations in the load-end shortening curves (LSCs) by modelling the critical characteristics of the LSCs in probabilistic terms. The probability distributions of the critical LSCs characteristics of the stiffened panels were developed based on a dataset

generated using empirical formulae and FE analysis results. The impact on the variability of the ultimate strength of the hull girder was assessed for four merchant ships and four naval vessels. A key finding from this study was that the mean ultimate strength predicted for all case study ships in hogging closely matched the CSR baseline, whereas for sagging the mean was approximately 95–97% of the CSR baseline. Georgiadis *et al.* (2023b) applied Bayesian statistical inference to estimate the uncertainty when using the Smith method. Engineering judgment and FE analysis data were formally combined through Bayesian analysis, while the uncertainty in the FE analysis results was explicitly accounted for through the likelihood formulation. Their work produced new probabilistic models for container ships to estimate uncertainty when using the Smith method. The authors applied the same approach in their study of double-hull oil tankers (Georgiadis and Samuelides, 2023a).

While design calculations must use specified minimum material values, analyses seeking to capture true ultimate strength behaviour require a decision regarding the choice of material properties. The choice between using the design or actual values is a key consideration. The actual properties of normal-strength steel typically exceed those provided by material manufacturers, implying that the ultimate strength of the actual structure could be higher than calculated. However, this safety margin tends to decrease for higher-strength steels. The same consideration applies to the assumed state of the structure, such as whether it is considered damaged or undamaged. Do et al. (2021) investigated the effects of local damage in stiffened cylinders after impact loads. In their simulations, the impact analysis defined geometric changes due to impact, including contact and strain rate effects. The resulting new nodal positions were mapped onto the structure for buckling analysis, thereby accounting for the effects of residual stresses. At this stage, the material was adjusted to elastic-perfectly plastic, neglecting material memory effects. This type of numerical analysis showed a reasonably good correlation with the experimental results, although some differences were observed in the pre- and post-ultimate strength behaviour between load (pressure) and the axial shortening (see Fig. 4).

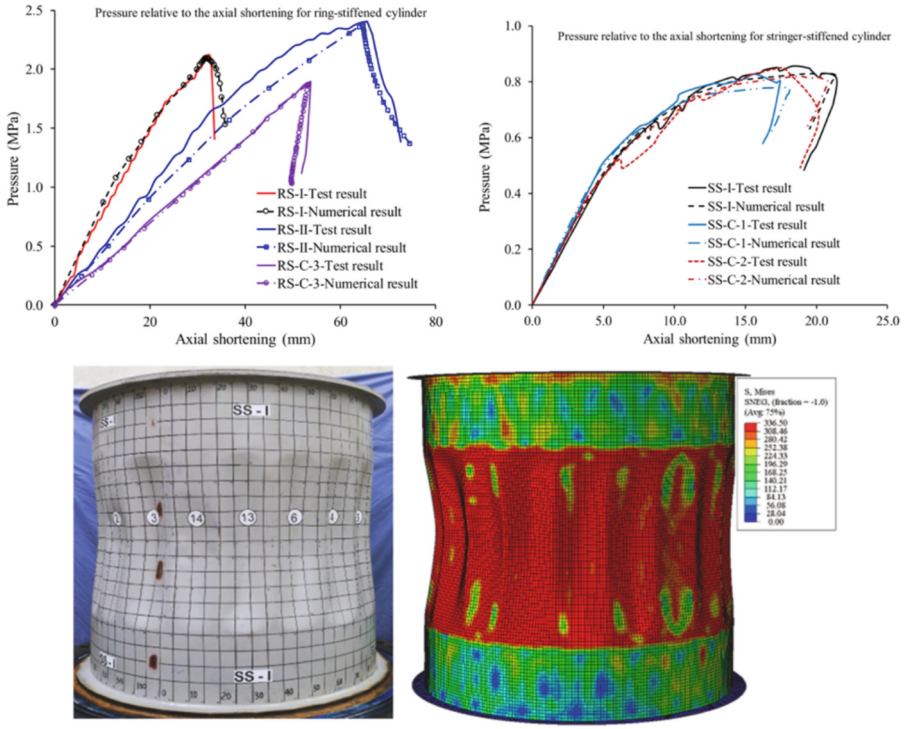

Fig. 4. Comparison of simulations and experiments on pre-damaged cylindrical shells (Do et al., 2021).

Kuznecovs et al. (2021) used FE analyses to investigate the effect of ship collisions on ultimate strength, predicting residual strength using the Smith method for tankers, with and without corrosion degradation (both general and pitting corrosion) included. They demonstrated the effects of collision damages along the hull girder length by utilising 3D demand-capacity plots to describe the relationship between horizontal and vertical bending moments at different sections along the prismatic body of the ship.

Li *et al.* (2021a) used a shell-element-based FE analysis to study the individual, combined, and superimposed effects of pitting corrosion and cracks in various orientations on the ultimate strength of box girders. Their findings confirmed the expected reduction in ultimate moment due to both types of damage but also highlighted the important role of structural integrity in ensuring that the connections of stiffeners and plating were appropriate for carrying loads and supporting the plate against buckling. Investigations by Piscopo and Scamardella (2023) utilised Monte Carlo simulations to estimate the statistical properties of plate ultimate strength of pitted simply supported plates. Similarly, the importance of stiffener integrity was demonstrated by Li *et al.* (2021c) who investigated the influence of residual stresses on the ultimate strength of ship panels under compression and noted that the residual stresses in the stiffeners may lead to beam-column type failure and thus a significant reduction in ultimate strength due to loss of support for the plate. Zhong and Wang (2021a) investigated the ultimate strength

of laser-welded web-core sandwich plates, demonstrating the combined effects of geometrical and material non-linearities on the resulting load-end-shortening path when compared to models solely considering geometrical non-linearity. Their results indicate that highly localized plasticity affects the onset of local buckling, which subsequently leads to overall buckling of the panel.

A quasi-static approach is typically assumed to be appropriate for loading; for instance, experiments and simulations are conducted such that strain rate and kinetic energy effects are negligible. Kong et al. (2021) investigated the dynamic buckling of a deck grillage with an opening subjected to in-plane loads, using both experimental and numerical methods. Their findings indicated that the dynamic buckling mode differed significantly from the failure mode of the structure subjected to quasi-static in-plane compressive load. Specifically, they observed that vertical displacements at the deck edge and axial displacements increased as impact frequency decreased. Their study also demonstrated the effects of dynamic buckling on hull girder failure. In their study, Jagite and Bigot (2023) further explored the evaluation of the ultimate strength of a hull girder when loaded dynamically by wave loads.

When choosing between solid, shell, plate, and beam structural models, as well as between analytical and numerical solutions, the accuracy of the stress field versus computational cost is one of the primary considerations in ultimate strength analyses. It is widely known that material failure is dependent on stress triaxiality, and single-layer shell and line-type beam elements cannot model stresses in all three directions directly. Approaches exist to approximate these omitted stresses in post-processing with certain assumptions. However, uncertainties may be introduced particularly in problems where damage localizes quickly, affecting the load-carrying mechanism of the structural system due to interdependent length scales. Another significant source of uncertainty lies in the level of idealization of the loads and boundary conditions used in simulations and their practical realism. When verifying and validating models, uncertainties can arise from the reproducibility of results under seemingly similar conditions, as well as from systematic and random errors in experimental data. This aspect is discussed in detail in the benchmark study presented in Sect. 6.

Wang *et al.* (2022b) investigated the buckling of aluminium extruded panels using FE analysis with both static and dynamic solvers. They discovered that the static solver, which is commonly used in buckling simulations, may not accurately model the experimentally observed bucking and post-buckling behaviour, as it neglects inertia forces. These forces were found to be crucial in driving the buckling process forward, especially when the stiffener-tripping mode occurred. Therefore, they recommended using the dynamic solver, as the inclusion of inertia effects improves numerical stability over time steps, thus avoiding severe overprediction of the ultimate load. Additionally, they noted that the residual stress model should be carefully selected since including the residual stress may strengthen the panels, resulting in an overestimation of the ultimate load. Consequently, they advised against using excessive residual stress levels. As noted by the ISSC 2022 Ultimate Strength committee (ISSC, 2022a), the focus of the post-processing of theoretically or experimentally obtained data is often the actual ultimate strength rather than residual capacity, resulting in an emphasis on the energy of the structural system beyond the ultimate strength. Therefore, in many comparative studies,

the focus is not on the tail parts of the load-end-shortening or moment-curvature curves, and thus the uncertainties are fundamentally related to the fact that these parts of the curves are overlooked or the communication in scientific papers is not highlighting this region carefully enough. This concern will be further examined in the benchmark study in Sect. 6. Advances in technology, such as digital image correlation (DIC), provide a valuable opportunity to address these gaps. With access to large datasets from both numerical and experimental sources, techniques such as DIC, which enables precise strain field measurements on actual structures, can be powerful. These approaches may enhance our understanding of uncertainties not only in the context of ultimate strength but also in the case of residual capacity following ultimate load. Such approaches could also be expected to enable a better explanation of variability across repeated experiments.

2.2 Computational Tools

2.2.1 Numerical Methods

Material modelling serves as input for all FE simulations, regardless of the selected element type. The manner in which load effects are incorporated into plasticity models influences the computational prediction of ultimate strength. The stress-strain curve consists of several regions: the linear-elastic region, the yielding plateau, the strain-hardening region modelling (which models plasticity), and the softening region (which models the reduction of material resistance to zero as strain increases). This monotonic representation of material stress-strain behaviour is a simplification that neglects the accumulation of damage due to cyclic loading, such as high- and low-cycle fatigue. These effects are always present in ships and offshore structures, but their effects over the life cycle of the modelled structure are difficult to reliably assess in practice. How these aspects are modelled will influence the failure behaviour of the material, influencing the structural response at larger scales. It is recognised that strain rate and temperature affect material properties and ultimately the capacity of the structural system. As noted, multi-scale and multi-physics approaches to materials and structural modelling (e.g., with computational tools like NASMAT) enable these complex simulations. Structures composed of different materials have unique characteristics that must be considered in numerical assessments of ultimate strength.

Cui and Ding (2022) used FE analysis to study the effect of various material models on the ultimate strength and fracture failure of hull-stiffened panels made from *steel* under cyclic loads. They varied the material modelling strategy among elastic-perfectly plastic, isotropic hardening, and Chaboche models (i.e., combined isotropic and kinematic hardening accounting for both monotonic and cyclic effects) to examine plastic accumulation during cyclic loading and its impact on ultimate strength under compression at the structural level and combined compression-tension at the material level. Plastic accumulation was highest in the initial cycles and decreased rapidly with constant amplitude loading in subsequent cycles, particularly in the weakest region of the structure where fracture typically occurs, and at higher load levels. Both stiffness and ultimate strength were reduced after unloading. The choice of hardening model significantly influenced results, with the Chaboche model providing the most stable accumulation of plastic strain. When plastic strain accumulation reached a specific threshold, it did not increase

further, and the point of final failure was governed by low-cycle fatigue. One key aspect in this type of plasticity modelling is the determination of material parameters experimentally, see for example Shi et al. (2013) and Ma et al. (2018), and the effects of the material model on the hull-girder ultimate strength under several load cycles, see for example, Preventas et al. (2021). In a series of studies, Barsotti and Gaiotti (2022; 2023a,b) analysed the cumulative process of buckling deformation on a stiffened panel subjected to uniaxial cyclic loading. They demonstrated that pure plane stress modelling with shell elements is insufficient to accurately capture the accumulation of plastic strain. Instead, solid elements were required in areas with regions of high plastic strain, such as stiffener intersections, where constraint effects resulted in a triaxial stress state. Kinematic compatibility between shell and solid elements was modelled with rigid links, and they applied a plastic bilinear model that was in accordance with the isotropic hardening law. Over one thousand load cycles with 90% of the structure's ultimate monotonic load, deformation accumulation rates were observed to increase with the number of load cycles.

Heat-affected zones (HAZ) significantly influence the welding connections of structures made from aluminium and high-strength steels; thus, their modelling should not be neglected when ultimate strength is to be assessed, even when it typically complicates the numerical modelling substantially. Wang *et al.* (2022b; 2024) investigated the effects of the HAZ, residual stresses, and initial imperfections on the numerical modelling of welded aluminium panels and considered inertia effects and compared the results from static and dynamic solvers. They concluded that inertia effects are important as they stabilise the numerical solution, particularly in the case of the rapid collapse of stiffeners. After comparing their results with those obtained through approaches guided by IACS and the computational tool developed by DNV (the panel ultimate limit state, PULS), they concluded that these methods yielded satisfactory results in cases where welding effects can be neglected. In *reinforced concrete structures*, durability degradation modelling is essential due to corrosive ion penetration and freeze-thaw cycles (FTCs), as reported by Peng et al. (2022). Modelling damage in concrete requires accounting for temperature distribution, pore water crystallization laws, and critical saturation under seawater FTCs to predict durability degradation accurately.

In *composite* materials and structures, material performance is strongly correlated with the structural model (beams, plates, or shells). Peeters et al. (2022) demonstrated the impact of high-fidelity kinematics on predictions of the buckling strength of composite aeronautical stiffened panels, where the composite layup was designed to trigger multiple buckling and failure modes within 10% of the lowest buckling mode. The Carrera unified formulation (CUF) was used, enabling natural activation of the relevant high-order kinematic terms without significantly increasing computational load. The model was validated through repeated experiments, and experimental and modelled results showed excellent agreement. Augello et al. (2022) expanded on this work, applying a refined equivalent single-layer model in which the critical point of buckling and post-buckling behaviour was modelled with excellent accuracy by using fewer degrees of freedom (DOFs). CUF enabled the development of equivalent 1D models, incorporating complicated stacking sequences through refined expansion functions (Lagrange polynomials). In cases where the shear transfer between material layers is incomplete or layers are

allowed to deflect differently to different extents, these kinematical changes become very important when assessing deformations, strains, and stresses. Insulated Glass Units (IGU) represent an extreme case in this respect. Heiskari et al. (2022; 2023) conducted numerical investigations on insulated *glass* units used on passenger ships; these units consist of a hermetically sealed void between two glass panes and their study focused on the impact load-sharing due to the void and the influence of von Karman strains on glass pane thickness. They assumed no influence of structural strength on glass strength and linear-elastic material behaviour. Results indicated a significant increase in predicted ultimate strength. These theoretical findings are currently being further explored in an experimental study, the results of which are expected to be published soon. The main idea is to learn about shear transfer, load-sharing effects, and geometrical non-linearities, and how these interact when glass structures are loaded to their ultimate limit.

2.2.2 Reduced-Order and Analytical Models

Dimension reduction is often necessary in engineering to reduce the computational effort required for assessments of ultimate limit state. In the ISSC 2022 Ultimate Strength committee report (ISSC, 2022a), dimension reduction strategies were characterised as presented in Fig. 5. At the highest level, reduction involves simplifying the physical problem size, for example, by isolating a panel from a larger structural assembly (such as a hull girder) and limiting the analysis to that panel. The second level of reduction involves reducing the degrees of freedom, often achieved by applying kinematic assumptions inherent in beam, plate, and shell theories. In the third level, problem size may be reduced through closed-form solutions by using semi-analytical, multi-scale numerical methods, or advanced structure-specific methods, such as the Smith method, which uses numerical methods with reduced degrees of freedom. Machine learning (ML) methods are emerging as a fourth model reduction method that can be used to explore the design space effectively without requiring exhaustive simulations or experiments, enabling faster predictions of structural behaviour. In the future, when computational resources increase, it is worth considering whether these computationally cheaper models with substantial idealisations and simplifications are used over more exact models with fewer simplifications, but higher computational costs. Such choices require substantial theoretical knowledge, practical experience, and skills from the analyst in balancing between accuracy and speed.

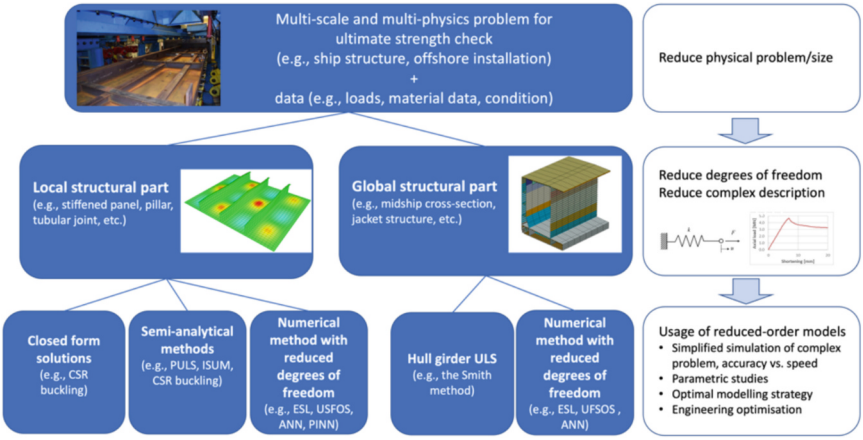

Fig. 5. Dimension reduction in ultimate strength assessment (updated from ISSC, 2022a).

Ma et al. (2022) extended the idealised structural unit method (ISUM) to the analysis of the dynamics of the ultimate strength of stiffened plates. In their approach, the Newmark method to solve the equations of motion, and the ISUM model comprised an ISUM plate and ISUM beam-column elements. The static solution was expanded to include mass and damping matrices (Rayleigh damping). They concluded that the effects of the strain rate and inertia of the structure increased ultimate strength. The computational tool for panel ultimate limit state developed by DNV (PULS, see Byklum and Amdahl, 2002), which is based on analytical, formulations, has been used as the basis for recent research seeking to incorporate the FE method. Assuming first-order shear deformation theory (FSDT) for plates, Putranto and Kõrgesaar (2021) and Putranto et al. (2021; 2022a,2022b) employed parametric FE analysis to derive non-linear stiffness models for unit cells in ABAQUS, which serve as input for non-linear FSDT plates with orthotropic material definitions. This approach, which accounts for both geometric and material non-linearities, demonstrated good agreement with high-fidelity 3D FE models of the actual geometry, both at the sub-structural level (e.g., stiffened panels) and at the structural system level (e.g., ships). However, recent investigations have highlighted challenges in addressing loads in the weaker direction, i.e., the direction normal to the stiffeners (Kõrgesaar et al., 2023). The prevailing differential equations are the root cause since they cannot distinguish between antisymmetric and symmetric out-of-plane shear strains, which negatively affect buckling strength (Romanoff et al., 2020). In FE analyses, this limitation can lead to mesh size-dependent problems in defining the bifurcation buckling load, which serves as input for the non-linear solution phase. The benchmark study presented in Sect. 6 will address this topic in further detail.

Ishibashi et al. (2024) developed a simplified method grounded in elastic large deflection plate theory to estimate the ultimate strength of simply supported rectangular plates under combined biaxial and shear loads, without requiring numerical iterations. Yielding was verified analytically in pre-defined locations identified through extensive non-linear FE analyses of steel plates representative of typical ship structure designs. While generally accurate, the method tended to overestimate the ultimate strength in thinner

plates subjected to certain tension/compression loading scenarios. Similarly, Li and Chen (2023a) developed explicit empirical formulae to estimate longitudinal and transverse ultimate strengths, based on non-linear FE analyses. These formulae share a common general format, providing practical tools for structural assessment.

Li *et al.* (2022a) estimated the ultimate strength of cracked plates using finite element analysis and ANNs. Their work focused on parametrising the problem through the load-end-shortening curve and key input parameters, such as plate slenderness, crack orientation, length and number of cracks. The results indicated that the ultimate strength, expressed as the peak stress of the plated element, can be predicted with relatively high accuracy ($\pm 5\%$ for 87% of the cases) for designs outside of the training dataset. However, the output data did not include details about the tangent modulus or energy absorption of the plated element. Although this was not discussed in this study, in principle if the ANN is trained to account for these factors, its predictive capabilities could be improved, allowing it to capture additional features related to load-end-shortening. Park and Kim (2022) investigated the sloshing-induced buckling failure of LNG cargo containment systems to investigate the efficacy of an ANN-based approach for multi-material systems under complex loading. Given the complexity of the problem, their ANN model utilised two hidden layers, with layer sizes optimised through trial and error to balance between under- and over-fitting. Both numerical and categorical variables were used to improve regression results; 85% of the total data was used for the development of the model and 15% for testing.

Ishibashi et al. (2024) investigated the ultimate strength of rectangular plates in the longitudinal and transverse directions through statistical modelling of the initial imperfections of 120 measurements of bulk carrier and pure car carrier deck and bottom plates. They assumed a double trigonometric shape model and estimated the component wave amplitudes through Bayesian linear regression. They concluded that the correlations between trigonometric component waves should be considered when deriving shapes for strength analyses. The true ultimate strength was estimated through non-linear FE analysis, linear-elastic perfectly plastic material models, and by estimating the ultimate strength numerically without accounting for residual stress effects. They concluded that (particularly in the case of thin plates) bimodal strength probability distributions can occur below the yield point due to mode shifts in plate shape from the initial imperfection to ultimate strength failure. In thicker plates, the shape remains unchanged, and the strength approaches that of the yield point. Lima et al. (2023) proposed a bi-fidelity Kriging model for reliability analysis of the ultimate strength of stiffened panels that leverages the accuracy of high-fidelity (HF) simulations and the coverage and efficiency of low-fidelity (LF) simulations by utilising distance correlations between the two sets of results. This multi-fidelity framework provided similar accuracy to computationally intensive HF modelling but with considerable computational time savings. Coraddu et al. (2023) developed a surrogate model approach based on non-linear FE analysis that enables the determination of the optimal design of the ultimate strength of stiffened panels in a given design space while accounting for residual stresses. Hernandez Ramos et al. (2024) integrated the non-dominated sorting genetic algorithm II (NSGA-II) and the original Smith method, which employs genetic operators, such as crossover,

mutation, non-dominated sorting, and population diversification to explore the connection between reduced-order models and their associated modelling errors. They used a Sigma function to evaluate force equilibrium errors and force vector equilibrium errors. The applicability and accuracy of their proposed approach were validated on a double-hull VLCC and demonstrated good agreement with methods proposed in ISSC reports on ultimate strength 2000 and 2012 (ISSC, 2000; 2012).

Physics-informed neural networks (PINNs) are an emerging machine learning technique for problems with established physical models, which can be used to augment data obtained from simulations and/or experiments. Incorporating these laws into the training process enables a reduction in the amount of learning data required, resulting in faster convergence rates. Several recent advancements have been made that could benefit future ultimate strength analyses. Zhuang et al. (2021) proposed a deep autoencoder-based energy method for addressing linear bending, vibration, and buckling of Kirchhoff plates, utilising the minimum potential energy principle to model the plate bending effectively in their selected benchmark cases. In turn, Yan et al. (2022) investigated shell structures made from composite materials and introduced the concept of an "extreme learning machine" in the context of PINNs for linear-elastic analysis of isotropic plates with a cutout and free vibration analysis of stiffened composite panels. Li *et al.* (2021d) highlighted that energy-based training is more efficient than PDE-based training due to the lower-order approximations of the displacement fields, while Petrolo and Carrera (2021) proposed the use of ANNs as an effective means for selecting the element kinematics in finite element meshes. Bastek and Kochmann (2023) explored the use of PINNs in the analysis of thin shells, specifically investigating shell element behaviour against locking. They considered three well-known benchmark case studies involving doubly-curved shells subjected to gravity and point loads under conditions of linear elasticity and low strain. Their findings suggest that the weak form, which is commonly used in FE analysis, performs better in the context of PINN than the strong form. They also noted that scaling differences in membrane, bending, and shear energies become particularly pronounced in the thin-plate limit. These investigations have implications for the fundamental underlying assumptions of ultimate strength analyses, particularly in the selection of the initial conditions of simulations, and simulation accuracy in general, highlighting the need for care to ensure realistic estimates.

Some studies have addressed the prediction of strength or failure. Huang et al. (2022) used physics-guided deep neural networks (PGDNN) to identify structural damage in large structures. Their approach focused on addressing two challenges: the large datasets required for pure data-based machine learning methods, which can be computationally infeasible, and the difficulty of achieving high precision in FE analysis-based damage identification. A loss function was developed to minimise the discrepancy between the simulation results and measured data, enabling the model to learn damage features from actual structures. The accuracy of the PGDNN was substantially better than that of conventional neural networks (CNN). Tran et al. (2024) also adopted a machine-learning approach in their investigation of the crack-tip cohesive law. They used PINNs to construct a fully functional form of the cohesive traction separation relationship at the crack tip based on far-field stresses and displacements. Leveraging Maxwell-Betti's reciprocal theorem and small-scale yielding enabled successful modelling of fatigue

crack propagation. This study demonstrated the efficacy of the PINN in stable cohesive zone extraction, suggesting the potential for extension to higher plasticity levels required for ultimate strength predictions.

2.3 Experimental Investigations

2.3.1 Full- and Model-Scale Experiments

Full-scale observations of the failure of built structures are vital when the design principles for ultimate strength are to be derived or updated, particularly for consideration of the interplay between environmental and strength modelling. The Norwegian Safety Investigation Authority (NSIA, 2023) reported on Viking Polaris superstructure window failures at the southeast of Cape Horn, November 22nd, 2022. The ship hit a breaking wave, which resulted in the breakage of the windows of seven staterooms of the cruise ship, with severe damage to both people (1 died, 8 injured) and materials. The crew were unable to predict the risk associated with the breaking wave, particularly the effect of the height of the wave on the hull or the force that might be exerted. The brittleness of the material led the structure to shatter after the ultimate strength was reached. This case motivated recommendations for updates to the current design rules.

Another branch of the literature has focused on investigating ultimate strength in carefully controlled laboratory settings. Zhao et al. (2022) conducted a series of experiments on the midship section of a fast ferry featuring two decks, multiple materials, and an opening in the deck, to assess the ultimate strength of large structural systems containing several connected plate fields and intermediate frames. Testing was conducted using a 1:5 scale model subjected to pure bending, and comparisons were made against FE simulations carried out using the ABAQUS and LS-Dyna software tools and the Smith method. Similar studies have been conducted for box-girders (e.g., Quispe et al., 2022). These results indicated good agreement between the simulation results and the experimental results, particularly in terms of the moment-curvature relationship. In another study, Shi and Gao (2021) explored the impact of a large superstructure on the load-carrying capacity of a passenger ship hull girder. While their model was simplified, their study demonstrated the effect of the interaction between bending moments and shear forces on the ultimate strength of the complex hull girder.

2.3.2 Experiments on Panels and Grillages

Understanding the behaviour of structural sub-systems behaviour is essential for validating numerical simulations and reduced-order models, which are used to accelerate the design process. Experiments play a critical role in testing the validity of the assumptions used in model development, thereby improving the accuracy and efficiency of the methods used to assess ultimate strength. While laboratory experiments offer well-controlled conditions, they often require idealized loading conditions and scaled-down specimens, which may not fully replicate real-world scenarios. Ideally, experiments would be repeated on similar specimens to increase confidence in the results; however, practical and economic constraints often limit the feasibility of multiple tests.

Xu and Guedes Soares (2021) investigated the impact of the size of the test unit, along with the applied loads and boundary conditions, on structural performance by

conducting experiments on small-scale panels. They relied on validated FE analysis to enable scale transitions between model-scale and full-scale specimens. They emphasised the importance of precise specimen geometry and support system design for accurate test results. Their experiments included stiffened panels with both two-span and three-span configurations, each with identical end-edge support; the two-span models demonstrated greater strength, attributed to increased rotational stiffness in the central span compared to the three-span setup. In 1/2 + 1 + 1/2 span configurations, failure typically occurred in the central span, aligning with expected outcomes, while in the three-span models, failure often began in the outer spans.

Several studies have sought to address the discrepancies arising from scale differences. Xu *et al.* (2021b) explored *partial* or *response* similarity methods in relation to the more complete *geometric* similarity methods. They found that the primary limitation of partial similarity methods is the alteration of collapse modes. Ma et al. (2023) developed a general scaled model technique for stiffened panels to preserve the similarity between full and model scale models, by focusing on plate and column slenderness, as well as non-dimensional lateral pressure. Their method involves a two-step process: first, the number of stiffeners needed to ensure plate slenderness is consistent between scales is determined, second, the dimensions of both the plate and stiffener are adjusted to maintain consistency in the sectional area. Liu *et al.* (2021b) conducted experiments to evaluate the compressive strength of long-span stiffened panels with large openings in the web frames and girders of passenger ship decks supported by tension pillars under combined uniaxial and lateral loads. The scaling factor for the lengths was 1:10, while plate thickness was scaled 1:2.33. Irregular shapes were observed in the scanned imperfections, and the ultimate strength results showed good agreement with FE simulations. However, due to the experimental challenges in applying loads and boundary conditions, the shapes of the stress-strain curves differed significantly between experimental and FE results. This discrepancy was attributed to the difficulty in retraining unloaded edges in physical experiments, whereas restraints are easily applied in FE analysis. Liu *et al.* (2021a) expanded their prior investigation to grillages with large openings typical of those found on the top decks of large passenger ships. Similar challenges with unloaded edges were observed experimentally. Their findings indicated that the complex shape of the grillage openings and the presence of reinforcements altered the overall buckling and collapse behaviour of the stiffened panel under compressive loads. This investigation also highlights the effect of edge stiffeners on the ultimate strength. Ma et al. (2021) performed experiments on biaxially loaded panels under lateral loads and used laser scanning to capture the shapes of initial imperfections. They concluded that incorporating these measured imperfection shapes into FE simulations led to significantly better agreement with experimental results compared to relying on the standard design equations. Xu *et al.* (2022b) used scaled experiments to validate their FE analyses on perforated rectangular specimens, finding good agreement in terms of ultimate strength, though initial stiffness alignment was less precise.

Guo et al. (2021) performed tensile experiments on laser-welded aluminium panels using DIC instrumentation to capture the strain field evolution and damage formation. This was complemented with a thermal-elastic-plastic analysis to assess the temperature field, welding deformations, and residual stresses. These data were combined to assess

the ultimate strength of the panels using non-linear FE analyses. This hybrid modelling approach, which combines measured strain fields with computed stress values (since these cannot be measured), effectively accounted for all significant effects and therefore resulted in excellent agreement in the force-displacement relationships of the tested panels.

Barsotti et al. (2025) performed experiments on a full-scale stiffened panel loaded in the transverse direction towards the deck stiffeners to study the failure mode differences for a scenario where the load acts in the weaker direction of the panel. This case, identified by Kõrgesaar et al. (2023) as challenging for reduced-order models, provided insights into multiple sources of uncertainty affecting agreement between experimental results and FE simulations. Due to these complexities, this experiment was selected as a benchmark for the current committee's study.

2.3.3 Experiments at the Component Level

Experiments may also focus on component and material specimen testing to better understand the effects of various environmental conditions, such as temperature, corrosion, or moisture, on material properties under applied loads, including strain or stress. These studies often examine factors such as strain rate, stress triaxiality, and material inhomogeneity, which may arise due to the material manufacturing process or joining methods that localise damage. Additionally, they may investigate how different material systems influence structural failure modes, particularly in composite materials where operational damage, moisture, temperature variations, and delamination significantly impact strength.

3 Construction, in-Service, and Life-Cycle Effects

The multivariate nature of ultimate strength prediction is reflected in both the inherent complications associated with prediction methods (as discussed in Sect. 2) and the very nature of the life cycle of a given structure. Aspects such as material properties, fabrication techniques, environmental effects, and structural maintenance all contribute to the ultimate strength prediction, which has further implications for design optimisation, service management, and potential life extension. Because there are uncertainties in all of these aspects, which are often difficult to quantify across structural scales, there is an uncertainty in the ultimate strength prediction. Research shows that a 10% uncertainty in the ultimate strength of plating may translate to a 20% variation in the ultimate strength capacity of a ship hull (Li *et al.*, 2021b). In the pursuit of more insightful analysis, research has been focused on the application of more realistic material models, more representative loads, improved geometry characterisation, and improved modelling formulations to account for uncertainties. Compared to the current industrial practice and classification society requirements, many of these applications are achieved at an increased computational cost. However, researchers have been adopting machine learning methods, such as ANNs, as a simpler tool to infer the current serviceability and remaining service life of a given asset, which would not be possible with an idealised model (Graves et al., 2023). Before delving into ship and offshore-specific topics, this

section reviews the latest literature on fabrication, as well as in-service and life-cycle effects, covering both metallic and non-metallic constructions.

3.1 Material Uncertainties

The uncertainties associated with material inputs strongly affect the ultimate strength prediction of both metallic and non-metallic structures. This section discusses key research advances in the past three years relating to this aspect.

3.1.1 Steel

The role of mechanical properties in the ultimate strength characteristics of steel structures is generally well established. The peak load prediction at the design stage is generally acceptable even when the minimum rule-required properties and a simplified bi-linear stress-strain relationship are utilised (Ringsberg et al., 2021). However, the true ultimate strength highly depends on the actual mechanical properties of individual structural members.

Zhao et al. (2022) conducted both experimental and numerical investigations of the ultimate strength of a ship hull girder model with large openings. As part of their experimental work, tensile tests were carried out on DH40 and DH36 grade steels. The tensile test coupons were made of different thicknesses, ranging from approximately 3 mm to 8 mm. The results were then fed into an FE model using a simplified stress-strain relationship (elastic-perfectly-plastic model). It was found that the failure modes of the strong girder and the first deck structure were relatively consistent between the simulations and model tests. However, this was not the case for the deformation direction of the panel centre of the second deck. The ultimate strength prediction error of the FE model was as low as 1.6%, implying that the second deck deformation effect was minimal. These results were fairly consistent with the findings from the ISSC 2022 Ultimate Strength benchmark study (Ringsberg et al., 2021); when the actual material properties were used in modelling, even with a simplified bi-linear stress-strain relationship, the ultimate strength prediction error was only 3%. However, the failure mode or plasticity location predictions at both the onset of yielding and the ultimate strength points proved to be a more difficult task. This implies that even though it may be possible to confidently estimate the magnitude of the ultimate strength with a small error, it is difficult to precisely predict the location of damage. Note that failure mode validation is more challenging than validating the ultimate strength value, as in most large-scale experiments in the literature, the failure mode is typically measured by strain gauges at discrete locations rather than through a full-field measurement. It is challenging to identify any onset of plasticity that can be compared with FE results.

Pan et al. (2023) addressed a gap in the applicability of existing load-end shortening formulae in the IACS Common Structural Rules for Bulk Carriers and Oil Tankers (CSR-H) in the case of hard corner elements. The assumption that hard corner elements follow elastic-perfectly-plastic collapse may lead to an overestimation of the ultimate load-carrying capacity due to the local buckling of plates. To more realistically reflect the progressive collapse behaviour under longitudinal compression of structural elements,

the authors proposed an improvement of the average load-end shortening curves in CSR-H. This was achieved via experimental results and non-linear FE analyses of hard corner elements to modify the CSR-H prescriptive load-end shortening curve formula, resulting in more realistic collapse behaviour and increased accuracy of the hull girder ultimate strength assessment. Therefore, it may be beneficial to assign more realistic material properties to hard corner elements in reduced-order/analytical methods, such as the Smith method. The authors also investigated the effect of steel grade, finding that steel grades with higher yield strength had lower plastic flows that may affect the equivalent stress distribution of the structural element; the lower the yield strength of the material, the more likely the structural element's response will be in the plastic region and the larger the increase in the errors of load-end shortening curves because of elastic-plastic buckling.

The role of yield strength in ultimate strength was further demonstrated during the ISSC 2022 Ultimate Strength benchmark study (Ringsberg et al., 2021). It was shown that the assumption of nominal versus actual material strength had the largest impact regardless of the numerical method selected. Also note that the examination of the M/V MOL Comfort accident conducted by ClassNK (ClassNK, 2014) found an 8% higher girder ultimate capacity when replacing the minimum mandated yield strength with more realistic values.

The effect of yield strength uncertainty manifests itself when considering cyclic loading. Jagite and Bigot (2023) analysed the ultimate strength of a container ship using a hydro-elastic-plastic model. The model permitted the application of time-dependent cyclic loads, determined from a long-term direct hydro-elastic analysis, rather than monotonic increasing loads. Interestingly, the authors concluded that the reduction of the ultimate strength of the hull girder due to cyclic loading was minor relative to the uncertainty in the material yield strength or the uncertainty in the effects of residual stresses and geometric imperfections. The authors recommended that such studies should be conducted on different ships of varying sizes and functions to gain a better understanding of the influence of cyclic loading on the ultimate strength of hull girders, with consideration of the probability of occurrence of "significant loading cycles". In addition, cyclic testing of steel materials typically used in ship construction was suggested to calibrate material models, such as the Chaboche model.

For cases where material coupons may be retained for testing, uncertainties surrounding mechanical properties could be addressed through testing efforts. However, in real-world structures or design-related analysis, this is not an option. In such cases, prior investigations into the uncertainty of steel properties must be examined. High-strength steels for marine use generally exhibit higher material property variation than mild steels (Storheim et al., 2018). Additionally, the former does not typically display a clear yield plateau, posing a challenge for modelling efforts that must consider using the 0.2% proof stress or proportional limit. Nahshon et al. (2018) applied various uncertainty quantification methods to examine the role of material uncertainties in the ultimate strength of a stiffened panel using available material and geometrical variability data from Hess et al. (2002). Using various statistical sampling methods to generate FE analysis input models that incorporated the statistical nature of steel material properties, as well as geometric imperfections and fabrication tolerances, they found a large range of possible

load-shortening curves, as shown in Fig. 6. It can be expected that such variation will manifest itself when a structural system is considered.

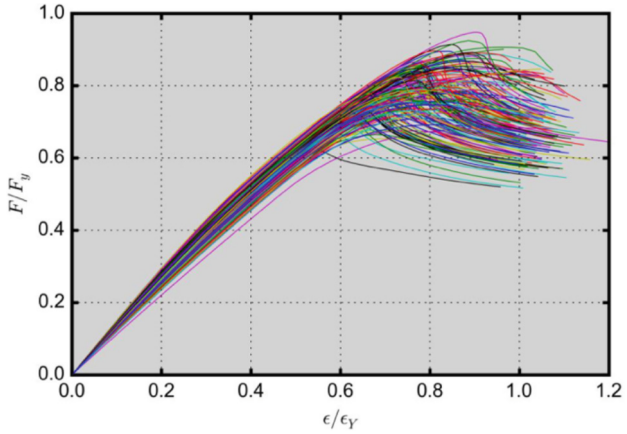

Fig. 6. Range of load shortening curves for typical stiffened panels, accounting for steel material, thickness, initial imperfections, and fabrication uncertainties (Nahshon et al., 2018).

Currently, steel grades for shipbuilding are capped at S460 (460 MPa minimum yield strength for container ships) by classification societies, although higher-grade steels are used extensively in naval, offshore and lifting appliance sectors. Ultra-high strength steels are often used for the construction of key sections of ice breakers and other specialised ships since they allow for a reduction in scantlings while maintaining the same design stress level. However, high-strength steels, while advantageous for their strength, present challenges, such as reduced toughness, high yield-to-tensile strength ratio (currently limited to 0.94 by classification societies), more complex welding processes, and lower ductility. These effects, combined with possible low operational temperatures, raise concerns regarding ultimate strength performance. Wong and Walters (2023) studied the decreased strain-hardening ability of high-strength steels and its effect on the elastic-plastic rotation capacity and local buckling of a stocky I-beam (with an overall cross-sectional slenderness below 0.51). The rotation capacity of a plastic hinge needs to be large enough so that the plastic hinge can maintain its strength until complete collapse. Both geometric and welding-induced residual stresses were included in the numerical models. A total of 217 beams with various yield strengths (from 460 to 960 MPa), yield-to-tensile ratios (from 0.80 to 0.99), and beam geometries were analysed. It was found that the rotation capacity of the beam was simultaneously dependent on all of the investigated parameters. Based on their findings, Wong and Walters suggested that a cross-sectional slenderness limit could replace the yield-to-tensile ratio limit to enable broader use of high-strength steels. However, their analysis appears to have been primarily informed by the rotational requirements for civil engineering applications, along with yield-to-tensile limits from classification societies, and slenderness requirements from IACS requirements for Polar Class ships. The differences in the assumed safety margins and design approaches in these requirements were not considered.

3.1.2 Aluminium Alloys

Liu *et al.* (2020a), Hosseinabadi and Khedmati (2021), and Wang *et al.* (2022d) published comprehensive reviews examining various factors and their interactions that influence the ultimate strength of aluminium structures. These included material properties, investigation methods, structural geometry/arrangement, initial imperfections, boundary conditions, loading conditions, and in-service degradations. Unlike steel structures, where an elastic-perfectly-plastic material model is commonly used, the Ramberg-Osgood approximation model is generally adopted for aluminium alloys (also required by classification societies). Aluminium structures exhibit a high level of sensitivity to temperature with rapid loss of stiffness above 100 °C. As such, it is crucial to prioritise the design at the member, joint, and structural levels, along with ensuring effective fire protection for the structural systems. They are also most likely to contain under matched heat-affected zones (HAZ) in weld areas, as opposed to overmatching in most steel welds. For example, Liu *et al.* (2020b) reported such characteristics for AA5083-H116 coupons (see Fig. 7), which were fed into their LS-DYNA model of butt weld and fillet weld joints. It was found the difficulties in predicting plastic responses were primarily due to the use of simplified shell elements and material properties; the actual material properties would vary with distance to the weld seams. In addition, ultimate strength prediction methods, such as ISUM and ISFEM, may require further evaluation for their applicability to aluminium vessels (Hosseinabadi and Khedmati, 2021).

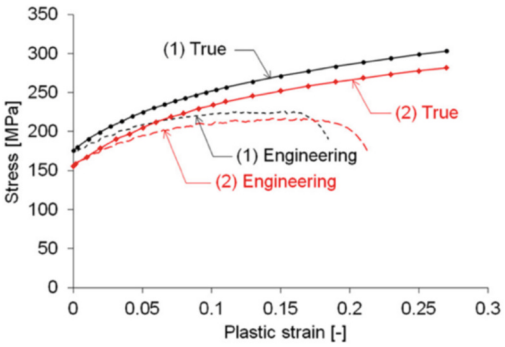

Fig. 7. Material properties of AA5083-H116: (1) base and welded materials, and (2) HAZ material (Liu et al., 2020b).

3.1.3 Composites and Sandwich Structures

The application of composites in marine environments has steadily expanded, encompassing applications from low/high-performance vessels and offshore renewable energy systems to wind-assisted propulsion systems and dock infrastructure. Given the diversity of factors, such as composite materials, layup configurations, and manufacturing techniques, it is essential to accurately characterise and correctly apply material properties in any structural analysis, especially when predicting strength capacity and failure modes. Lowde et al. (2022) conducted an in-depth review focused on the prospect/feasibility of

building over 100 m long composite ships. Their review included manufacturing processes, material properties, and economic and life cycle considerations. One of the key obstacles preventing scaling up to longer composite ships is the lack of a comprehensive database of material properties. In addition, new materials, such as 2D monolayers and nanotubes, are often costly and are available in limited quantities. Nevertheless, research continues, and novel methods are being used to improve methods for accurately predicting material properties and failure modes.

Barsotti et al. (2020) reviewed industrial developments in limit state assessment and design approaches for marine composites, with a focus on pleasure yachts/crafts and naval ships. They concluded that experimental testing was the most reliable method for determining material properties and failure modes. However, when experiments are infeasible, designers often rely on established rules, the research literature, and manufacturer reports. The use of cohesive elements in FE modelling represents the state-of-the-art approach in the assessment of delamination, which is one of the most critical failure modes. Despite the effectiveness of this approach, cohesive elements are limited to small-scale applications due to computational demands and the complexity of calibration. Additionally, the joining of composites with other materials (for example, for repair) has become an increasingly explored area of research in recent years.

Liu et al. (2023) performed a multi-scale analysis on glass-fibre-reinforced polymer (GFRP) materials. The micro- and mesoscale representative volume element (RVE) models of components used in GFRP materials were established, incorporating failure criteria and stiffness degradation models through a user-defined subroutine (VUMAT) in ABAQUS. The equivalent material properties at the micro-scale (mesoscale) obtained by a homogenisation method were used to define the mesoscale (macro-scale) mechanical properties in the FE analyses. It was shown that the ultimate strength of the GFRP stiffened panels was primarily determined by the failure of chopped strand mat (CSM) fibre bundles and woven roving (WR) yarns. The findings from this work suggest that the parametric study of meso-mechanics could be an effective guiding method in the optimisation of macro ultimate strength capacity in stiffened panels.

Jafarzadeh and Khedmati (2020) modelled the midship section of a 50 m long WR/polyester GFRP vessel subjected to four-point bending to assess its ultimate strength behaviour. Due to the 45-degree fibre orientation, symmetry conditions could not be applied, necessitating a full model of the section. Modelling was conducted (in ANSYS using SHELL281) based on first-order shear deformation theory. No initial imperfection was included. The Tsai-Wu failure criterion was employed, and bending moment versus displacement was analysed for both hogging and sagging conditions. In both cases, failure was observed to initiate in the deck structure. Validation was performed through a comparison with numerical results from the literature, showing relatively good agreement.

Based on the active learning Kriging (ALK) model and the Hashin failure criterion, Wang *et al.* (2023a) proposed a new reliability evaluation model for composite stiffened panels and conducted a reliability analysis of their ultimate bearing capacity. They also studied the importance ranking of the input variables. Comparing the results of the ALK model with those from the Monte Carlo method demonstrated the model's accuracy and efficiency in various cases. Their discussion of the effects of longitudinal elastic

modulus and fibre-direction tensile strength on post-buckling failure probability provides valuable insights and references for the optimisation and design of composite stiffened plates. An ANN was used by Sun *et al.* (2021b) to predict the ultimate strength of composite hat-stiffened panels under in-plane shear. The database for training the ANN was generated using FE models, which considered several material parameters. The ANN model achieved over 98% accuracy in predicting the buckling load and the ultimate load. However, its performance with input parameters outside its training domain (i.e., its generalisability) remains uncertain.

Aluminium alloy honeycomb sandwich (AHS) structures are known for their excellent impact-absorption capabilities and high stiffness-to-weight ratio. Compared to composites, they also offer improved recyclability without sacrificing their lightweight character. Research has explored hybrid lightweight ship designs that combine steels with AHS structures to improve energy efficiency. For example, Garbatov et al. (2023) introduced a hybrid bulk carrier design in which part of the cargo holds was replaced with AHS panels. The ultimate strength of the hull girder was incorporated into a multi-objective optimisation design process, and two designs were selected for further reliability analysis, which will be discussed in detail in Sect. 3.4. Corigliano et al. (2023) conducted both experimental and numerical studies of an AHS panel subjected to uniaxial compressive loads. The numerical studies were based on a modified Smith method and the Johnson-Ostenfeld formulation. Relatively good agreement of the load-shortening curves was obtained between the two methods. However, the numerical method did require calibration based on experimental results.

Honeycomb sandwich structures produced by additive manufacturing were investigated by Garbatov et al. (2024). The core material consisted of thermo-plastic nylon reinforced with 10% chopped carbon fibres, manufactured using the classical fused deposition modelling technique. The skins were made from thermoplastic nylon reinforced with continuous carbon fibres, produced via continuous fibre co-extrusion technology. Printed samples were subjected to 3-point bending tests, which fed into a subsequent numerical approach for the prediction of the progressive compressive failure modes. The response of the compressed face (global and local buckling followed by delamination) governed the flexural response of the structure. On a larger scale, Zhong and Wang (2022) conducted a numerical analysis to study the ultimate strength of sandwich box girders. The analytical results were validated through comparison with experimental results. Their findings indicated that increasing face plate thickness while reducing web plate thickness led to higher warping stress in the box girder, ultimately decreasing the ultimate bearing capacity. However, further research is needed to understand these structures' performance under ship-specific design conditions.

3.2 Fabrication Uncertainties

Consideration of initial imperfections has always been a key part of ultimate strength assessment. Most imperfections stem from structural connections (often seen as weak spots). The quality of both traditional welding and non-metallic bonding is influenced by the materials used, fabrication procedures, and workmanship. This section reviews the recent literature that discusses the consideration of these uncertainties when predicting ultimate strength.

3.2.1 Welding-Induced Distortions and Residual Stresses

Steel

Welding of steel structures introduces distortions and residual stresses that have a profound effect on ultimate strength at the structural element, grillage, and system levels. As such, approaches to account for these effects have been a longstanding research topic. Within the context of FE analysis, efforts generally focus on direct or implicit simulation of distortions and residual stresses through imperfection generations in a deterministic, statistical, or stochastic manner. In contrast, reduced-order models such as the Smith method consider these effects through modification of the underlying load-shortening curves of structural elements to perform progressive collapse analyses.

Given the large temperature variation during a welding process, temperature-dependent material properties play an essential role in welding-induced imperfections. However, there are limited material data, especially at high temperatures available in the public domain. This research gap motivated Chen and Guedes Soares (2021) to conduct tests with metal inert gas T-joint fillet welding tests on rectangular steel plates. Subsequently, a 3D sequentially coupled thermo-elastic-plastic modelling approach was developed, with both welding-induced distortion and residual stresses validated against experiments. A simplified temperature-based material model was then proposed which could be used in welded structure models.

The uncertainties associated with welding-induced distortions and their effect on ultimate strength were also investigated by Li *et al.* (2022c). The authors conducted FE analysis case studies on a steel grillage model and tested both deterministic and probabilistic geometric imperfections. This work emphasised that, beyond influencing the magnitude of the ultimate strength, the selection of a particular distortion mode also has implications for model convergence and hence prediction robustness. It was also concluded that adopting a stochastic modelling approach could provide more realistic assessments of structural responses.

A new probabilistic-based imperfection model was introduced by Georgiadis and Samuelides (2021a) via a spectral representation method. The method was based on random field theory and actual measurements of ship structures. The impact of stochastic geometric imperfections on the ultimate strength of plates was assessed using Monte Carlo simulations. The proposed imperfection model was then applied to a tanker under extreme sagging conditions to predict the stochastic ultimate strength of the hull-girder by training an ANN. Figure 8 shows the comparison with conventional imperfection models and the Smith method. Notably, the proposed model resulted in a reduction of ultimate strength by up to 4.5% compared to the commonly used “hungry horse” imperfection mode. The use of an ANN makes it feasible to incorporate the full spectrum of input uncertainties in ultimate strength assessments.

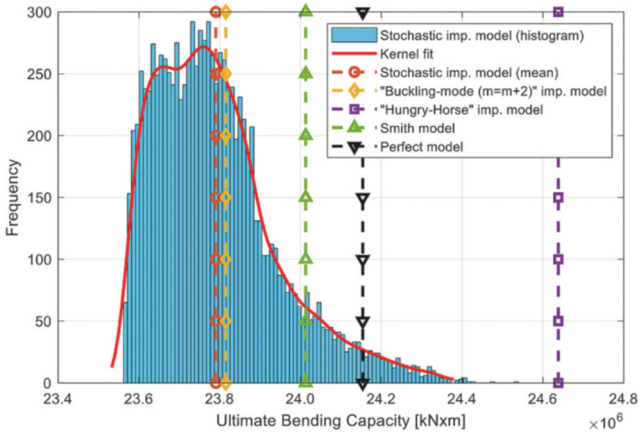

Fig. 8. Histogram of stochastic ultimate strength of a VLCC in sagging compared to conventional imperfection models and the Smith method (Georgiadis and Samuelides, 2021a).

Graves et al. (2023) proposed a new method for mapping point cloud data obtained from laser scanning or photogrammetry to FE models to characterise geometric imperfections. Mapping was performed using Kriging methods that inherently smooth out noise in the point cloud data and effectively fill data gaps. The method was then applied to FE analysis calculations of a typical tee-stiffened steel grillage. Results were compared to those performed using a typical spectral-distortion approach. The proposed method provides a robust approach for incorporating measured in-service distortions when commonly assumed welding-induced distortion shapes (e.g., eigenvalue buckling mode or hungry horse) are unsuitable. Such in-service distortions could be located where deck repairs are made, or impact damage has occurred.

Residual stress can be redistributed or relaxed under applied loads during service. Elastic shakedown involves initial cycles of plastic deformation that adjust plasticity-induced residual stresses, redistributing them to achieve internal equilibrium after unloading. Consequently, the original welding residual stress state is modified. Gadallah et al. (2024) developed a numerical procedure to analyse the relaxation of welding residual stress due to elastic shakedown in various welded components. They found that early cyclic loading, especially near weld toes, significantly altered the initial welding residual stresses, highlighting the importance of accounting for this redistribution. Hayama et al. (2024) conducted *in situ* X-ray stress measurements to assess fatigue properties and relaxation behaviour throughout the fatigue process. They found a linear correlation between the relaxation threshold stress and initial compressive residual stress with specimen hardness, which aligned with the compressive yield strength. This underscores the importance of using relaxation threshold stress for quantitative evaluations to predict fatigue limits, particularly considering the compressive residual stress induced by surface treatments.

Aluminium

Ultimate strength analyses of aluminium structures present additional challenges compared to similar analyses of steel structures due to (1) the significant impact of

welding on the reduction of local material properties (softening in the HAZ), (2) the use of extruded structures, and (3) the generally lightweight scantling of these structures. Having reviewed the welding-affected material properties in Sect. 3.1.2, it is notable that understanding and data on initial deflections in welded aluminium structures lag somewhat behind those of steel structures. The majority of aluminium stiffened panel models in the literature apply similar methods as for steel structures, e.g., using Fourier series to generate initial deflections. Typical amplitudes are summarised in the review by Hosseinabadi and Khedmati (2021). Soleimani et al. (2020) carried out a numerical buckling analysis of a midship section of a real high-aspect-ratio twin hull (HARTH) vessel, made of AA5083-H321 plating and AA6062-T6 stiffeners. A HARTH vessel has a smaller waterplane area than conventional catamarans, and experiences reduced hull drag, allowing it to more easily break through the water during movement. However, it also means that the vessel is more susceptible to buckling in rough seas. Initial geometric imperfections in plates were considered using a half-wave distortion mode as described by Smith et al. (1987), incorporating plate aspect ratio, plate thickness, and an average distortion factor for aluminium plates, as recommended by Paik et al. (2008). These initial imperfections play a critical role in the buckling behaviour of thin plates (particularly those less than 8 mm thick). While the plate aspect ratio has minimal effect on overall strength, it significantly influences the failure mechanism. Welding residual stresses and heat-affected zone properties were not included in this analysis.

3.2.2 Non-welded Connections

The impact of manufacturing technology (welding versus extrusion) on the ultimate compressive strength of aluminium-alloy stiffened panels has been explored through a series of FE analyses (Liu et al., 2020a). Assuming similar levels of initial distortion, the load-carrying capacity of extruded panels was reported to be 4.6% higher than welded panels due to the consideration of HAZ properties. The use of large aluminium extrusions is common in high-speed craft such as passenger ferries. However, research on extruded structures is still limited (Hosseinabadi and Khedmati, 2021).

L-joints, such as those typically found between the hull's outer shell and the upper deck, are a common feature in ship structures. Kai et al. (2020) showed that changes in the structural transitional area of such joints can change the failure mechanisms under tensile loads (see Fig. 9). Joints with a radius of 45, 90, and 180 mm were tested and analysed using FE analyses with a new damage criterion, which differentiated between matrix and fibre response under both tension and compression. The foam core was modelled using an ideal elastic-plastic model, and debonding between the stiffener and the panels was included via a cohesive zone approach. The authors subsequently proposed an improved L-joint, where the common bonding mechanisms at the end of the joint were replaced by integrated-moulding T structures with rounded corners. This design incorporated a larger no-damage zone and had a higher ultimate strength than conventional designs. It must be noted that this improved design was only studied numerically. Although no experimental validation was provided, the numerical model was validated against the original tested geometries. The damage and failure prediction maps presented in the paper (Fig. 9c) aid in understanding the failure mechanisms and optimising joint design.

3.3 In-Service Effects: Degradation and Damage

This section focuses on the effect of material degradation and mechanical damage on ultimate strength. Both aspects have been intensively investigated in the past few years to better estimate the remaining strength capacities of structures, which has key implications for the optimisation of the design and life-cycle management of a given asset. The effects of asset-specific accidental damage, such as collision and grounding, are outside the scope of this section and will be covered in Sects. 4 and 5.

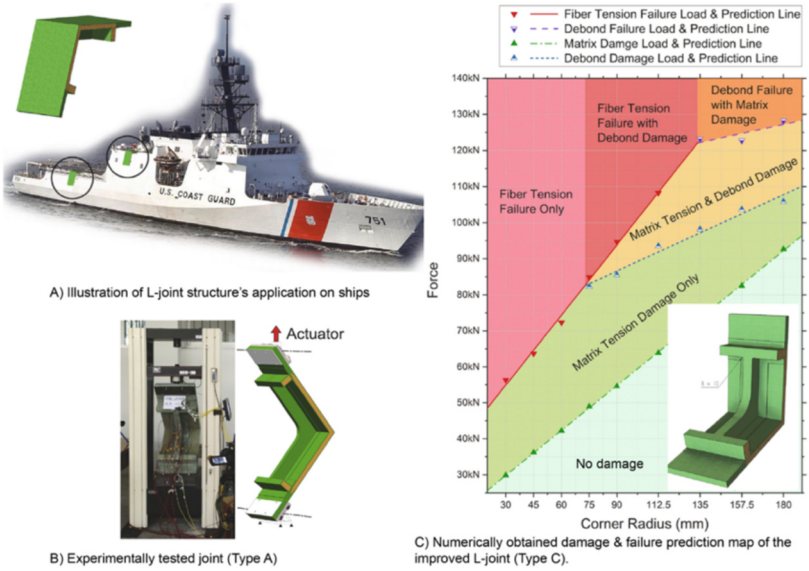

Fig. 9. (a) L-joint application case in ship structures, (b) experimental testing of the L-joint, and (c) damage and failure prediction map of the improved L-joint (Kai et al., 2020).

3.3.1 Corrosion and Material Degradation

Degradation of Metallics

Requirements for and advancements in coating applications for metallic structures exposed in marine environments highlight the significant threat posed to ultimate strength capacity by localised corrosion in the form of pitting or crevice corrosion, as it results in localised thinning, eventually leading to perforation (often covered by rust and/or coating) that is difficult to detect. Understanding how and when this process takes place, what the controlling parameters are, and how they correlate with one another in the context of ultimate strength analysis is essential for developing more robust and reliable evaluation procedures and fitness-for-service practice codes. Consequently, there has been a continuous research effort on this topic in recent decades.

In their consideration of structural members, Feng et al. (2020) focused on the ultimate strength characteristics of three stiffened panels with pitting corrosion distributed

on both plates and webs. A random as well as uniform distribution of circular through-thickness pits was employed, and their influences on the ultimate strength were investigated. Their findings indicated that pitting distribution and pitting severity were less harmful in the context of ultimate strength reduction when they occurred on the webs rather than on the panels. These results support previous findings related to corrosion wastage effects where web pitting was found to be less influential on ultimate strength. Based on these results, the authors proposed an empirical formula for predicting the ultimate strength of stiffened panels as a function of the ratio of the corroded volume to the undamaged volume of the reinforced panel. The robustness of this formula was verified against 243 simulated cases with random pitting distributions and degrees of severity. These findings may provide valuable information for supporting maintenance decisions and emergency stop protocols.

Mursid et al. (2023) investigated the effect of pitting corrosion on a ship bottom plate damaged by grounding. They found that the pitting location played a significant role in the ultimate strength of a structure by conducting a very detailed FE analysis, where 14 scenarios were simulated using different pitting positions on the bottom plate. The simulation results indicated that the location of pitting corrosion impacts stress concentrations, crack initiations, load re-distribution, and penetrating position when the crack nucleates. For example, a configuration comprising four small pits near the centre of the indenter will exhibit a peak force that is approximately twice the force that would be experienced if occurring away from the indenter. These findings indicate that the critical position of pitting significantly affects the load-carrying capacity of the bottom plate, especially as the relative spacing between pits increases radially. Zhang et al. (2022) also investigated the combined effects of pitting and cracking on the ultimate strength of stiffened panels under compression, addressing a gap in research on how these defects impact load-carrying capacity. Their study aimed to confirm the interactive effects of cracks and pitting with plate and column slenderness ratios on ultimate strength.

A more general framework for assessment of the ultimate strength of a bulk carrier subject to pitting corrosion was developed by Piscopo and Scamardella (2021). They modified the well-established incremental-iterative method (IACS, 2020a,2020b) to study the ultimate strength of a hull girder and the combined effects of random pitting corrosion wastage. In their approach, the authors introduced a slight modification to the existing expression using an extended version of the Faulkner equation (Faulkner, 1975). This method incorporates plate panels as part of grillage structures, whose ultimate capacity is provided by the Faulkner formula, which enables allowance for a certain degree of rotational restraint along the longitudinal edges of the plate panels. This correction provides an explicit strength check criterion for the ultimate strength assessment of pitted plating, which is not considered by current rules and guidelines. The reliability of the proposed method was evaluated against results obtained from a benchmark study using four reference scenarios, characterised by different locations and the extent of pitting corrosion wastage. In their study that also focused on ship structures, Shi et al. (2021) proposed a new method to study the ultimate strength of a pitted ship hull through a series of numerical analyses with various levels of corrosion damage and damage locations. Using a series of Monte Carlo simulations, they demonstrated a strong

relationship between the criticality of corroded structures and the sensitivity of related factors impacting hull collapse.

In their work related to general/uniform corrosion, Kim *et al.* (2022a) introduced a Bayesian inference model to address uncertainties in corrosion prediction. They proposed a probabilistic model in which the parameters introduced in the corrosion wastage model were treated as random variables and the probability distribution of these random variables was updated accordingly when measurement data were obtained. This iterative updating approach estimated corrosion depth distributions with approximately 95% and 99% reliability. The predicted corrosion depth from posterior results decreased at each time point, reflecting the incorporation of new data through Bayesian inference. This model could support health monitoring and assist in determining optimal times for periodic inspections. Similarly, Garbatov (2020) developed closed-form solutions for determining the corrosion allowance of ship structures based on probabilistic and risk principles. It is worth mentioning that the proposed set of equations takes into consideration the time-dependent degradation factor for wastage estimation in cargo ships coupling with the Two-Areas-At-Time (TAAT) analysis to determine corrosion allowance in different environments. Although this model assumes uniform thickness reduction without local pitting, it offers a practical probability-based approach for predicting general corrosion wastage.

General corrosion wastage was also indirectly studied by Liu (2021) through FE modelling of lattice corrugated panels made of E690 for offshore applications. The panels were subjected to quasi-static and low-speed impact loading. Uniform thickness reduction representing general corrosion was assumed to circumvent complex material dissolution modelling. It was found that corrosion in the inner part of the structure had a more severe effect on the structural strength than the outer surface corrosion. In a similar analysis using uniform thinning to represent corrosion, Zhang et al. (2024) conducted experimental and numerical analyses of "corroded" concrete-filled double-skin steel (CFDST) subjected to eccentric compression. CFDST is increasingly being used as an alternative to circular steel tubes (CST) for offshore structures, such as wind turbine jackets, for enhanced structural resilience. Partial uniform thinning of the outer steel skin of the tube was considered. Four levels of corrosion and two types of cross-sections were analysed. It was found that CFDST exhibits enhanced robustness and energy dissipation capacity against sudden damage due to local buckling compared to CST. The authors also recommended further research on CFDST structures, considering both dynamic loading and the effects of corrosion.

To simulate more realistic corrosion morphologies on steel structures, Georgiadis and Samuelides (2021b) studied the effect of non-uniform thickness reduction on stiffened panels subjected to compressive loads using random field theory. Their findings indicated that thickness data collected from inspections could be used to inform spatial variations in the material, enabling more reliable vessel-specific predictions of ultimate strength. However, this conclusion cannot be a priori extrapolated in the case of pitting corrosion in areas with pronounced stress concentrations. Zhang and Zaghi (2023) used 3D scanning of heavily corroded steel bridge structures to estimate their residual strength. They generated FE models directly from 3D point cloud data of the damaged structures, incorporating perforations and thickness reductions. It was demonstrated that

corrosion substantially changed the failure mode and encouraged failure to occur at the damaged location where longitudinal and transverse structures intersected, as illustrated in Fig. 10. Although this study focused on bridges, the corrosion features and resulting analysis framework could be equally valuable for understanding failure modes in ship and offshore structures under similar conditions.

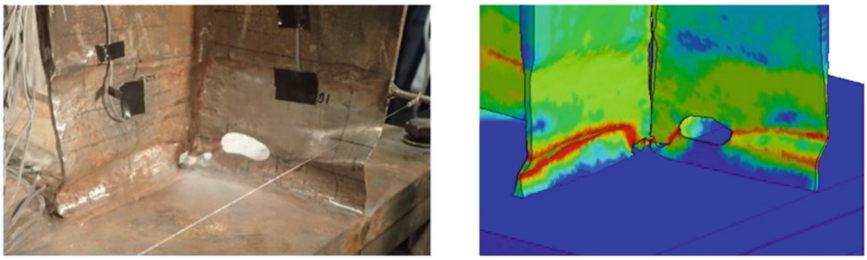

Fig. 10. Failure mode of corroded girder (Zhang and Zaghi, 2023).

Tekgoz et al. (2020) summarised key factors influencing changes in the ultimate strength of ship structures that have aged or experienced damage during their operational lifetime. They showed that the ultimate strength of corroded structures is influenced not only by thickness wastage but also by microstructural changes that may occur during the environmentally assisted degradation processes, which eventually undermine mechanical performance. In ship design regulations, the net scantling approach is applied to oil tankers and bulk carriers covered by the CSR, as well as to other ship types as directed by some classification societies. The full corrosion addition is deducted from the scantling for buckling analyses, whereas for hull girder analyses, only 50% of the corrosion addition is removed. IACS specifies corrosion additions in the CSR for tankers and bulk carriers, UR-S11a for container ships, and UR-S21 for hatch covers/coamings. Based solely on general corrosion, these guidelines were derived from extensive survey thickness measurements collected by classification societies over several years, followed by statistical analysis. Final corrosion additions also account for coating life, coating failure period, and survey intervals.

Structural integrity assessment standards for the offshore sector, such as API 579 (2021), define corrosion degradation as either local metal loss (LML) or general metal loss (GML) for in-service structures. As specified in API 579, every structure is designed with a corrosion allowance (CA). Inspections that find metal loss exceeding the specified CA necessitate the evaluation of the suitability of the structure for continued use, as well as predictions of future corrosion progression to guide inspection frequencies and protocols.

Assessment procedures are based on point thickness readings and thickness profiles for a prescribed grid. For GML, the minimum thickness measurement is often used as a baseline across the plate or structure, providing a conservative estimate. As in the procedure for LML, if the GML assessment does not meet basic criteria, more advanced assessment methods are available. When calculating the minimum required wall thickness, including the CA, engineers often assume that the steel is purchased at a standard

thickness, which is usually greater than needed. This practice introduces an additional safety margin beyond the design requirements due to the excess material. These considerations are particularly important for evaluating the ultimate strength behaviour of offshore structures, as corrosion progression may bring the structure closer to its limit state over time.

Degradation of Composites

The growing use of composites has raised concerns about their structural integrity, particularly under marine environmental degradation, where the underlying mechanisms are not fully understood. This has spurred intensive research efforts to gain further understanding of the interaction between the matrix material and surrounding conditions with applied stress. Recently, Vizentin and Vukelic (2022) investigated composite degradation experimentally. Coupons made of glass fibre with epoxy and polyester resin were immersed in real sea environments for up to 12 months. Material characterisation and tensile tests were subsequently conducted. It was found that the 0/45/90 layout for the polyester/glass combination showed the greatest resilience to seawater. However, the polyester coupons were produced using a hand-layup process, and the impact of this method was not assessed. It was reported that microorganism growth resulted in voids in the resin matrix and affected the mechanical properties. However, this mechanism must be further researched.

Accelerated ageing tests were conducted by Ghabezi and Harrison (2022) on glass/epoxy and carbon/epoxy samples in artificial seawater at room and elevated temperatures for over 180 days. Failure modes and locations were recorded using the 3-part failure mode code from ASTM D3039. Experiments showed that mechanical-based damage, such as softening and swelling, is the primary source of physical degradation of polymer resins. Even after water penetration reaches the saturation point, water molecules still react with the epoxy over time, causing irreversible chemical changes (chain scission) and reduced material properties. Bonsu et al. (2022) also performed tests in artificial seawater and evaluated the failure mechanisms of plain glass and basalt fibre-reinforced composites, as well as a selected glass/basalt hybrid composite sequence. The results showed that some hybrid laminates with sandwich-like and alternating sequencing exhibited superior mechanical properties and ageing resistance than plain laminates. For instance, a $[B_2G_2]_S$ (where B stands for basalt fibre and G stands for glass fibre) hybrid composite with basalt fibre outer plies retained 100% tensile strength and 86.6% flexural strength after ageing, which was the highest among all the laminates. However, $[BGBG]_S$ specimens with alternating sequencing retained the highest residual impact strength after ageing. Scanning electron microscopy (SEM) analysis of the failed specimens showed fibre breakage, matrix cracking, and debonding caused by fibre-matrix interface degradation due to seawater exposure. However, various hybrid configurations significantly hindered crack propagation across specimens, thereby altering their overall damage morphology.

Wang *et al.* (2022c) developed a progressive damage model that included the effect of hygrothermal conditioning on both the strength and stiffness of glass fibre composite structures. The model was developed based on quasi-static tensile and compressive tests on open-holed specimens under both dry-state room temperature and hygrothermal conditions. Failure models, including both the Hashin and maximum stress criteria, were

adjusted to match the experimental data. While the authors reported good agreement between numerical analyses and experimental results, discrepancies were noted in the displacement and strain values at which the ultimate load was reached. Based on these findings, the authors concluded that the ultimate strength of these high-strength quasi-isotropic panels decreased by approximately 35–40% for both tension and compression when tested at 70 °C with equilibrium moisture absorption. For compressive loading, the failure mode remained consistent, but for tensile loading, the failure morphology shifted from an X-shape around the hole to an I-shape. This study underscores the importance of accounting for hygrothermal effects when evaluating composite materials for ship and offshore applications.

3.3.2 Mechanical Damage

Cracks in metallic marine structures are commonly observed along weld lines and at the intersection of stiffening elements. Understanding the impact of cracks on structural strength is necessary for preventing complete failure and informing maintenance strategies, yet studies on cracked aluminium panels are limited despite extensive literature on the residual strength of aluminium residual strength. Attia et al. (2023) conducted a series of FE analyses on cracked AA5083 H116 panels, varying crack length, location, and orientation to evaluate their effects on ultimate strength. It was found that the location of the crack significantly impacted the ultimate capacity, equivalent stress distributions, and deformation shapes for transverse and inclined cracks, whereas this was not the case for longitudinal cracks. As the crack length increased, the ultimate capacity of the panel decreased. Taking the loading rate into account, Shi *et al.* (2023a) analysed the dynamic ultimate strength of cracked, thin steel plates under compression. Steel with 315 MPa yield strength was modelled using non-linear FE analysis. An empirical formula was then derived accounting for loading rate, crack, and plate geometry. It was reported that cracks caused up to a 61% reduction in the dynamic ultimate strength of plates when compared to uncracked specimens. Both a longer crack and a larger crack angle reduced the ultimate strength. Similar to the findings by Attia et al. (2023), the transverse location of the crack also influenced the dynamic ultimate strength more than the longitudinal location, with a decreased effect observed as the crack approached the unloaded side of the plate. The length and aspect ratio of the plate were found to influence the dynamic ultimate strength, while the slenderness ratio had little impact at a high strain rate.

Through a combination of non-linear FE analysis and the use of an ANN, Li *et al.* (2022a) found that the ultimate strength of plating is significantly influenced by crack orientations and configuration features. The combined effect of these influential factors was captured through an empirical mathematical expression derived by the ANN. The machine learning algorithm was trained and validated with an independent database to evaluate the accuracy and applicability of the suggested approach. The impact of the crack location on the ultimate strength of the hull girder was examined by Babazadeh and Khedmati (2021) for a bulk carrier. Their study indicated that the presence of cracks in deck structures and the side structures near the decks has the most significant effect on ultimate strength under both sagging and hogging conditions.

Low cycle loading is another key source of damage affecting the ultimate strength of marine structures during service. Li *et al.* (2019a) presented an analytical method

to predict the collapse behaviour of plates and stiffened panels under severe low-cycle loading scenarios where loading magnitudes approach or exceed ultimate strength. The method was developed by performing parametric FE studies. This study included an investigation of the effects of kinematic versus isotropic hardening. The model was then formulated in a manner suitable for introduction into an ultimate strength framework based on the Smith method, thereby facilitating rapid predictions of potential hull disintegration. Deng et al. (2022) conducted experiments as well as FE calculations on single and double-hulled girder test sections with large deck openings to investigate severe cycling loading beyond the ultimate strength of the girder. This work included numerous details related to the tested structures, such as material stress-strain curves, residual stress measurements, and initial distortions. Additionally, 3D scanning was performed after every load cycle to characterise the damage progression. The corresponding FE simulations demonstrated the accumulation of residual stress, damage, and reduction in structural capacity as a result of cyclic-loading-induced damage, see Fig. 11.

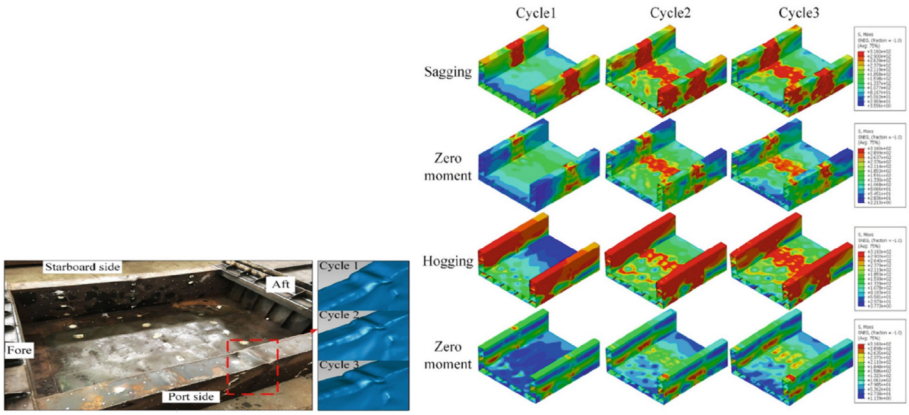

Fig. 11. Experimental setup and corresponding FE analyses for a double-hulled case showing residual stress accumulation during severe hogging/sagging cycles (Deng et al., 2022).

Studies have also been conducted to investigate the combined effects of cracks and cyclic loading. Hu et al. (2022) studied the failure mechanism and behaviour of cracked panels under cyclic loading. They concluded that when the buckling half-wave number is odd, the crack location at the trough/crest of the buckling mode results in larger deformation in the adjacent area around the crack. This accelerates strain accumulation near the crack tip, promoting crack propagation and leading to greater ultimate strength reduction. Conversely, when the buckling half-wave number is even, its effect is insignificant. This was found to be true for cracks either located in the centre or at the edge of the panel. Kang et al. (2022) investigated cracked steel panels under extreme cyclic loading and developed a formula to predict the ultimate strength for different types of crack propagation. FE analysis revealed that cyclic loading induces smaller deformations than monotonic loading due to lower load amplitudes. Hence the ultimate strength of a non-cracked panel remains relatively unaffected by an increase in cycles. However,

increasing the load accelerates crack propagation and decreases ultimate strength for all crack positions. Double-edged cracks exhibited the fastest crack growth and ultimate strength reduction, while thicker panels facilitated greater crack extension. The study conducted by Song et al. (2022) focused on the effects of pre-existing and low-cycle fatigue (LCF) cracks on the residual ultimate strength of steel plates. An elastic-plastic analysis was carried out to determine the bearing capacity of plates under various loading conditions for cracks with different lengths and locations. FE analysis was then used to replicate buckling and collapse behaviour. A lower bearing capacity was observed as the crack propagated when compared to static cracks. Additionally, cyclic tensile loading produced deflection in the opposite direction of initial deflection, which improved compressive bearing capacity. However, higher cyclic load amplitudes increased deflection and reduced ultimate strength. Future improvements to the proposed LCF model may include consideration of the crack surface contact effect.

Openings in composite stiffened panels can cause cracking. Liu *et al.* (2022b) investigated the effect of open cracks on the residual bearing capacity of a single-hat-stiffened composite panel, using an ANN model. The model input parameters included crack orientation, length, width, and angle. The main emphasis of the study was on producing an ANN with a satisfactory learning rate without overfitting. The network was trained using approximately 90% of the 3830 FE analyses that included a Hashin criterion for the in-plane failure, and a cohesive zone approach for the possible debonding between the stiffener and panel. The use of the ANN allowed the authors to study the effect of the input parameters of the crack on the residual buckling strength.

The buckling and post-buckling behaviour of J-type composite stiffened panels were theoretically predicted and tested both numerically and experimentally by Wu et al. (2023). The authors also investigated the influences of adhesive layers, the layup configurations of both the stiffened rib and skins, geometric dimensions, and accidental impact load positions of the J-type ribs on the structural buckling responses. It was found that the failure modes included delamination, debonding, skin crushing, and rib fracture. The skin between the ribs was the first buckling location. The load-bearing capacity was found to be sensitive to the impact energy when the back of the rib was impacted.

3.4 Life-Cycle Management Analysis

Life-cycle analysis can provide a rational basis for the management of ageing ships and offshore structures with reduced ultimate strength. Uncertainties that may arise from time-varying deterioration phenomena (e.g., corrosion, crack, delamination), loads, or load effects, and modelling/prediction techniques dictate the use of probabilistic approaches for life-cycle management. Structural reliability and risk-based methods constitute important performance indicators for structural safety in the presence of uncertainties, based on which key actions and decisions related to life-cycle aspects (e.g., maintenance, inspection, repair, service life extension) can be obtained. This section discusses the state-of-the-art research related to the life-cycle analysis of ships and offshore structures, including inspection, maintenance, service life extension, damage detection, and monitoring. Moderate progress has been made in the field. Risk-based analysis tools

are the most commonly used analysis method, whereas digital twin and machine learning applications are emerging as viable solutions to facilitate more effective life-cycle management.

Inspection planning is an important aspect of ship life-cycle management. Unlike standard periodic class surveys, optimal inspection planning seeks to reduce costs and minimise unnecessary downtime while maintaining structural safety. Machine learning techniques offer a promising approach for optimising inspection decisions. Cheng et al. (2022) proposed a reinforcement learning method to optimise the dynamic inspection policy of ship structures. Unlike fixed inspection policy, dynamic inspection policy allows inspections to be based on the actual state and can avoid unnecessary or insufficient inspections. Results indicated that dynamic inspections can effectively reduce the expected life-cycle costs of a vessel. Acquiring information from inspections can assist in future inspection planning (e.g., selecting the next inspection time) and life-cycle management by reducing the uncertainties in the prediction models (e.g., crack propagation or corrosion wastage models). Bayesian inference is another powerful mathematical tool for this purpose. Liu *et al.* (2021c) used a Bayesian inference technique to reduce the uncertainties related to crack propagation and refine the prediction of fatigue-induced structural deterioration. Kim *et al.* (2022a) also employed a Bayesian inference tool in an analysis of inspection data to update corrosion wastage model predictions. Other relevant studies have been published over the past decade, see ISSC (2022a).

In the context of material/structural degradation, recent work has focused on optimising corrosion addition. Gong et al. (2020) introduced a risk-based framework that allows decision-makers to determine the economically optimal corrosion addition and the benefits realisable through reducing expected life-cycle costs. This framework incorporates reliability analysis in ultimate limit state (ULS) assessments and considers the impact of periodic dry-docking maintenance on the life-cycle cost estimates of an oil tanker. The study found that the expected life-cycle cost of a hull girder with added corrosion allowance is significantly lower than that of a net scantling design.

A first-order reliability analysis (ultimate limit state) was carried out by Garbatov et al. (2023) on two lightweight hybrid bulk carrier designs containing aluminium honeycomb sandwich panels in the inner hull over their service lives. A two-stage corrosion model was used for the honeycomb structures, assuming a coating life of 5 years and a coating-break-down transition time of 6–7 years (as opposed to 4 years for steels). This was also combined with a cost-benefit analysis including factors such as loss of cargo, human life, and cost of CO_2 emission. However, only general corrosion was considered, whereas corrosion of aluminium alloys in marine environments is primarily pitting/localised.

Recent research has also examined the impact of corrosion on the operational life of traditional offshore platforms. Mohd et al. (2022) applied Melcher's two-stage empirical corrosion model to assess the global ultimate strength and reserve strength ratio (RSR) (the ratio of base shear ultimate strength versus its design strength with a 100-year return period) of a platform through push-over analysis, considering both average and severe corrosion levels. The PETRONAS guideline requires an RSR of 1.5 to be adopted for manned platforms and 1.32 for unmanned platforms. The study found that, with an RSR of 1.5, the platform could safely operate for up to 50 years under average corrosion

conditions, but only 35 years under severe corrosion. Furthermore, the authors concluded that the corrosion in the atmospheric zone did not affect the global strength of the structure (Othman et al., 2023). Corrosion in the immersion zone was found to be more critical than that in the splash zone for platform life extension. The corrosion model led to a 6-year extended life span for all the studied jacket offshore platforms. However, only uniform corrosion (thickness reduction) was considered in these studies and the sensitivity of the corrosion model to life span estimation was not assessed.

The offshore wind sector has widely adopted supervisory control, data acquisition, and condition monitoring systems during operations (Yeter *et al.*, 2022b). However, as the industry pushes to reduce costs further, there is a growing need for "smarter" life cycle management and life extension strategies. These strategies should not only draw on experience from conventional offshore platforms but also integrate "big data", AI-based predictive models, and intelligent decision-support tools. Yeter *et al.* (2022b) published a comprehensive review of AI-aided life extension studies of offshore wind structures. They discussed key challenges, including data acquisition, preprocessing (such as noise filtering algorithms), and risk/reliability-based machine learning approaches. The authors highlighted the importance of reassessing structural capacity for various failure mechanisms (linked to different levels of risks), such as the ultimate strength of corroded leg components, to inform the decision-making process. Additionally, they explored a cycle-by-cycle approach for structural integrity assessment to extend the life of wind turbine support structures (Yeter *et al.*, 2022a). Although this research primarily focused on the operational stage, the interconnected nature of design, manufacturing, life extension, and decommissioning stages suggests that AI-based approaches will see increasing applications across the offshore wind sector shortly.

The final key aspect of a life-cycle analysis is determining an optimal end-of-life strategy, i.e., service life extension or decommissioning. Service life extension of ship structures has become increasingly important due to sustainability goals and the significant costs associated with new ship construction (Liu *et al.*, 2020c). Risk-based analysis is a viable tool to assess the performance of hull structures beyond their intended design life and for planning necessary maintenance actions. Liu *et al.* (2021c) presented a risk-based cost-benefit analysis for extending ship service life by addressing hull structural failure. Two cost-benefit indicators, benefit-cost ratio and net present value, were used as financial performance indicators to guide optimal end-of-life decision-making. This framework provides a structured approach for determining optimal strategies across various oil tanker sizes.

4 Ships

Section 4 is focused on the ultimate strength of ship structures. Unlike fixed offshore structures, ships are inherently meant for transit operations. As the world becomes increasingly focused on addressing climate change and reducing emissions, ship operations need to become more environmentally sustainable. Naval architects can contribute to resolving the ongoing energy crisis by designing lightweight ship structural systems or developing tools that enable the design of such systems. These novel systems should facilitate increasing the amount of cargo transported per unit of energy spent. This must

be balanced with the need for ship structures to withstand imposed loads over their lifetimes with a sufficient margin of safety. Optimising the design and construction of ship structures can enable weight reductions and increased efficiency, which can ensure significant fuel savings and a corresponding reduction in emissions. However, the design of such lightweight structures is a compromise between efficiency and safety. In other words, lightweight efficient designs must not compromise the safety of structures, operators, or people at large. Therefore, we need to be more aware and knowledgeable of the ultimate limit states of ship structures, and phenomena that affect ultimate strength. With this aim, this section presents the most relevant findings from recent years.

4.1 Loads

This section provides an overview of the loads (or load effects) acting on ship structures and their effect on ship response. Broadly speaking, these loads include (i) static loads and (ii) low- and high-frequency dynamic loads caused by waves. Static loads are caused by the uneven distribution of weight and buoyancy, while dynamic loads result from various forces, such as wave-induced pressure on a hull's wetted surface, inertial force, sloshing, slamming, whipping, and green water on deck.

4.1.1 Non-linear Wave Load Effects

The assessment of the ultimate strength of hull girders is a central element in ship structural design. Ensuring the safety of the ship structure from an ultimate strength perspective necessitates designing hull structures that have a load-carrying capacity that surpasses applied loads. This underscores the importance of investigating the loads applied to hull girders, particularly focusing on the vertical wave bending moment, to assess the safety of the ship structure in terms of its ultimate strength.

The response of a ship structure to time-varying loads is inherently a dynamic event. However, it is convenient to analyse this response as a quasi-static problem. The frequency domain approach for determining design load in ship structural design has been extensively employed. However, this approach inevitably introduces approximation errors resulting from the linearisation of complex problems. For instance, the frequency domain-based analysis method assumes identical hogging and sagging wave bending moment magnitudes, while in reality, large waves acting on a container ship can produce a significantly larger sagging bending moment. To address these errors, attempts are being made to directly calculate irregular wave loads using computational fluid dynamics (CFD). Choi et al. (2023) proposed a method that applies high-order spectral (HOS) to model non-linear ocean waves, and rapidly generate the necessary irregular waves for structural analysis by interpolating the fluid domain information of the modelled non-linear ocean waves using 3rd and 4th order B-spline interpolation. The method is computationally more efficient than CFD-based wave generation using linear superposition and provides a more accurate non-linear description of waves.

Takami et al. (2023) introduced a method for predicting the extreme distribution of the vertical wave bending moment in ships considering non-linear wave fields that include freak waves by combining the higher order spectrum method (HOSM) and the first order reliability method (FORM). They scaled down a 6,600 TEU container ship

to create two hypothetical vessels with lengths of 100 m and 200 m, respectively, and estimated their extreme hogging vertical bending moments. They found that the shorter vessel was more sensitive to the effects of wave shape non-linearity. Therefore, traditional linear methods may underestimate the wave-induced vertical bending moment (VBM) because they exclude non-linear wave shape effects. The influence of wave non-linearity on ship motion and vertical wave bending moment was also investigated numerically by Houtani et al. (2023). The simulations involved varying the wave height and wave non-linearity order, specifically considering the first and fifth orders, for a wall-sided ship with the same dimensions (length, width, and depth) as a 6,600 TEU container ship with a large flare. They found that both the shape of the ship and the non-linearity of the wave shape can significantly affect the wave-induced VBM. These studies demonstrate the importance of non-linear wave shapes on wave-induced VBM, which becomes more pronounced in large waves. Moreover, the incorporation of these methods in the design for ultimate strength allows consideration of more realistic loading scenarios (dynamic and non-linear effects) and scenario-based modelling as advocated in the ISSC 2018 Ultimate Strength committee report (ISSC, 2018a), which should result in higher fidelity ultimate strength analysis.

4.1.2 Dynamic Load Effects

Dynamic load effects on ultimate strength have historically received limited attention, as noted in the ISSC 2018 Ultimate Strength committee report (ISSC, 2018a). However, recent research shows growing interest in this area. Xiong et al. (2023) developed an empirical formula to predict the dynamic ultimate strength of stiffened panels under longitudinal compressive impact loads, addressing the scarcity of studies on rapid dynamic loads in extreme wave conditions. Using FE analysis, they evaluated steel panels with varying yield strengths (315–340 MPa) and analysed parameters like impact duration, shape, and plate geometry. The findings indicate that impact duration significantly affects dynamic ultimate strength, with longer durations reducing strength, while factors like amplitude, impulse, and impact shape have minimal influence. The study emphasizes the need to further investigate in-plane impact loads.

Zhong and Wang (2021b) studied the dynamic ultimate strength of steel-stiffened panels under in-plane impact load and lateral pressure, focusing on rapid dynamic loads like explosions. Using non-linear FE analysis, they found lateral pressure minimally affects dynamic ultimate strength for short impacts but becomes significant for longer durations. Short-duration impacts exhibited higher dynamic ultimate strength, which was influenced by the model range. The strength was notably impacted by local plate deflection, showing an inverse correlation with impact load impulse. Additionally, increased lateral pressure led to a reduction in quasi-static ultimate strength.

Guo et al. (2024) examined the dynamic ultimate strengths and deformation behaviours of stiffened plates under various loading cases using non-linear FE analysis. The study confirmed that dynamic ultimate strength decreases with longer slamming load durations, with collapse modes transitioning from local buckling to edge collapse. Lateral loads significantly reduced strength after 20 ms of slamming duration, while transversal in-plane compressive loads further decreased strength due to global buckling.

Jagite et al. (2022) used FE analysis to investigate the ultimate strength of large containerships under dynamic loading scenario due to slamming induced whipping. Novelty of the work relates to realistic loading conditions and the way dynamic effects are calculated. Namely, dynamic effects are quantified by considering two scenarios: a wave scenario, and a wave-whipping scenario wherein high-frequency whipping-induced stresses are superimposed to the low-frequency wave-induced stresses. The dynamic collapse effect was calculated as the relative value between whipping and wave scenarios, and it quantifies the increase of structural capacity due to slamming-induced whipping. In considered case, the effect varied from 1.05% to 2.26%. This was considerably less than obtained with traditional approach 4.8% to 8.4%, which quantifies the effect as the ratio between the dynamic ultimate strength and the quasi-static one. The authors stress that the obtained results with new calculation method align well with long-established industry practice which considers the wave loads as quasi-static and disregards any dynamic effects associated with the wave loads.

Kong et al. (2021) investigated the ultimate strength and damage mechanisms of a steel deck under quasi-static and dynamic in-plane compression loading through experimental and numerical methods. A structural model was used for quasi-static testing, while simulations analysed the effects of load amplitude, frequency, initial stress, and deflection on strength and failure modes. Dynamic buckling modes differed from quasi-static ones, with buckling strength decreasing proportionally to pre-applied quasi-static loads. Certain load frequencies induced dynamic buckling even at amplitudes near static load capacity. Geometry, boundary conditions, and material properties influenced buckling, with dynamic loads causing more damage than static ones. The study emphasized further testing to understand post-buckling behaviour under in-plane impact loads.

Shi and Gao (2020) analysed two container ships (14,500 TEU and 19,000 TEU) that failed due to whipping loads to assess the impact of whipping on hull girder reliability. Using the first order reliability method (FORM), they identified significant variability in whipping moments, model tests, and calculations. It was also found that evaluation criteria for hull ultimate strength are not the same across all classification guidelines. Therefore, large container ships should have their minimum ultimate capacity increased to maintain a safe failure probability. The authors recommended that more case studies be carried out on other ships to improve their analysis.

4.1.3 Other Load Effects and Load Combinations

Empirical models, FE analysis, and machine learning based approaches have been employed to improve the accuracy of strength predictions under complex loading conditions. These approaches aim to enhance the safety and reliability of structures by addressing factors such as external pressure, cyclic loading, and temperature effects.

Seyffert et al. (2019) presented an interesting approach that employs the non-linear Design Loads Generator (NL-DLG) process to efficiently estimate the lifetime performance of stiffened panels under combined loading. The approach allows for a direct comparison between panel options and highlights critical panel parameters that are strongly related to design robustness. The approach was used to compare the failure probabilities of six different stiffened panel designs for a specific vessel in a long exposure to harsh ocean excitation. The comparison was especially interesting since some class society

had previously vetted all designs. It was demonstrated that the NL-DLG process yields similar statistical characteristics to those of brute-force Monte Carlo simulations, while reducing simulation time by a factor of 87,000.

Ma and Wang (2021) investigated the effect of lateral pressure on the collapse behaviour of stiffened plates under combined loading, developing an empirical formula verified through numerical analysis to provide a faster, reliable method for estimating ultimate strength. They found that lateral pressure influences initial deflection and pre-buckling strength, significantly reducing ultimate strength, especially for thinner plates. Longitudinal ultimate strength may increase for column slenderness above 0.7 with periodic symmetrical collapse modes, but lateral pressure impacts longitudinal and transverse strength differently. Thicker plates or those with larger stiffeners were less affected. The authors recommended refining the empirical formula by analysing parameters influencing ultimate strength and validating it with additional data.

Li and Chen (2023b) investigated the effects of extreme cyclic loading and lateral pressure on the collapse behaviour and ultimate strength of continuously stiffened panels using non-linear FE analysis. The study focused on parameters such as slenderness, stiffener geometry, and load characteristics under combined loading scenarios, addressing gaps in prior monotonic loading studies. Findings showed that cyclic loading can induce buckling, especially with smaller stiffeners, and strength reductions increase with panel thickness, stiffener size, and cycle numbers. Weak stiffeners combined with thick panels were identified as particularly detrimental. Under combined loads, lateral pressure can prevent overall buckling, but this effect decreases with an infinite number of stiffeners and is more significant for slender panels. The authors recommended further study of complex loading parameters to refine collapse and strength predictions for stiffened panels.

Hu-Wei and Ping (2018) proposed a simplified approach to represent the stress-strain relationship of plates under monotonic uniaxial compression using the envelope of the stress-strain curve from cyclic uniaxial compression. The approach was validated against previous tests and analyses. Tests were conducted on six square-column models to simulate the collapse behaviour of hull plates under cyclic compression, and the results were compared with the predictions from the simple approach. The results from simple approach showed good agreement with experimental results (see Fig. 12). The study concluded that the method's accuracy could be enhanced by incorporating residual stress and uneven plastic deformation effects.

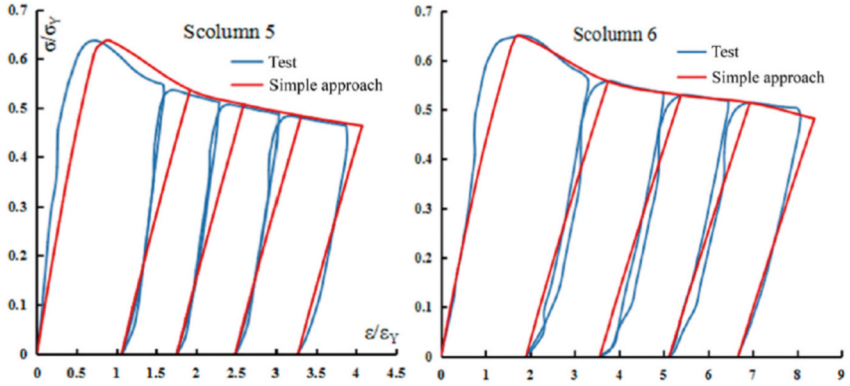

Fig. 12. Curve comparison between the simple approach and experiment (Hu-Wei and Ping, 2018).

Park and Kim (2022) utilized an ANN to predict the ultimate strength of a GTT LNG cargo containment system under sloshing impact, reducing reliance on complex numerical analyses during design. The ANN, with two hidden layers and 64 neurons per layer, was trained on 24191 FE analyses, achieving high accuracy. The study also evaluated the influence of including more realistic onboard boundary conditions, sloshing rise time, load area, and temperature. The onboard conditions significantly affected ultimate buckling strength compared to rigid boundaries. A key limitation was that the ANN is applicable only within the scope of the training data.

4.2 Structural Elements

Stiffened panels are the fundamental building block and load-carrying component of ship structures. This section reviews recent developments in the ultimate strength analysis of stiffened panels, considering aspects such as material properties, geometric imperfections, residual stresses, and load combinations. With improved access to computational resources, these models have become increasingly detailed, which can influence the final collapse mode of stiffened panels. Additionally, there is a clear trend toward developing computationally efficient, machine-learning-based methods to incorporate all these complex details.

4.2.1 Stiffened Panels

Various influences on the ultimate strength of the stiffened panel were investigated, such as initial imperfections of the actual panel, stiffener misalignment (Chen et al., 2023), small and large openings (Liu *et al.*, 2021b), residual stresses (Guo et al., 2021), welding techniques (Mun and Ri, 2022), and corrosion (Zhu et al., 2021; Mokhtari et al., 2023).

Different buckling failure modes in stiffened panels lead to variations in ultimate strength. To address this, Zhang *et al.* (2023a) performed a series of non-linear finite element analyses with a stiffened panel benchmark model, including appropriate initial imperfections, boundary conditions, and mesh size. Compared with earlier closed-form

analytical expressions for ultimate strength (Paik and Thayamballi, 1997; Zhang and Khan, 2009), which considered column slenderness λ, plate slenderness β, web height to thickness ratio h_w/t_w, their evaluation additionally accounts stiffener tripping slenderness λ_e parameter. Thereby, the fitting equation accounts for beam-column buckling, local plate buckling, stiffener web buckling, and stiffener tripping. Comparison with earlier closed-form expressions and FE results demonstrates the increased accuracy of the fitting expression especially in the range where stiffener failure is expected (see Fig. 13).

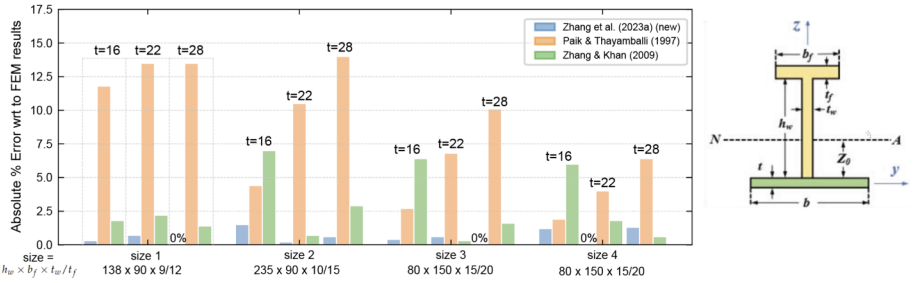

Fig. 13. Table 8 from Zhang *et al.* (2023a) converted to a figure showing the error of different fitting formulas with respect to FE analysis results.

Another fitting formula for the ultimate strength of stiffened panels was derived by Hanif et al. (2023). However, compared to Zhang *et al.* (2023a), their fitting equation focused on the imperfection mode, with separate parameters for column, torsional, and local imperfections. A total of 750 stiffened panel configurations were investigated using a non-linear FE analysis. Regression analyses performed across studied cases showed that plate slenderness and local imperfection modes had the largest influence on strength. Furthermore, their sensitivity analysis revealed that, among the imperfection modes considered, the local imperfection mode had the strongest influence on the normalized strength, confirming the results of Li *et al.* (2022c). The derived formula demonstrated good accuracy when compared with the FE analysis results, with a mean absolute percentage error (MAPE) of 1.9%. The model was also compared against six other fitting equations, with the best showing a 6.89% MAPE. This confirms its validity as a reference for evaluating the ultimate strength value in scenarios where an initial geometric imperfection is present.

Li *et al.* (2022c) provide recommendations for selecting an imperfection model for buckling analysis of ship-type stiffened plated structures based on their comparative study regarding the effects of different imperfection modelling approaches on the ultimate compressive strength. Models were categorized into deterministic and probabilistic approaches. Deterministic models included hungry-horse (HH), Admiralty Research Establishment (ARE), and critical buckling (CM) mode, which correspond better to as-built panels rather than in-service panels. In contrast, the probabilistic approach treats initial imperfections as a random field generated from specified statistical parameters and is thus believed to be applicable for both as-built and in-service panels. The authors conclude that it is difficult to conclusively suggest the best imperfection model for collapse analysis. Different models have different advantages, but recommendation given by the

authors take into account the convergence of numerical simulations and the effect on accuracy. Considering the randomness of imperfections authors advocate the use of probabilistic imperfection model but concede that it is more complicated than deterministic approaches.

One approach to account for mechanical damage to a stiffened panel is to consider the damaged geometry as a form or type of imperfection. Chujutalli et al. (2020) investigated the ultimate strength reduction of stiffened panels under compression due to indentation damage. The ultimate strength, failure mode, and deformation field were measured experimentally for selected scaled stiffened panels, which were used to validate the simulation model. The validated FE model was subsequently used for parametric study to gauge the effects of indentation dent depth, indenter diameter, indentation location and stiffener slenderness. It was found that depending on the stiffener type used (flat bar or T-stiffener), the indentation parameters have a different effect on the response.

Xu *et al.* (2021b) proposed a partial similarity method to account for buckling and distortion when assessing the ultimate strength of small-scale stiffened panel models. Complete similarity methods are unsuitable for use on slender/thin elements, therefore, highlighting the need for a more accurate similarity method that can predict the ultimate strength of a full-scale ship from a smaller model, as the proportions of members on a small-scale model are not necessarily reflective of those on a full-scale model. This study was also driven by a need to consider plate buckling on the scaled model. AH32 steel coupons were tested and used in the verification of the FE model. It was concluded that for partial similarity, plate and column slenderness govern beam-column buckling, while plate torsional slenderness governs tripping buckling. Partial similarity methods can lead to dimensional distortion across different buckling modes, potentially altering the collapse mode and load-carrying capacity of stiffened panels. The collapse mode and governing parameters should be carefully considered during model scaling to minimise dimensional distortion. Complete geometric similarity may be applied to small-scale models for validation. Based on results for collapse mode pre- and post-buckling average stresses, partial similarity can be used to guide the design of test models if key parameters specific to the collapse mode are considered.

It is well established that distortions in a structure's geometry resulting from fabrication and manufacturing processes significantly influence the ultimate strength and structural stability of the system. However, existing methods for quantifying these distortions heavily rely on assumptions that limit their practicality. With the growing use of full-field 3D measurement and inspection techniques such as light detection and ranging (LiDAR) and photogrammetry, it is now possible to inspect and quantify distortions during inspection activities or even continuously during operations. The capability, use, and availability of such data will only increase over time. This trend has sparked interest in the use of quantitative 3D inspection data to create digital twins of structures for the production of data that can be used to update FE models so that they accurately reflect the actual state of the structure. As noted in the ISSC 2018 Ultimate Strength committee report (ISSC, 2018a), these data are also essential for reliability analysis, this data is crucial for reliability analysis, though the problem was previously unaddressed in the literature at that time. By integrating inspection data with FE models, strength reductions can be assessed, enabling more accurate insights into current serviceability

and remaining life than an idealised model could provide. For instance, Graves et al. (2023) presented a process for incorporating point cloud measurements of distortions into FE models through a Gaussian process interpolation that inherently filled in gaps in data, eliminated outliers, and provided quantitative measures of uncertainty. They demonstrated the utility of this approach for the provision of strength estimates that were comparable to established methods and its wider applicability to a range of cases where the quantification of a performance envelope for risk analysis would be useful.

As large amounts of data become available and data analysis techniques evolve, data-driven approaches are expanding to the field of structural engineering. One such data-driven approach was implemented by Li *et al.* (2022b) to estimate the ultimate strength reduction factor of stiffened panels caused by welding residual stress. Various machine learning (ML) methods were compared based on their ability to predict this reduction factor. The data consisted of 136 simulated scenarios of simply-supported two-bay and two-span stiffened panel models under uniaxial compression. The simulation model had been previously introduced by the same author (Li *et al.*, 2021a). The authors reported that the best ML method had a 99% prediction accuracy for panels within the limits of the dataset and 96% accuracy for panels with configurations which deviated from those used for learning by up to 15%. The approach demonstrates the potential of data-driven approaches in the realm of ship structural design, which often requires expensive non-linear numerical simulations, but as shown here, can be replaced by a computationally inexpensive data-driven method.

Hosseinpour et al. (2022) used FE models to study the behaviour of steel plates with a central circular hole subjected to compressive axial loading. A total of 270 holed steel plate configurations were modelled and analysed using the ABAQUS software. The effects of four main variables including plate length, hole diameter, plate thickness, and yield stress were discussed. Using the database provided by the FE analyses, the ANN method was used to develop a predictive model to estimate the ultimate strength of steel plates with a circular hole in the centre. The accuracy of the ANN-based formula was compared and confirmed with formulations presented in previous studies. Lima et al. (2023) also introduced a method to replace computationally expensive structural reliability models with a surrogate model based on a bi-fidelity Kriging model. The results suggest that the proposed bi-fidelity framework, which used the correlation between high-fidelity (HF) and low-fidelity (LF) non-linear FE analysis models (as shown in Fig. 14), can provide an accurate failure probability estimation with less computational cost compared to solely using HF non-linear FE analysis.

Most numerical studies exploring the ultimate strength of ship structures utilise a large number of calculations to explore the parameter space. Papanikolaou and Anyfantis (2022) employed a design of experiments (DoE) and response surface methodology (RSM) combined with numerical non-linear FE analysis to develop a surrogate model for the ultimate strength of stiffened panels. It was demonstrated that the buckling response with respect to the nondimensional slenderness ratio could be fitted with nine runs per stiffener geometry. The T-bar stiffener surrogate model was found to be sufficiently accurate for ultimate stress prediction in the practical design space, while the surrogate models for angle bars and flat bars demonstrated a difference between 10 and 30% from common structural rules (CSR).

The equivalent single-layer (ESL) homogenisation method was presented by Putranto et al. (2021). ESL transforms a 3D stiffened panel into a plate with equivalent stiffness with comparable mechanical behaviour. ESL stiffness was obtained through unit-cell analyses based on the stiffened panel where periodicity was imposed with boundary conditions based on the first-order shear deformation theory (FSDT). Stiffnesses were determined from the first derivative of the membrane force and bending moment obtained through numerical simulations. The effect of the initial imperfection shape was included in the analysis to account for local and global buckling behaviour. ESL with non-linear stiffness was implemented in the ABAQUS UGENS subroutine, allowing incremental evaluation of stiffness. The key aspect of this analysis was the use of non-linear ESL stiffness, as linear analysis was unable to detect the point at which the grillage reached its ultimate strength capacity. The method was computationally efficient and allowed for considerable reduction in modelling effort by smearing of stiffeners. The method was further validated by authors in Putranto *et al.* (2022a) for combined compression and in-plane shear.

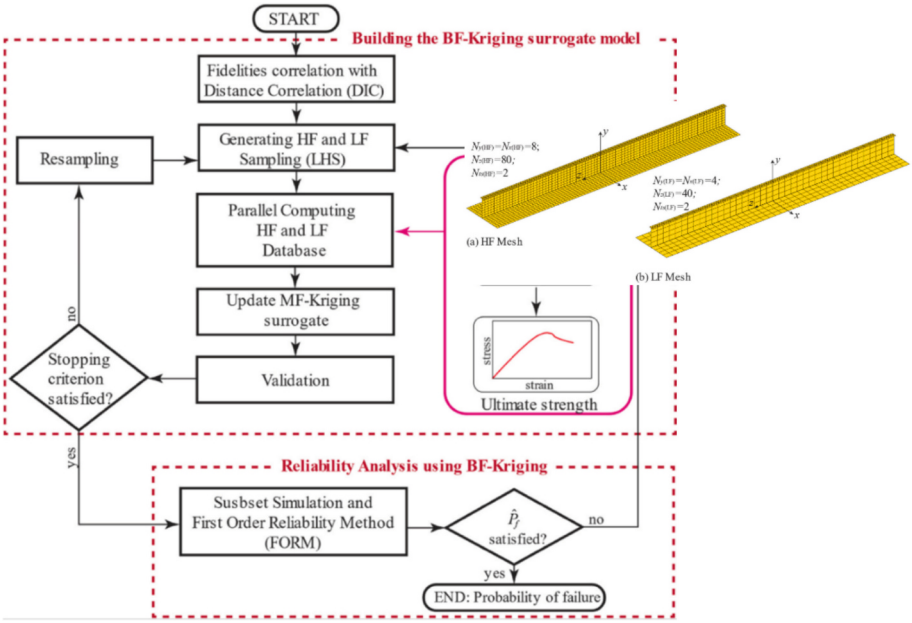

Fig. 14. Flowchart of the bi-fidelity Kriging framework.

Kõrgesaar et al. (2023) demonstrated the applicability of the ESL approach for the ultimate strength assessment of stiffened panels under various loading combinations of uniaxial (longitudinal and transverse), biaxial and shear. Using the ESL approach, the 3D stiffened panel was replaced with its ESL representation, and the tertiary stiffening elements were excluded from the FE model, as shown in Fig. 15. This approach

offers significant time savings in modelling the final structure. ESL analyses were conducted using both the ABAQUS implicit and explicit subroutines to compare numerical efficiency and accuracy between the two schemes.

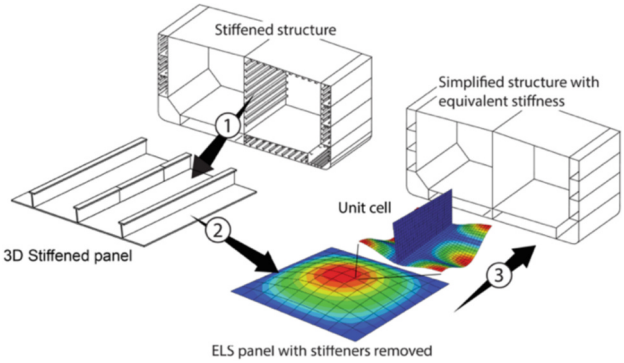

Fig. 15. FE model simplification using ESL approach (Kõrgesaar et al., 2023).

Long-span stiffened panels, which often utilise girders with deep webs and multi-web openings, are commonly employed in open spaces without stanchions to create large open spaces, such as theatres and lounges in large passenger ships. These panels are often supported with in-tension pillars to decrease deck deflection and out-of-plane deformations, but their effect on the compressive strength of supported panels is unknown. Liu *et al.* (2021b) presented experimental and FE analyses of the ultimate compressive strength of two long-span stiffened panels subjected to combined uniaxial and lateral loads. The comparison with experimental results demonstrated that the in-tension pillars only marginally increased the ultimate compressive strength of the stiffened panels. The experimental results aligned with the numerical simulations, and this study provides insights into the buckling and ultimate behaviour of long-span stiffened panels, including their progressive collapse processes.

Extruded aluminium structures are increasingly being used for high-speed craft. Such structures are often stiffened using floating girders to achieve lightweight and affordable ship hulls. Sun *et al.* (2021a) conducted uniaxial compression experiments with simply supported boundary conditions to investigate the differences in ultimate strength and collapse behaviour between a novel aluminium stiffened panel with a floating girder (SPT) and a fixed girder (SPX) (see Fig. 16). These experiments showed that a novel aluminium SPT had a higher ultimate strength than an SPX. The former experienced web tripping, while the floating girder panel exhibited girder buckling.

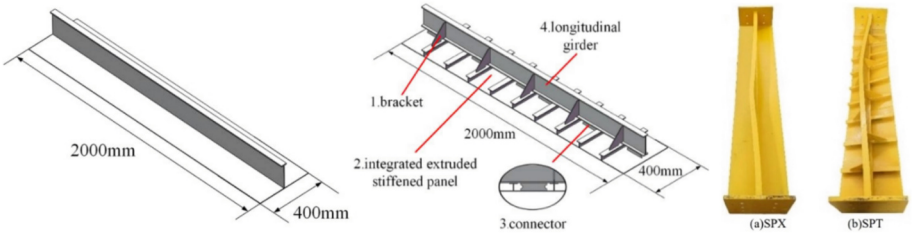

Fig. 16. Appearance of stiffened panel with fixed girder (SPX) and floating girder (SPT), and comparison of collapse deformation.

4.2.2 Curved Stiffened Panels

Unstiffened and stiffened cylindrically curved plates are often used in ship structures, such as in cambered decks, side shells at the fore and aft sections, and the circular bilge area. Park et al. (2020) conducted numerical analyses to investigate the ultimate collapse response of stiffened curved plates commonly used in ship structures. Various stiffener geometries shown in Fig. 17 were evaluated under axial compressive loading, considering quasi-static and cyclic loads, with initial imperfections and geometric non-linearity included. Results showed that increased stiffener height and plate curvature improved the elastic and elastic-plastic buckling strengths. Furthermore, elastic buckling exhibited complex secondary behaviour, absent in elastic-plastic buckling due to plasticity effects. The study emphasized designing for elastic-plastic buckling to account for the geometric instability and material non-linearity of curved plates compared to flat plates.

Alinia et al. (2019) studied the shear buckling and post-buckling behaviour of thin curved panels under lateral pressure and increasing in-plane shear forces, considering lateral pressure magnitude, the radius of curvature, and the panel aspect ratio. Theoretical buckling load predictions were compared with experimental results. The results showed that inward pressure eliminated the snap-through phenomenon and softening stage in shallow panels but had minimal effect in on moderately curved panels under low pressures. Increased inward pressures significantly reduced the ultimate shear capacity of highly curved panels, leading to unstable buckling and suppressed hardening stages due to released strain energy.

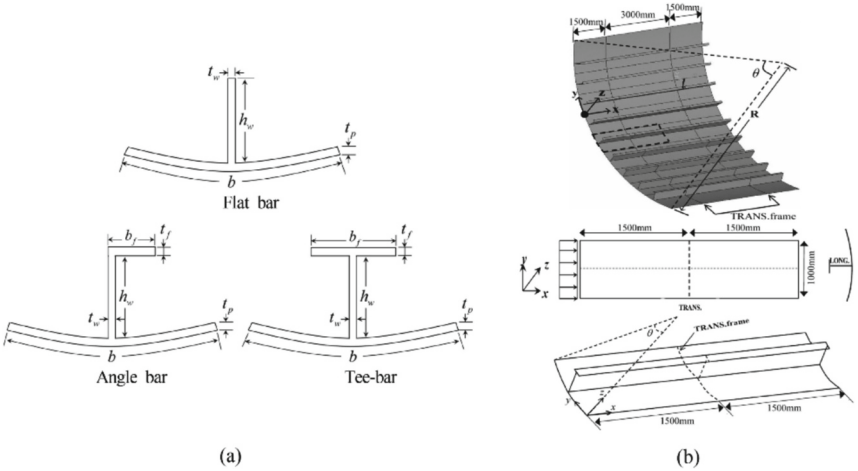

Fig. 17. (a) Typical shapes of curved plate and stiffener, and (b) double span/double bay model of a stiffened curved plate (Park et al., 2020).

Kim et al. (2021) developed empirical design equations to predict the ultimate strength of curved plates under longitudinal compressive loads. Their study included experiments on buckling collapse, considering factors like flank angle, slenderness ratio, and aspect ratio. Detailed finite element analyses were conducted to investigate buckling and collapse behaviour of curved plates under elastic-plastic large deflection conditions. The proposed approach allows for estimating collapse using these geometric characteristics.

Cho et al. (2022) employed a deep learning model to predict the ultimate strength of curved plates under compression. While the fully connected network provided satisfactory estimations, discrepancies in mean squared error results between training and validation sets emerged post the 500th epoch. Exploring alternative regularization techniques or learning rate schedulers could have mitigated this issue. Furthermore, due to the non-linear input-output vector relationship in one-dimensional space, the use of a "tanh" activation function might enhance performance. Despite these challenges, the deep learning-based predictions for ultimate strength showed notably superior accuracy compared to empirical formulae.

Shiomitsu et al. (2023) found that critical yielding locations impacted the ultimate strength of curved plates under axial compression. Yielding occurred along the longitudinal edges when dominated by membrane action, while it manifested at locations of maximum curvature when influenced by combined bending and membrane actions. The study proposed a straightforward approach for predicting the ultimate strength of simply supported curved plates under axial compression, which was verified through nonlinear finite element analysis outcomes for various flank angles.

4.2.3 Composite Elements

This section explores various methods for analysing and predicting the behaviour of composite materials under compressive loading, with a particular focus on delamination

and failure mechanisms. Techniques such as FE analysis, neural networks (NN), and progressive damage models are typically utilised to assess the strength and structural integrity of laminated strips. Experimental studies complement these models by examining the effects of material properties, temperature, and moisture on the mechanical behaviour of composites.

Alizadeh et al. (2022) conducted FE analyses to evaluate the residual ultimate strength of composite strips with different layup configurations and a single through-the-width delamination under compressive loading. Using solid 8-noded layered elements delamination growth was modelled via the strain energy release rate calculated with the virtual crack closing technique, offering an efficient method to predict delamination regions. Two layups, $[0/90/90/0]_4$ and $[90/0/0/90]_4$ were analysed, with delamination introduced between the 5th and 6th plies. The first layup exhibited stable load stages, while the second showed a sudden capacity drop. This approach provides a straightforward assessment of delamination effects on compressive strength of laminated strips.

Liu *et al.* (2022b) built neural networks (NN) to examine the effect of crack characteristics – length, orientation, and width – on the compressive residual strength of single hat-stiffened composite panels. A network with five hidden layers, each containing 5 to 30 neurons, achieved optimal accuracy without overfitting. The model was trained on 90% of 3,830 FE analyses, which utilized the Hashin criterion for in-plane failure and a cohesive zone model for stiffener-panel debonding. This NN effectively predicted the influence of crack parameters on residual buckling strength.

Wang *et al.* (2022c) developed a progressive damage model to evaluate hygrothermal effects on strength and stiffness, based on tensile and compressive tests of open-holed specimens under dry and hygrothermal conditions. Failure models incorporating Hashin and maximum stress criterion were updated with the fitted relationships. While numerical predictions aligned well with experimental ultimate loads, discrepancies occurred in displacement or strain levels at failure. Results showed a 35–40% reduction in ultimate strength for both tension and compression under 70 °C with equilibrium moisture absorption. The compressive failure mode remained unchanged, but tensile failure shifted from an X-shape to an I-shape. This study emphasizes accounting for hygrothermal effects in composite material evaluations for marine applications.

Xu *et al.* (2022a) conducted experimental and numerical studies to investigate the failure behaviour of GFRP L-joints with a PVC core. They used a material model based on Shokrieh et al. (1996), a 3D adaptation of the Hashin criterion, to model fibre and matrix failure, shear failure, and delamination. Cohesive zone elements were employed to simulate core-laminate debonding, with a Maxwell element added to capture loading rate effects from the viscoelastic behaviour of the adhesive. FE analyses, conducted in ABAQUS with 8-noded linear brick elements, were compared to tensile ultimate strength tests. Incorporating viscoelastic adhesive behaviour provided better agreement with experimental results, especially in capturing post-linear behaviour and failure modes.

4.2.4 Complex Loading

Li and Chen (2023a) proposed empirical formulae for assessing the ultimate strength of continuous hull plates under combined biaxial compression and lateral pressure. Based on 4,800 numerical analyses using non-linear FE methods, the formulas treat longitudinal and transverse strength separately, enhancing applicability and accuracy. Anyfantis (2020) evaluated the ultimate strength of stiffened panels under combined uniaxial thrust and bending moments. Using design of experiments and non-linear FE analyses, the study found that non-uniform thrust significantly impacts ultimate strength of stiffened panels.

Woloszyk *et al.* (2021b) analysed the effect of boundary conditions on stiffened plates under compressive loads. The study, comparing FE analyses with experimental tests, showed similar ultimate strength and post-collapse shapes across different boundary conditions, though discrepancies were noted for fully clamped setups. Barsotti and Gaiotti (2024) studied residual displacements accumulation in HSLA steel stiffened panel under cyclic loading. They found a decrease in ultimate strength under alternating tension-compression loads compared to compression-only loading, with material hardening law significantly influencing results under alternating loading.

4.2.5 Empirical Formulae

This section explores methods for predicting the ultimate compressive strength of steel-stiffened panels using physical testing and empirical formulae. New empirical models are being developed to improve structural design and safety predictions under various loading conditions.

Useful empirical formulae have historically been developed by fitting curves to data from relevant testing databases. An example of this is the Paik-Thayamballi (Paik and Thayamballi, 1997) formula which provides a closed-form function of plate and column slenderness ratios that was developed by fitting to available data. Since 1997, high-precision data-acquisition equipment has been used to gain insights from large-scale physical models built from modern steel types (e.g., AH32) using modern manufacturing technologies (e.g., flux-cored arc welding technique). It is essential to assess the compatibility of these advanced testing data with established empirical formulae. In a study conducted by Lee *et al.* (2023b), benchmark studies were conducted to evaluate this compatibility, focusing specifically on the Paik-Thayamballi formula. This study offers valuable insights into the alignment between the advanced testing data and the established empirical formulae.

Li and Chen (2023a) focused on the development of empirical formulae for hull structural design and safety estimation. They verified and adopted an equivalent sequential loading method for biaxial compression to decouple the conventional implicit strength relationship of plates expressed by the elliptic function. A total of 2,737 and 1,944 scenarios, involving different combinations of slenderness ratio, aspect ratio, and applied loads, were selected for non-linear FE analysis to assess longitudinal and transverse ultimate strength, respectively. Based on their numerical findings, the authors proposed two empirical formulas with the same general explicit form using the response surface method. These formulas are versatile, accommodating various load scenarios, including

combined biaxial compression, lateral pressure, and other load combinations. Statistical analysis showed that the equations aligned closely with ABAQUS simulation results (R^2 = 0.993 and 0.996), validating their effectiveness as a practical approach for ultimate strength assessment in design.

Kim *et al.* (2022b) proposed a simplified empirical formulation to predict the ultimate strength of initially deflected plates subjected to longitudinal compression. The applicability and accuracy of the empirical formulation were verified through comparison with a non-linear FE analysis. A total of 700 plate scenarios with initial deflections, modelled based on assumed buckling mode shapes, were used as input data. A generalised empirical formula was developed from the input data to simplify the plate design process, yielding a reliable closed-form expression that aged well with results from the non-linear FE analysis ($R^2 = 0.98$ to 0.99). Additionally, Kim *et al.* (2022c) proposed an empirical formula to predict the ultimate strength of initially deflected plates subjected to combined longitudinal compression and lateral pressure. This formulation was validated using the ALPS/ULSAP method, analysing a total of 5,600 plate scenarios that included variations in geometry, material properties, and applied loads. These examples, along with a detailed user guide, provide valuable resources for structural analysis.

4.3 Structural Systems

In this section, hull girder, intact and damaged residual strength, superstructure inclusion, and their effects on the ultimate strength of ships are discussed by reviewing recent advances in the structural systems of ships. Emphasis is placed on numerical investigations using FE simulations and combined loading effects.

4.3.1 Intact Hull Girder

Combined loading effects have become an increasingly important topic in ULS assessment because of the M/V MOL Comfort and M/V MSC Napoli accidents. Therefore, this sub-section explores various methods, including FE analysis, incremental-iterative techniques, and empirical models, to assess the impact of combined loads, initial imperfections, residual stresses, and corrosion on the ultimate strength of hull girders. The findings emphasise the need for advanced models and surrogate techniques to improve the accuracy and efficiency of predicting the structural behaviour of ships under complex loading conditions while highlighting areas for further research, such as fatigue in sandwich decks.

The combined effect of hogging and bottom local loads (double-bottom effect) on the hull girder's ultimate strength prediction and annual failure probability in container ships was investigated in Georgiadis *et al.* (2023b). The estimate of uncertainty based on predictions from the conventional Smith model was decreased by including a model correction factor that combined engineering judgment and FE analysis data, which included the double-bottom bending effect. A formal method based on Bayesian analysis was developed to explicitly account for the uncertainties in FE analysis results. The findings show that a significant increase in the failure probability of container ships was due to the double-bottom effect in hogging conditions.

Tatsumi and Fujikubo (2020) evaluated the ultimate hull girder strength of container ships subjected to combined hogging moment and bottom local loads using FE analysis. They concluded that there was a significant reduction in hull girder strength due to the influence of bottom local loads. These results were used in a companion study by Tatsumi et al. (2020) to develop a simplified method for the analysis of the progressive collapse of container ships under these combined loading conditions. The authors proposed an extension to the conventional Smith method, to account for the effects of bottom local loads. The extended Smith method was validated through a series of FE analysis results showing good agreement between the two approaches.

Lindemann et al. (2022) investigated the ultimate strength of a double-hull VLCC using non-linear FE analysis under pure vertical, horizontal, and biaxial bending, considering both initial imperfections and residual stresses due to welding. They concluded that welding residual stresses had a negligible effect on the progressive collapse of the hull girder. In a subsequent study, Lindemann et al. (2023) examined the impact of various methods and model parameters on the ultimate strength of ships in bending, comparing results from a non-linear FE analysis (frame space model), application of the Smith method, and a deep neural network (DNN) model trained using results from the application of the Smith method. Consistent with their earlier findings, they concluded that initial deflections have a greater impact than welding residual stresses. All methods showed good agreement in terms of moment-curvature and neutral axis shift for an intact hull girder; however, the DNN tended to overestimate the residual hull girder strength for scenarios that included damage. It is the opinion of the committee that while the application of surrogate models, such as DNN, is certainly attractive from the perspective of computational efficiency, the assumptions and limitations of these methods should be well communicated, and training data should be free of any bias or modelling errors. Furthermore, surrogate models inherit the limitations of the models used in training, raising the question of which base model (a simplified Smith method or more detailed FE analysis results) should be used as a standard. Both have their advantages, which need careful consensus within the community to ensure the advancement of the field.

Lindemann et al. (2024) also investigated the applicability of the ISUM method to determine the ultimate strength of ships under bending. They found that ISUM predicted slightly higher final bending moments than the Smith method. Consistent with their previous findings, they noted that welding residual stresses had a negligible effect on ultimate strength in horizontal bending. In a parallel study, Lindemann and Kaeding (2024) further explored the applicability of ISUM for performing progressive collapse analyses of welded box girders in bending. They discussed the versions of ISUM and proposed a combined ISUM plate/beam-column element to model the progressive collapse behaviour of welded box girders in four-point bending. The results were compared to experimental data, with additional comparisons made using non-linear finite element analyses.

Faqih et al. (2023) evaluated the ultimate strength of the hull girder of a bulk carrier exposed to various corrosion damage rates. Two corrosion conditions, standard and severe, were considered, and the effect of corrosion was modelled as thickness reductions over various service times (0, 10, 15, and 20 years). Ultimate strength was assessed using incremental-iterative methods based on IACS-CSR, both with and without accounting

for the inclination of stiffened panels relative to thrust load (referred to as non-uniform uniaxial thrust). The findings from the study suggest that considering non-uniform uniaxial thrust reduces the ultimate bending moment, and severe corrosion has a pronounced negative impact on the ULS of the structure.

Xu *et al.* (2022c) analysed the collapse severity of a steel hull girder under extreme loading, along with and its influencing parameters. Due to the limitations of experimental setups in replicating the extreme wave loads encountered at sea, this study aimed to assess the magnitude of collapse events and post-ultimate strength behaviour through analytical methods. Experiments typically cannot produce sufficiently large loads to induce collapse or reliably elicit dynamic responses, and post-ultimate strength behaviour is challenging to observe in tank experiments. An analytical approach was proposed to predict the collapse severity of a box girder under extreme loading across all unloading phases to address these gaps. The study found that collapse severity is reduced when there is a gradual capacity drop in bending moment-curvature, whereas a rapid drop in capacity increases the severity of collapse. While collapse modes and behaviours have been explored in other studies, specific focus on collapse severity under extreme loading remains limited.

Recent studies of the ultimate strength of hull girders with sandwich decks have shown promising results. In a comparative study, Zhong and Wang (2022) numerically analysed a hull girder with an upper laser-welded web-core sandwich under various loading conditions, including vertical bending, horizontal bending, torsion, and combined loads. The results indicated that hull girders with sandwich decks offer substantial advantages in ultimate strength over traditional hull girders. The stiffness of the hull girder under sagging was improved by using the laser-welded web-core sandwich deck. The sagging ultimate strength of the hull girder was increased by 15%, and the horizontal bending ultimate strength was increased by 6.2%. Interestingly, the finite laser weld rotation stiffness was found to have no significant effect on the ultimate strength of the hull girder with the upper sandwich deck, which suggests that the welding technique used for the sandwich deck does not compromise the overall strength of the hull girder. This conflicts with earlier findings by Jelovica et al. (2012) who observed that laser welds affect buckling sandwich plates. It is possible that the global analysis conducted by Zhong and Wang (2022) may have smoothed out local effects from the laser welds, warranting further investigation. The study also established high-accuracy ultimate strength interaction relationships for hull girders under combined two- or three-moment loads, providing a valuable predictive tool for practical applications.

The failure modes of the hull girder with the upper sandwich deck were also investigated. Under sagging conditions, failure occurred through global buckling and local buckling of the sandwich deck. Horizontal bending led to buckling of the outer side plates as well as the deck and bottom plates on the compression side. Under torsion, shear buckling of the outer side plates and the bottom plates was more pronounced compared to the prototype hull girder. Overall, this study highlights the potential utility of laser-welded web-core sandwich decks for the improvement of the ultimate strength of hull girders. However, future investigations should clarify the applicability and limitations of sandwich panels from other limit state perspectives (e.g., fatigue).

4.3.2 Residual Strength of Damaged Hull Structures

This sub-section focuses on advances in the assessment of the residual strength of damaged ships, particularly using methods, such as the Smith method and non-linear FE analysis. Studies show that asymmetrical bending, damage from collisions or groundings, and corrosion significantly impact the residual strength of ships, with variations between different vessel types like bulk carriers and oil tankers. Recent work includes the development of rapid assessment tools and empirical formulae for estimating strength loss after damage, providing critical insights for emergency response and structural optimisation.

Residual strength assessment has progressed significantly over the past decade. Cerik and Choung (2020) investigated the hull girder strength of intact and damaged ships using the incremental-iterative method developed by Smith for progressive collapse analysis. The authors extended the Smith method to address the asymmetrical bending of beams with arbitrary cross-sections by determining the translation and rotation of the instantaneous neutral axis at each curvature increment. They conducted a series of analyses on a double-hull VLCC and a bulk carrier, considering various loading plane angles and damage conditions. These analyses confirmed the earlier findings by Fujikubo et al. (2012), which indicated that the rotation of the neutral axis had minimal impact on the strength of oil tankers but significantly affected bulk carriers, where it can lead to a faster loss of strength after reaching the collapse load.

Kuznecovs et al. (2020) compared the ultimate and residual strength of a vessel using non-linear FE analysis and the Smith method proposed by Fujikubo et al. (2012). Their case study examined both an intact hull and a hull damaged by collision, under two conditions: newly built (non-corroded) and aged due to corrosion. The calculation of a residual strength index showed a greater reduction in strength in the FE analysis compared to the Smith method. The difference in residual strength index was more pronounced in the damaged and corroded cases, as the Smith method simplified the effects of damage and corrosion.

Li and Kim (2022) evaluated the residual ultimate strength of grounded ships using numerical and Smith-based methods. A residual strength versus damage index (R-D) diagram was developed, which accounts for varying extents of damage across various types of double-hull oil tankers. This R-D diagram serves as a valuable tool for quickly assessing the residual ultimate strength in emergency response situations.

Kuznecovs et al. (2021; 2022) introduced a methodology called SHARC for simulating and analysing a ship's damage stability and ULS conditions following a collision. SHARC integrates three methods: advanced non-linear finite element simulations that simulate the collision scenario, a dynamic damage stability simulation tool called SIMCAP, and a modified Smith method for the ULS analysis of a collision-damaged ship structure. They demonstrated the capabilities of the SHARC analysis approach by applying the methodology to a case of an intact and a damaged oil tanker under both non-corroded and corroded structural conditions across various sea states. Corroded structures resulted in larger damage opening and penetration depth of the striking bow, but the damage was limited to the same internal compartments. Consequently, this resulted in similar floodwater volumes and distributions, with the corroded tanker reaching the steady state faster due to the larger damage opening area.

Komoriyama et al. (2024) investigated the collapse behaviour and ultimate longitudinal bending strength of damaged box girders in upright and inclined conditions through experimental and numerical analyses. These experiments involved applying four-point bending loads to box girders with elongated holes. The authors concluded that the Smith method can estimate the ultimate strength of damaged box girders similarly to the FE model. They suggested further research to investigate different hole sizes, shapes, and locations, as well as real ship structures.

Understanding the remaining/residual ultimate strength of a ship post-collision or grounding is key for deciding on appropriate remedial actions. However, such studies have been relatively scarce in the literature. Do et al. (2024) conducted a comprehensive numerical analysis of the post-collision ultimate strength of a handy-size container ship mid-section. The non-linear FE method using the Hosford-Coulomb crack model was first validated against a previously published box girder impact and bending test, with up to 9% difference in the residual ultimate strength between the simulation and test. This was followed by a parametric study of a container ship mid-section with classic T-bone damage from a bulbous bow, see Fig. 18. The influence of impact velocity (1 m/s to 11 m/s), bow shape of the striking vessel, and boundary conditions of the FE model were investigated. The results were used to develop an empirical formula for rapid estimation of the ultimate strength reduction. Similar studies on different ship types would be valuable not only for optimising scantling designs but also for informing emergency responses upon damage occurrence.

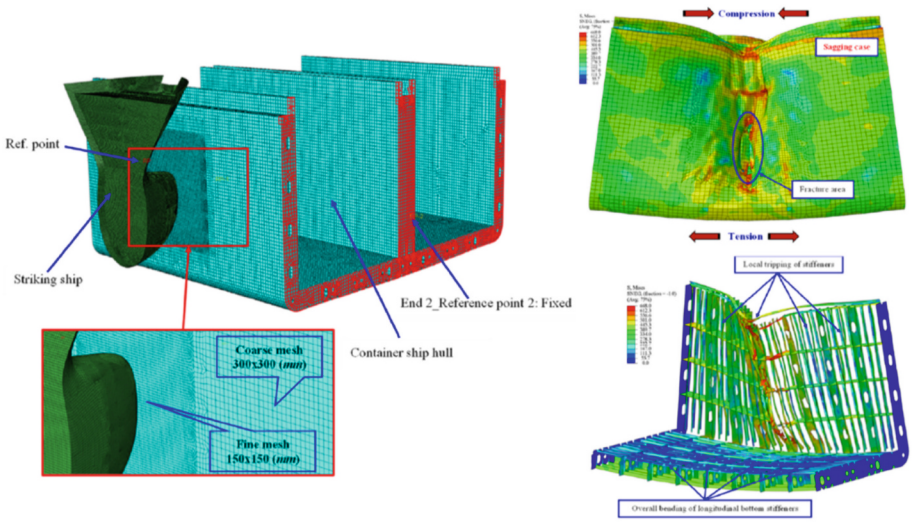

Fig. 18. Container ship mid-section FE model subject to collision damage and sagging bending moment (Do et al. 2024).

4.3.3 Load Combinations

Previous ISSC Ultimate Strength committee reports, e.g., the ISSC (2018a) report, have identified the need for investigation of the combined load effects on ULS. Zhang *et al.*

(2023a) investigated structural dynamic ultimate strength under combined bending, torsion, and lateral pressure (slamming) using non-linear FE analysis with ABAQUS as a solver. The analyses were performed with a partial length model of 26 m even though the Official Discusser in the ISSC 2018 Ultimate Strength committee report (ISSC, 2018b) suggested that torsion cannot be adequately assessed using partial length models. Their analyses showed that when slamming duration was on the order of seconds there was little difference between the dynamic and the static ultimate strength. For shorter events, the dynamic ultimate strength of the hull girder was higher than the static ultimate strength. Although not explicitly noted by the authors, this suggests that modelling slamming events as quasi-static is a conservative approach. However, these results require further scrutiny.

Lee and Paik (2020) investigated the ultimate strength characteristics of as-built ultra-large containership hull structures under combined vertical bending and torsional moments. The analysis was conducted using the intelligent supersize finite element method (ISFEM) and the ALPS/HULL3D program. Their results showed that the ultimate strength of the hull structures was influenced by ship size and the combination of vertical bending and torsional moments. This study provided insights and structural design recommendations for enhancing the ULS capacity of containership hull structures and achieving robust structural design for ultra-larger containerships. Containership hulls with large deck openings may be vulnerable to structural failure due to torsional moments combined with vertical bending, and this vulnerability becomes more significant with an increase in containership size.

Dynamic loads play an important role in structural safety analysis. Shi *et al.* (2023a) investigated the dynamic elastic-plastic response and ultimate strength of a box girder under a bending moment. One set of results was validated with previously conducted experiments, which were then used as a basis for six different box girder models that were used to gauge the effect of model length, plate thickness, mass density, and load excitation period. Based on the structural dynamic response, they proposed an evaluation criterion of the dynamic limit state for the box girder under a bending moment. However, it is left to the reader to interpret how this can be exploited in an actual ship analysis procedure.

4.3.4 Progression Sequence of Failure

Deng et al. (2022) presented numerical and experimental findings for the ultimate bearing capacity and collapse behaviour of ship hull girders with large deck openings under cyclic ultimate bending moments. These results provide valuable insights into structural behaviour, validate numerical models, and support previous findings that cyclic plastic loading reduces the capacity of the hull girder in subsequent load cycles. Notably, the double-hull structure exhibited a higher margin of residual strength in subsequent loading cycles than the single-hull structure, which the authors attributed to better stiffness distribution and load redistribution capability. Liu and Guedes Soares (2020) similarly demonstrated that the ultimate strength reduction of hull girders due to cyclic loading can be captured through numerical simulations. They used a kinematic hardening material model to account for both the ratcheting and Bauschinger effects. While these results demonstrate the capabilities of numerical simulations, the question remains of

how to integrate these relatively costly simulations into ship structure analysis and rule development. Simplified approaches developed for this purpose would be beneficial for future investigations (see, e.g., Preventas et al., 2021), as ULS analysis under monotonically increasing bending moments is already complex and numerical simulations under cycling loading further increase simulation time and complexity.

Jagite and Bigot (2023) questioned the accuracy of the approach proposed by Liu and Guedes Soares (2020) due to the effects of load amplitude, period, and cyclic load magnitude. Motivated by the lack of research on the cyclic ultimate strength of ship hull girders, they analysed the influence of cyclic loads on structural capacity by considering realistic loading scenarios through a long-term hydro-elastic analysis. The ultimate strength of a containership was analysed numerically on a partial structural model using non-linear FE analysis. Their study clearly explains the assumptions and modelling principles, providing a solid foundation for future research. They compared cyclic ultimate strength to traditional ultimate strength obtained with monotonically increasing loads, finding that cyclic loading had an unfavourable, but negligible 1.2% effect on the ultimate strength, which is considerably lower than the 10% reduction reported earlier by Liu and Guedes Soares (2020). Jagite and Bigot (2023) attributed this difference to the more realistic loading assumptions of their approach and called for further experimental studies on the cyclic loading behaviour of typical marine structural steels to advance the field.

Hu et al. (2022) investigated the ultimate bending moment of a cracked stiffened box girder using a series of FE analyses, focusing on the effects of crack length and location under cyclic loads. The study found that crack location had minimal impact on the, focusing on the effects of crack length and location under cyclic loads. The study found that crack location had minimal impact on the ultimate bending moment of stiffened box girders under monotonic bending and bi-directional cyclic bending, but it did have some influence under unidirectional cyclic bending. However, crack length played a more significant role in affecting the ultimate bending moment under both unidirectional and bi-directional cyclic bending. The authors concluded that the ultimate strength reduction under extreme cyclic bending was attributable to the coupling effect of fatigue crack damage and accumulated plastic damage.

Zhou et al. (2023) modelled the progressive collapse behaviour of ship structures considering fluid-structure interaction effects using ABAQUS StarCCM coupling. The difference between ship structure collapse under pure bending and ship structure progressive collapse under different wave conditions was compared. They found that wave load significantly influenced both the ultimate strength and deformation mode of the ship structure. Additionally, wave parameters, such as wave height and wavelength, had a notable impact on the structural response of the ship.

4.4 Rules and Guidelines

Merchant ships have historically been primarily designed and sized following the rules prescribed by ship class societies, while naval ships have historically been designed and sized based on naval methods and guidelines. These ship design rules and guidelines were largely derived from the principles of structural mechanics as well as from the wide experience of individual ships in operation over prior decades. This section focuses on

current methods and new developments given by class societies and IACS, concerning buckling and the ultimate strength assessment for ships.

The global ship fleet continues to evolve with increasing vessel sizes, greater cargo capacities, and specialised vessel types for various purposes. Different approaches to buckling requirements exist across ship types, and classification societies have specific buckling procedures tailored to different vessel designs and structural arrangements. During the design phase of a ship structure, ultimate strength checks are conducted on both a global and local level: (i) a global ultimate hull girder strength check (e.g., the Smith method), and (ii) a local buckling check for individual structural members (e.g., explicit design rules).

4.4.1 Development of Rules and Regulations

A ship's structure must be designed to withstand severe wave environmental loads, and for global operations, the North Atlantic scatter diagram is typically used in these structural designs. The International Association of Classification Societies (IACS) has recently undertaken substantial work to update the wave scatter diagram currently provided in the IACS "Rec. No. 34" (IACS, 2022b), which is used as a basis for the designs of nearly all commercial shipping vessels worldwide. Austefjord et al. (2023) presented some of the background theory and discussed the recent IACS updates. The updated wave scatter diagram was derived from state-of-the-art hindcast datasets, incorporating bad-weather avoidance patterns observed in real ship voyages, using a comprehensive position database from automatic identification system (AIS) data. The spectral shape and spreading were adjusted based on these datasets, resulting in a slightly narrower spectrum. Additionally, AIS data were post-processed to derive statistics of ship speed and heading and their correlation with significant wave height. The updated wave data generally result in reduced loads; this reduction is consistent with the calibration factors currently used in the design rules.

In response to the IMO Goal-Based Standards (GBS) observation on requirement FR1–8/OB/02, and to ensure that the wave data used in ship design rules accurately reflect North Atlantic conditions, IACS (2022a, 2022b) has allocated significant technical resources and applied modern methodologies to update Recommendation No. 34, "Standard Wave Data". Revision 2 now offers an extensive, comprehensive dataset that provides a more accurate representation of the North Atlantic Sea state (IACS, 2022b). Building on the work in Recommendation 34, IACS has also initiated a large-scale project to develop design wave loads based on the updated wave scatter diagram. This project will re-evaluate all wave loads in the Common Structural Rules (CSR), including, hull girder loads, sea pressures, and accelerations, to establish a detailed technical foundation and implement necessary rule changes. Additionally, for other ship types, hull girder loads such as wave bending moments and shear forces will be reviewed, and if necessary, several IACS Unified Requirements may be updated.

4.4.2 Class Requirements: Ultimate Hull Girder Strength Assessment for Ships

Assessments of ultimate hull girder strength commonly use the Smith method (Smith, 1977), which is an incremental procedure to compute the ultimate of a ship's hull girder

structure. A summary and a more detailed review of this approach are presented in ISSC (2018a; 2022a). The Smith method, which is used by most class societies, is applied to incrementally calculate the hull girder bending capacity for each cross-section of the ship, under hogging and sagging conditions. This method has not been further developed since its first implementation in the CSR for bulk carriers and oil tankers (IACS, 2023a).

Hull girder ultimate strength assessment is currently required by most class societies for ships over 150.0 m in length. However, this mandatory assessment typically only considers global vertical bending moments. Assessment of hull girder ultimate strength capacity for ships under horizontal bending moment or torsion is not required by class societies. Darie and Rörup (2017) showed that large containerships operating in oblique seas experience maximum horizontal and torsional loads that are as relevant to the ship's integrity in terms of hull girder strength capacity as the vertical bending moment (head sea conditions). The effect of torsion and horizontal bending moment on hull girder ultimate strength capacity, particularly for ships with large deck openings requires further exploration.

Local loads, such as external pressure, cargo load, and ballast loads are not directly considered in the ultimate strength assessments mandated in class requirements. These local loads, which have a notable effect on the ultimate strength capacity of a ship, are currently only addressed through partial safety factors. For example, to account for double-bottom bending due to local loads on bulk carriers in hogging conditions, IACS (2023a) requirements specify a partial safety factor of 1.25 to reduce the hull girder ultimate strength capacity of the cross-section. Similarly, the mandatory IACS (2020a) requirements for container ships include a partial safety factor of 1.15 to address the local bending effect on the double-bottom in hogging conditions. This factor applies specifically to the midship region, and it may be adjusted in narrower double-bottom areas, such as the engine room, where it can be reduced to 1.0. However, recent increases in the size and capacity of certain ship types, particularly very large containerships with greater width and draught, have resulted in significantly increased local loads on the double-bottom structure. This suggests that the partial safety factor for double-bottom bending effects on hull girder ultimate strength may need to be re-evaluated, potentially using finite element calculations, to ensure accuracy for these larger vessels.

The approach for calculating the hull girder ultimate strength implemented in the requirements presented in IACS (2020a, 2020b; 2023b) is based on a net scantling concept. This concept involves deducting half of the corrosion addition values, as specified by the rule's scantling requirements, from all structural elements of the cross-section under consideration. Since all IACS-classed ships undergo regular surveys by classification societies to examine their corrosion status, the net scantling concept provides a safety margin for hull girder ultimate strength. IACS also requires a partial safety factor of 1.05 (IACS, 2020a, 2020b) or 1.1 (IACS, 2023a) for hull girder ultimate strength, which is intended to account for uncertainties in the construction materials used. An additional partial safety factor, specifically applied to the vertical wave bending moment, is set at 1.2. This factor further enhances the safety margin in assessing hull girder ultimate strength for ships under the IACS classification.

The whipping effect is another important factor influencing the hull girder's ultimate strength of the ships. Whipping is often experienced on large container ships, commonly

occurring in head sea conditions, and can reduce the hull girder's ultimate strength capacity, as evidenced in accident analyses of the container ships M/V MSC Napoli and M/V MOL Comfort. Currently, IACS (2020a, 2020b) advises that classification societies consider the whipping effect in hull girder ultimate strength assessments for container ships; however, it does not provide a specific calculation method. In developing these rules, classification societies have conducted extensive research—including theoretical studies, model testing, and numerical verification across various ship types. This research led to the development of hydro-elastic load calculation software and established a technical approach for evaluating hull girder ultimate strength under whipping, characterized through specific class notations. These specific technical requirements are presented in Table 1.

IACS established working group PH38 to produce the study "Whipping on Container Ship" (IACS, 2022a). After theoretical analysis and comparison with real ships, the first draft of Annex 4 of UR-S11A "Functional Requirements for Ultimate Strength Assessment of Hull Beams Under Whipping Effect" was developed (to be released), which provides a foundational method for evaluating hull girder ultimate strength considering the whipping effect in large container ships. It includes core requirements for hydro-elastic analysis, a long-term method for analysing whipping loads, and guidance on the application of whipping factors.

Table 1. Class notations for ultimate strength assessments including whipping.

Classification (Acronym)	Class Notation	Reference
ABS	WIP	ABS (2025)
BV	WhiSp2, WhiSp3	BV (2024)
CCS	WAU	CCS (2018; 2022)
DNV	WIV	DNV (2021; 2022a)
KR	WHIP	KR (2022)
LR	WDA1, WDA2	LR (2022)

4.4.3 Local Buckling Assessment for Individual Structural Members

Local buckling assessments are conducted for individual structural members, such as stiffened panels, plates, and pillars, under various load conditions. Given the complexity of a ship structure, where multiple load cases must be evaluated for each stiffened plate, it is essential to use computationally efficient tools. These include explicit design rules employing closed-form methods or semi-analytical tools. For specific cases not covered by existing design rules, other more advanced methods, such as FE methods can be used. However, due to the high number of structural elements and load cases, using non-linear FE analysis extensively would be impractical.

Traditional methods for local buckling assessments, such as CSR and UR-S35 (IACS, 2024), often rely on empirical approaches. These methods typically involve plastic corrections to the elastic buckling strength or curve fitting based on non-linear FE analyses.

Semi-analytical approaches offer an alternative to these conventional methods. A recent study by Ishibashi et al. (2024) introduced a semi-analytical method that employed elastic large-deflection theory combined with trigonometric functions to derive analytical solutions describing the elastic post-buckling behaviour. The ultimate strength was then predicted by assessing the yield at critical locations within the plate. This approach is akin to the PULS buckling procedure (DNV, 2023). A key distinction between the two methods is that PULS employs an iterative process with a series of trigonometric functions to compute response and ultimate strength.

4.4.4 Harmonisation of IACS Buckling Procedures

IACS is responsible for numerous ship strength regulations, including both generally applicable Unified Requirements and specific rules tailored to different ship types. There are varying approaches to buckling requirements across vessel types, with rule sets, such as UR-S11, UR-S11A, UR-S21, UR-S21A (IACS, 2010; 2015a, 2015b; 2020a), and CSR (IACS, 2023a). These rule sets collectively cover 90% of ships worldwide. Currently, IACS is working towards harmonising these procedures to create a single, unified buckling standard.

Based on insights gained over the past several years gained through the application of the buckling methodology in CSR for bulk carriers and oil tankers, IACS decided to adapt the CSR buckling assessment procedure for use across all ship types. The objective is to establish a buckling procedure accepted by most IACS members, applicable to all relevant Unified Requirements related to ship strength without reservations. Following this decision, a dedicated project team was established by IACS and a new set of unified buckling strength requirements UR-S35 (IACS, 2024) was issued in 2024. In addition, some improvements to the existing CSR were introduced, as presented in Sect. 4.4.3. The new UR-S35 is a separate document and will function as a toolbox for the various unified requirements for buckling, as shown in Fig. 19. This new rule set of buckling formulae is already in effect for hatch covers, replacing buckling formulae in the previous rules (IACS, 2010; 2015b). The longitudinal strength standards, UR-S11 and UR-S11a, stipulate that the longitudinal strength members of a ship hull must be checked for buckling. However, before incorporating the new buckling requirements, updates to the wave loads are needed.

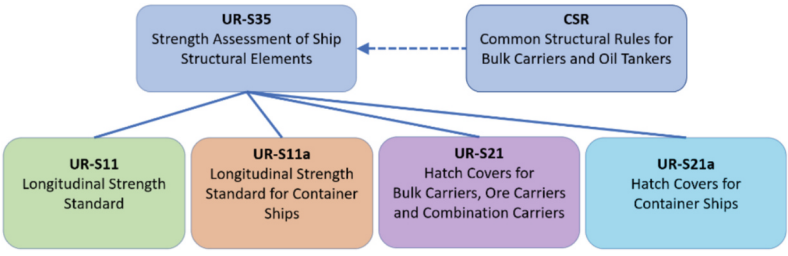

Fig. 19. UR-S35 as a buckling toolbox for all unified requirements in IACS.

Alongside efforts to harmonise buckling strength formulations, another IACS expert team has been updating the wave loads mentioned above. In addition to the harmonisation of buckling strength assessments and updating wave loads, a consequence assessment must be completed before the rule changes for longitudinal strength can be put into force. This involves evaluation of various aspects, such as corrosion additions, slenderness requirements. IACS is actively working on these aspects as part of the ongoing effort.

4.4.5 Recent Updates to the CSR

IACS has focused on the improvement and harmonisation of buckling assessment methods, with recent advancements led by an IACS project team established in 2018. The buckling procedure within the CSR has been incorporated into the new unified requirements, UR-S35 (IACS, 2024). As noted, one objective is to adopt this approach for longitudinal strength checks across all vessel types, which would encompass over 90% of the global fleet. Some of the improvements implemented by this project team, particularly in the context of the stiffener buckling approach, have been presented in Brubak et al. (2023). Additional background theory for these updates can be found in the technical background for CSR (IACS, 2023b). Issues identified with recent updates in the CSR buckling approach are summarised below:

- Buckling of global stiffeners
- Buckling of torsional stiffeners
- U-type stiffeners
- Sniped stiffeners
- Plates with openings
- Plates with one free edge

Only minor corrections have been implemented for the first two cases since the publishing of ISSC (2022a), and a short summary is presented here for the completeness of this report. In global stiffener buckling, out-of-plane deflections are computed using orthotropic plate theory rather than an equivalent beam, which has improved accuracy in certain cases, such as for plates with long, slender stiffeners under transverse loads. The formula for torsional elastic buckling was updated, and a load-dependent expression for torsional capacity was introduced. Further details, including comparisons with CSR and FE analysis, are available in the CSR technical background documents (IACS, 2023b) and the literature (see, e.g., Brubak et al., 2023).

The updated approach for U-type stiffeners incorporates the effect of rotational stiffness due to the closed profile, replacing previous CSR formulae that treated U-type stiffeners as equivalent T-stiffeners using beam theory. In the updated formulae, orthotropic plate theory is applied to U-type stiffeners, using global bending stiffness coefficients specific to the closed profile. Additionally, for local plate buckling between stiffeners, the extra rotational stiffness along the edge provided by U-type stiffeners is now considered.

A new approach was recently introduced in the CSR buckling procedure for sniped stiffeners, incorporating an additional bending moment due to the eccentricity of axial loads, as shown in Fig. 20. In the original formula, the impact of sniped stiffeners was accounted for by including an additional imperfection in the calculation of the

bending moment for second-order effects. This may be realistic for plates with pure axial loads in the stiffener direction. However, for combined loads, including transverse stress and shear stress, the original formula can produce unrealistic results. For example, under the original approach, increasing plate thickness could appear more effective than increasing stiffener size to prevent stiffener buckling, since the increased plate thickness would reduce the initial imperfection. This is counterintuitive, as increasing stiffener size is generally more efficient in preventing stiffener buckling. Additionally, the CSR buckling formulation has been updated for plates with a free edge, which is particularly relevant for plates with openings. In these cases, the buckling procedure for plates with a free edge applies to the individual plate segments on either side of the opening, as illustrated for the plates P1 and P2 in Fig. 21.

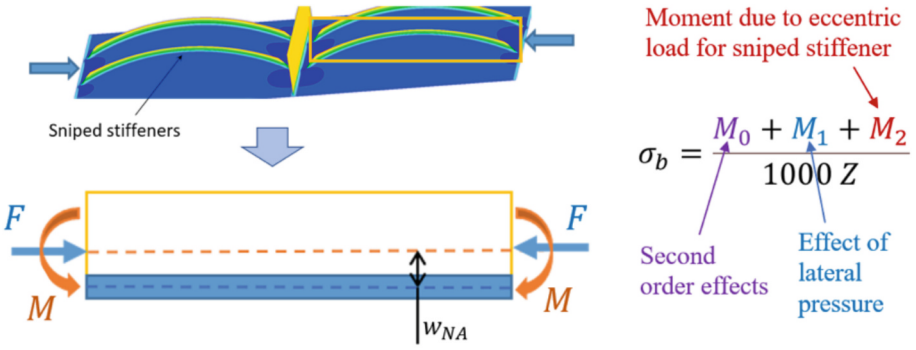

Fig. 20. Bending stress for sniped stiffeners with additional bending moment M_2 to account for the load eccentricity.

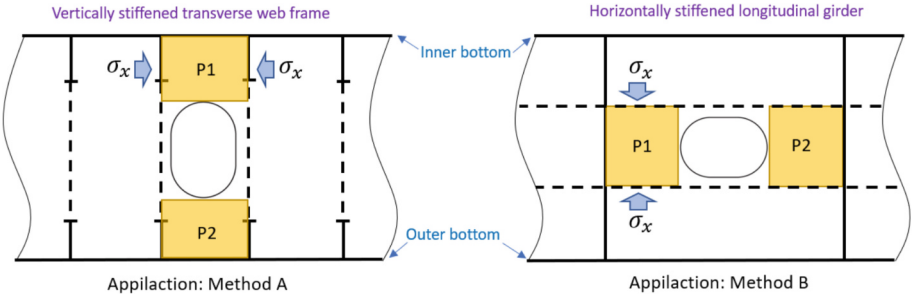

Fig. 21. Plates with opening where buckling formulae with a free edge are used for two different applications (Method A and B).

This update was prompted by industry feedback indicating that the existing formulae could be overly conservative, as demonstrated in the technical buckling documentation for CSR (IACS, 2023b). An additional application was introduced to address this, reducing conservatism in certain special cases. Consequently, there are now two applications

for a plate with a free edge, as illustrated in Fig. 22. In the left figure, the loaded edges are forced to remain straight and parallel (i.e., displacement-controlled), which is referred to as Method A in CSR. This application is suitable for plates where the neighbouring plates in the load direction are continuous, as illustrated to the left in Fig. 21. In such cases, the plate can re-distribute stresses, allowing it to retain reserve strength beyond its elastic buckling limit. Method B is applied in other applications, as illustrated on the right in Fig. 22. In this case, there is less in-plane support along the loaded edges, which are free to move in-plane. This is approach is equivalent to the method outlined in the original CSR and is more conservative. Method B is applied to plates without a continuous structure in the load direction, as illustrated to the right in Fig. 21. In these scenarios, the plate lacks reserve strength beyond elastic buckling because the loads are transferred directly into the plate, preventing stress redistribution.

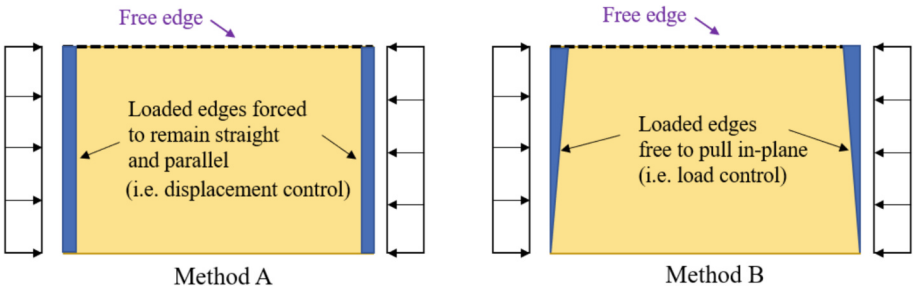

Fig. 22. Two different applications for a plate with one free edge.

5 Offshore Structures

Offshore structures, including oil and gas platforms and wind farms, are essential infrastructures in marine environments for harnessing valuable resources and energy. These structures must withstand the harsh conditions of the open sea, including extreme weather events, waves, and corrosive saltwater. Recent advances and future research needs are presented in this section, along with a summary of the latest updates in relevant design standards and regulations. Research on the ultimate strength of oil and gas offshore structures appears to be in decline, likely due to the global transition from fossil fuels to renewable energy. Furthermore, there is limited literature on the ultimate strength of other offshore structures, such as very large floating offshore structures, floating production storage and offload systems (FPSOs), and floating solar panel structures.

5.1 Loads

Extensive research has been conducted on the impact of load effects on the ultimate strength of traditional offshore structures. However, there has been a growing interest in relatively new structures, such as offshore wind turbines, arctic offshore structures, and composite risers.

5.1.1 Load Effects on Offshore Wind Turbines

Offshore wind is now recognised globally as one of the principal energy sources for combatting climate change. The development of offshore wind energy is forecasted to increase globally to over 290 GW by 2030 (Musial et al., 2023). Zavvar et al. (2022) presented a numerical study of the wave-induced motions and loads on the free-float capable tension leg platform (TLP) named CENTEC-TLP with a 10 MW floating wind turbine (FWT). The study analysed the response of the TLP to various wave conditions and wind speeds in ANSYS® AQWA. A 1:50 scale model of a TLP FOWT supporting a 5 MW wind turbine was designed and tested under combined wind and wave conditions by Ren et al. (2024). The tests conducted included free-decay tests, regular and random wave tests, as well as tendon-broken tests. The experimental results indicated that following tendon failure, the tendons adjacent to the broken tendon experienced a significant increase in tension force.

Li *et al.* (2024b) analysed the tower and blade responses of a spar-type floating offshore wind turbine (FOWT) to the original freak wave crest and subsequent changes. The study concluded that significant blade edgewise deformations occurred, and the tower resonated with the floating foundation. The most noticeable influences were observed in the fluctuation degree changing waves. Ding et al. (2024) described an experimental investigation into the non-linear wave forces acting on a monopile offshore wind turbine foundation under various wave conditions. Utilising a phase-based harmonic separation method, the study explored multi-directional and bi-directional wave interactions, achieving a clear separation of harmonic components even in complex wave scenarios. The results highlighted that non-linear loading could account for up to 40% of the total under certain conditions, with a reduction in non-linear high-order harmonics observed in wider wave spreading. A study by Wang and Moan (2024) investigated the influence of load effects on ultimate strength in the case of semi-submersible hulls for FWTs. A multi-body floater model integrated within a fully coupled aero-hydro-servo-elastic system was developed, enabling precise calculation of cross-sectional forces and moments under complex environmental conditions. This approach combined global load effects with lateral pressures to assess ULS, providing insights into critical design parameters and safety factors, which are essential for optimising hull and column structures in FWTs.

The impact of second-order wave hydrodynamic loads combined with aerodynamic loads on the dynamic responses of semisubmersible FOWTs was investigated by Shi *et al.* (2023b). Three water depths (50, 100, and 200 m) were examined to understand the depth effect. Simulation results demonstrated that second-order hydrodynamic loads were significant factors in motion and structural responses under extreme sea conditions, regardless of whether aerodynamic loads were included in the analysis. Additionally, aerodynamic loads were observed to substantially impact the dynamic responses of all semi-FOWTs during normal operational conditions. Among the three FOWTs analysed, the V-shaped semi-FOWT exhibited the highest pitch motion responses in extreme sea conditions.

The ship collision responses of a semi-submersible FOWT, i.e., the OO-STAR floater with DTU 10 MW blades, were investigated by Yu et al. (2022) using USFOS. It was revealed that the FWTs exhibit a higher capacity to withstand higher energy impacts

without collapse compared to bottom fixed installations. Notably, collisions with operating FOWTs tend to have more severe consequences, with the worst-case scenario occurring when the vessel strikes from the opposite direction of the wind. An aero-hydro coupled method was proposed by Zhang and Hu (2022) to analyse the dynamic response of FOWT under ship-FOWT collision under wind-wave conditions. Though the structure can withstand the ship collision at the beginning, the residual strength of FOWT may not be enough to withstand the continuous wind-wave loads. Therefore, a lower impact velocity could cause the tower to collapse in wind-wave conditions, in contrast to still-wave conditions.

The presence of energetic steep or breaking waves (ESBWs) in the targeted locations for OWTs can significantly contribute to the overall loading of the structure, impacting the ultimate limit state (ULS). Martin et al. (2022) utilised the computational fluid dynamics (CFD) solver Code Saturne to model the wave-breaking slamming phenomenon on a cylinder. Figure 23 illustrates the test model of a 1:55 scale representation of a 31m diameter rigid vertical column situated at a water depth of 121 m. The comprehensive test program encompassed 354 irregular wave tests lasting 3 h each in full-scale time in the SINTEF Ocean Basin laboratory. Slamming panels were installed on the area of the column facing the incoming waves.

Among the various load scenarios, the most critical for ULS assessment in FOWTs are those involving combined extreme wind and wave conditions, particularly during parked or shutdown states. These can induce significant tower base bending moments and tendon overloads. Additionally, tendon failure scenarios, as observed in experimental studies (Ren et al., 2024), can lead to load redistribution and localized overstressing, making them critical for collapse assessment.

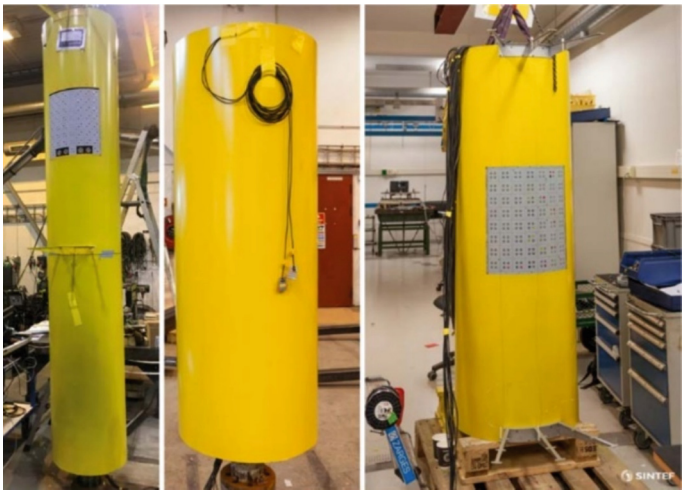

Fig. 23. Test model of a vertical column: (left) the full model, (middle) the lower column, and (right) the upper column (Økland et al., 2022).

5.1.2 Ice Load on Arctic Offshore Structures

The Arctic area is known for its abundant oil and gas resources, accounting for 13% of the world's unproved reserves and 30% of the world's total reserves (Zhang *et al.*, 2023b). Truong and Jang (2022) presented a FE analysis on the interaction between a moving offshore structure and fixed-level ice to estimate ice-load distributions and structural response characteristics, where the sophisticated procedure of ice load estimation using the influence coefficient method (ICM) was derived. Braun et al. (2022) introduced an approach to determine combined load spectra for offshore structures and standardised time series for wind, wave, and ice action. The load interaction of a monopile support structure in the Baltic Sea was numerically assessed based on over 3000 simulations of different load conditions, each lasting 600 s, for four design load cases (DLCs). It was concluded that combined stress spectra for wind, wave, and ice action on an OWT differed significantly from standard load spectra without ice contribution. This can be attributed to the occurrence of very high ice-related load cycles, which can lead to overload effects similar to those seen in storm events. Therefore, applicable damage accumulation sums for such spectra should be determined experimentally.

The definition of ice loads varies based on measurement techniques, encompassing terms such as contact pressure, contact forces, and line load, which depend on whether pressure gauges or shear strain gauges are employed. Li *et al.* (2024a) delineated ice load measurements, discussing direct methods using pressure panels and indirect methods that infer loads from structural responses. This included the use of strain gauges which, despite introducing uncertainties due to assumptions about load locations and heights, remain a prevalent practice for quantifying ice loads due to their practical applicability in field conditions.

The construction of OWTs in sub-arctic areas, such as the Baltic Sea and the Bohai Bay, presents a unique challenge, primarily due to the presence of sea ice (Hammer et al., 2023). In the numerical assessment conducted by Tabri et al. (2022), the ice involved in the interaction with a wind turbine foundation in the Baltic Sea was treated as an isotropic, brittle material. The behaviour of the ice was described using stress-strain curves to analyse its response during the interaction process. Barooni et al. (2022) also presented a suite of ice load models using a coupled aero-hydro-servo-elastic numerical model to study the dynamic response of FOWTs in regions with cold climates and the presence of sea ice. The findings of this study suggest that aerodynamic loads from wind inflow primarily control the dynamic response of wind turbines. When operating at the rated wind speeds, ice loads have little impact on power output and are statistically insignificant for floating spar-buoy wind turbines. Future work may pursue a further investigation of the effect of stochastic ice loads on the dynamic response of floating offshore wind turbines across various operational modes.

An experimental study was conducted to estimate the effects of hydrodynamics on the ice impact rate and load between an approaching iceberg and a moored FPSO by Huang et al. (2023). A probabilistic analysis was initially conducted to identify potential scenarios contributing to the design of iceberg loads, focusing on the iceberg population and environmental conditions on the Grand Banks and a standard FPSO. Three iceberg sizes and their corresponding environmental and test conditions were selected for the

study. The experiments indicated that the hydrodynamic effect led to a decreased probability of impact for smaller icebergs compared to the platform. Further experiments are suggested to investigate the influence of hydrodynamics on larger icebergs. The influence of hydrodynamic effects might be significant in some scenarios and should not be ignored for estimating iceberg design loads. Gu et al. (2023) conducted a comprehensive review of ice detection and mitigation technology for bottom-fixed offshore wind turbines deployed in the Arctic. The ice mitigation technologies were divided into two categories: passive technologies, including ice-phobic coating and black paint, and active technologies, such as heating resistance, pneumatic, ultrasonic, and hot air injection techniques.

For Arctic offshore structures, the most critical ice load patterns for ULS assessment are those involving high-velocity ice crushing and bending failure against vertical or inclined structural members. These loads are particularly severe at the waterline and can lead to local or global structural failure. The interaction of ice with compliant structures, such as monopiles or jackets, under dynamic conditions can also result in significant stress concentrations that govern ULS.

5.1.3 Load on Composite Risers

In response to the increasing need for sustainable and versatile materials, the offshore industry is progressively adopting composite materials. Their unique combination of lightweight properties, corrosion resistance, thermal insulation, and fatigue resistance makes composite risers an attractive choice for deep-sea operations. Chang et al. (2022) concluded that the internal flow velocity, external ocean current velocity, fibre orientation angle and top axial tension have a substantial impact on the coupled vibration stability and frequency-locking characteristics of composite risers.

Amaechi (2022) presented the locally tailored design of deep-water composite risers subjected to burst, collapse, tension, and combined loads. ANSYS ACP was used for modelling composite risers with different material configurations. Figure 24 illustrates the structure of the risers and their common loadings. Internal pressure was identified as the most critical factor of all the loadings investigated since it imposed the highest level of stress on the riser layers.

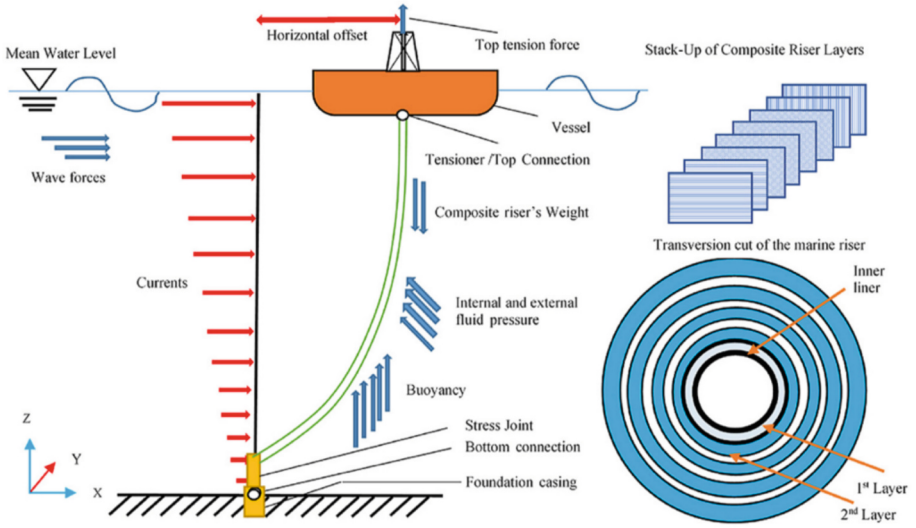

Fig. 24. Schematic of a composite marine riser highlighting loads, stack-up and transversion-cut of plies (Amaechi, 2022).

Hastie et al. (2022) conducted a failure analysis for a thermoplastic composite pipe (TCP) under loads illustrative of deepwater riser operation by FE analysis using ABAQUS. The analysis considered temperature-dependent material properties, examining various laminate stacking sequences. A multi-angle stack was found to be effective for both small and large tension operating scenarios. They concluded that TCP designed for extreme operating conditions will inevitably necessitate the use of large-diameter storage spools. He et al. (2023) conducted both theoretical and FE analysis to investigate the behaviour of thermoplastic composite pipes subjected to axisymmetric loadings. Their study found that the axial stiffness of the pipes remained constant regardless of the internal and external pressures. However, there was a slight decrease in stiffness as the prescribed temperature increased.

Theoretical and numerical models of composite flexible risers under axisymmetric loads were proposed by Sun et al. (2024). It was found that the structural radial stiffness of high-modulus glass fibre is better than that of high-strength glass fibre. Specifically, when the fibre volume fraction (FVF) of high-modulus fibreglass reaches 53.3%, it can achieve an equivalent stiffness to high-strength fibreglass with an FVF of 80%. An overview of the developed modelling approaches and the CFD results from verifiers in blind tests were provided by Yeon et al. (2022), and CFD was employed to analyse the model of an offshore floating structure. Results from these approaches were investigated in a comparison benchmark study, which included test results from existing models for both a semi-submersible rig and an FPSO. Through the Joint Industry Project (JIP), it was determined that CFD readiness for estimating wind loads on offshore floating structures was quite high. However, a major obstacle to achieving accurate CFD modelling was the need to repair geometry to ensure a watertight surface from CAD, especially when numerous defects were present.

5.2 Structural Elements

5.2.1 Tubular Joints

Research on tubular joints has recently focused on analysis methods and local strengthening of different joint types. Saberi and Fantuzzi (2022) analysed results from prior experiments on reinforced/unreinforced tubular T-joint components subjected to tension-compression loading conditions via the open-source finite element package Code_Aster. The code produced accurate predictions for ultimate load resistance against ovalisation for large deformation settings. Configurations with a brace-to-chord diameter ratio greater than 0.5 exhibited higher load-bearing capacity compared to those with a lower diameter ratio, where the failure mode was local yielding, causing the brace to yield before the joint. Nassiraei and Yara (2023) investigated the local joint flexibility of K-joints reinforced with external plates subjected to axial loads. An FE model was developed and validated against experimental results, with 150 K-joints simulated to analyse the effects of reinforcing plate size and joint geometry. Key findings include that external plates effectively reduce local joint flexibility in K-joints and the creation of a design formula to predict the local joint flexibility factor for reinforced K-joints under axial loads.

Kadry et al. (2022) presented a mathematical formula to calculate the capacity of a symmetrically loaded multi-planar KK joint. A verified ANSYS model was used to generate 172 records for parametric study with different geometries, member sections, and material properties. The novelty of the developed model lies in its ability to predict joint capacity as a true 3D joint, rather than an approximated 2D joint, as in prior studies. The results of the developed formula were compared with experimental test results and showed an average accuracy of 92.5%.

Feng et al. (2021) conducted a numerical study on the ultimate strength of stainless-steel hybrid tubular X-, T-, and Y-joints with square braces and circular chords (SHS-to-CHS). A parametric study using 288 FE models was performed, with half representing T/Y joints and the other half X joints. Various geometric properties were adjusted, revealing that the load-carrying capacity of the joints was particularly sensitive to the brace width-to-chord diameter ratio. A comparison of the results with current design guidelines indicated existing design codes inaccurately predict the strength of stainless steel SHS-to-CHS hybrid tubular T/Y- and X-joints. Consequently, improved design equations were proposed.

The effects of FRP on SCFs in uniplanar KT-joints reinforced with different fibre-reinforced polymers Glass/vinyl ester, Glass/epoxy (Scotchply 1002), S-glass/epoxy, Aramid/epoxy (Kevlar9/Epoxy), Carbon/Epoxy (AS/3501), and Carbon/epoxy (T300/5208) under five axial loading conditions were numerically investigated by Zavvar et al. (2023). The commercial FE software ANSYS was used to create 5184 finite element models with different geometries defined by dimensionless parameters, FRP materials, and several FRP layers/orientations. This range of dimensionless parameters effectively covers a broad spectrum of tubular connections used in offshore structures. In related work, Pandey and Young (2021) conducted experiments on novel joint configurations, including brace-rotated (BR), square bird-beak (SBB), and diamond bird-beak (DBB) T-joints, to assess their load versus deformation behaviour and static joint resistances, see Fig. 25. The joint failure resistances of BR, SBB, and DBB

T-joints were 1.53, 1.34, and 1.53 times the joint failure resistances of identical traditional RHS-to-RHS (rectangular hollow section) T-joints, respectively. Moreover, the joint ultimate capacities of BR, SBB, and DBB T-joints were 1.84, 2.12, and 2.24 times the joint failure resistances of identical traditional RHS- to-RHS T-joints, respectively. The authors also performed numerical FE simulations of the SBB joint and proposed accurate and reliable design equations for predicting the static strength of the SBB T- and X-joints.

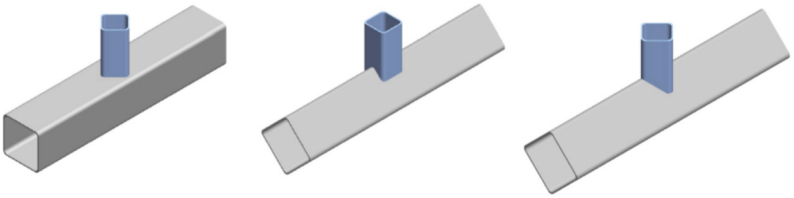

Fig. 25. Three-dimensional models of BR, SBB, and DBB T-joints (Pandey and Young, 2021).

5.2.2 Tubular Members

Tubular structural members, from pressure vessels and line pipes to piping and fittings at smaller scales, are often subjected to stresses and loads that can exceed design limits. These extreme conditions can bring components to a critical state, potentially compromising structural integrity. There are two distinct cases when referring to extreme loading conditions. One is when the extreme load causes actual damage to the structure, thereby reducing its residual or ultimate strength. The other is when the extreme load is used as a design scenario to assess the structure's capacity under ULS or ALS without prior damage. The former affects the remaining strength and may require damage-tolerant design or repair strategies, while the latter is used to verify that the structure can withstand extreme but undamaged conditions.

While large-scale experiments provide valuable insights, they can be costly and time-consuming, especially for certain structural components. As a result, computational tools are highly valued for their cost-effectiveness, speed, and ability to conduct parametric analyses. However, these benefits come with certain drawbacks, particularly in terms of reliability and accuracy. Despite extensive research over recent decades to address these issues, challenges remain that warrant further improvement.

Li *et al.* (2023a) conducted comprehensive computational analyses on multiaxially loaded pipe components with defects, made from 316L stainless steel, to assess plastic collapse and compare results with safety limit load requirements. The modelling included low-temperature behaviour, incorporating kinetic phase transformation and temperature-dependent yield strength formulations to capture mechanical responses at near-cryogenic temperatures (Paredes et al., 2020). This study was largely motivated by the need for long-distance modular transportation of liquid natural gas (LNG), where components are subjected to complex loading conditions, such as combined torsion, bending, and internal pressure, in Arctic-like environments. The findings were compared with analytical solutions from standards, such as ASME (2017), Rules for in-service inspection

of nuclear power plant components: boiler and pressure vessel code, section XI; and ASME (2017), boiler and pressure vessel code; see Fig. 26.

Yuan et al. (2022) focused on the plastic collapse behaviour of subsea-lined pipes deployed using the S-lay installation method. During this process, the lined pipe was subjected to combined tension-bending loading which typically leads the liner material to detach from the pipeline due to severe ovalisation. Using a custom numerical framework with quasi-two-dimensional and three-dimensional models, they investigated two loading sequences of bending and tension on lined pipes with both perfect and imperfect geometries. The results indicated that tension, either applied before or after bending, affects the growth of ovalisation and liner collapse, the extent of which depends on the load path followed. The authors also demonstrated that bending with modest levels of internal pressure delays the onset of liner collapse, but the threshold pressure varies for different load paths.

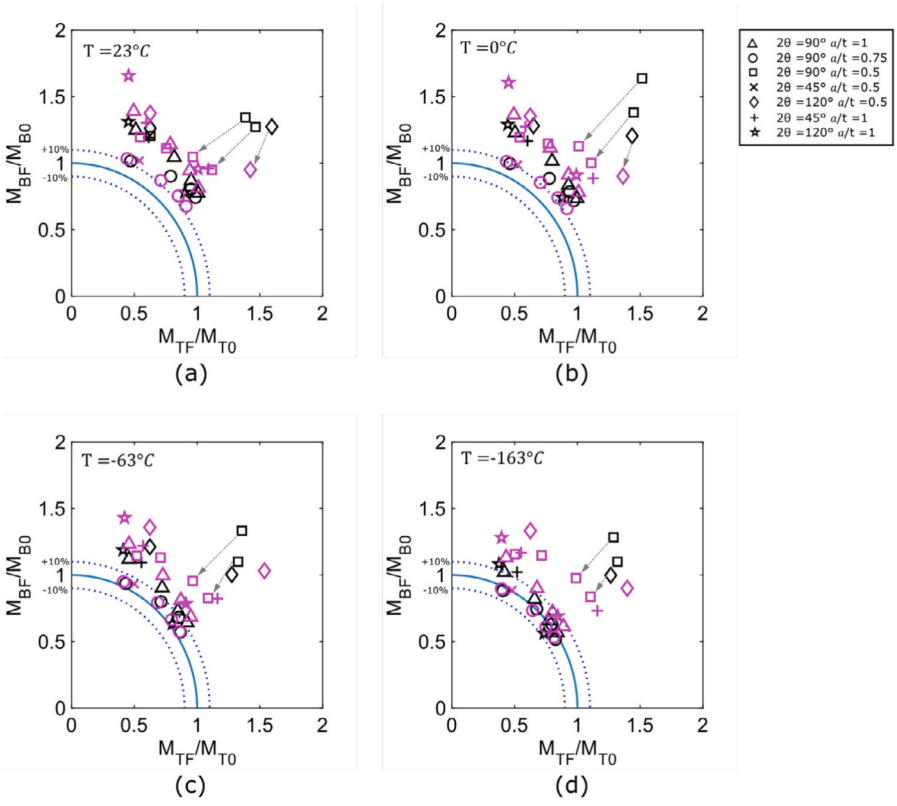

Fig. 26. Failure interaction curves for distinct temperatures: (a) 23 °C, (b) 0 °C, (c) − 63 °C, and (d) − 163 °C. The black open symbols represent simulations without internal pressure (p_i = 0 MPa), while the magenta colour marks depict pressurized pipe configurations (p_i = 20 MPa); Li *et al.* (2023a).

5.2.3 Reinforced Tubular Members

With the increase in the rated power of offshore wind turbines, the size of support structures has also grown, posing new challenges in the design of monopile tower barrels and support systems. To address these requirements, tapered concrete-filled double-skin steel tubular (CFDST) structures have recently been proposed by Wang *et al.* (2023b) (see Fig. 27). They developed an analysis tool for the evaluation of axial compression strength and torsional capacity for tapered CFDST members. Their investigation addressed the torque versus deformation response, interaction behaviour, and component contributions, as well as the influence of various parameters on the torsional capacity.

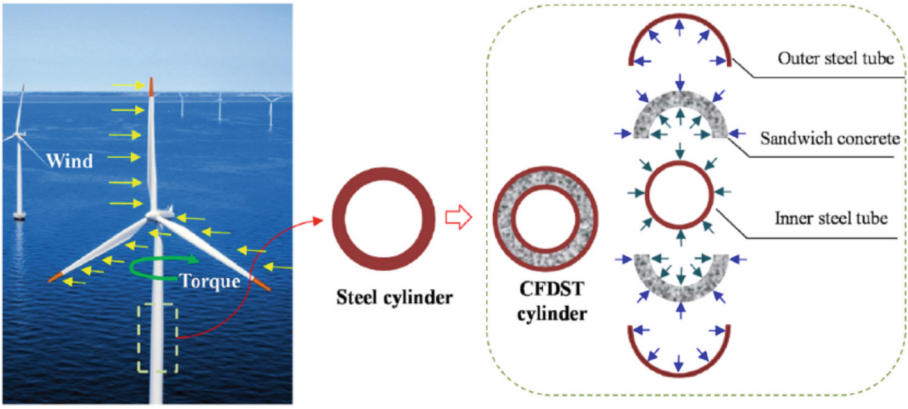

Fig. 27. Potential application of CFDST members in support structures (Wang *et al.*, 2023b).

Sundarraja and Prabhu (2011) demonstrated experimentally that the external bonding of the carbon-fibre reinforced polymer (CFRP) to concrete-filled steel tubular (CFST) structures provides effective confinement pressure and delays the local buckling of the steel tuber under axial compression. It is now well established that the presence of CFRP sheets considerably enhances the ultimate strength and deformation of traditional CFST columns. Therefore, different approaches have been proposed to predict the ultimate strength of FRP-CFST columns (e.g., Güneyisi and Nour, 2019) and their performance has been investigated under different combinations of variables (e.g., Shen et al., 2019). Wang *et al.* (2022a) conducted a comprehensive FE analysis, offering insights into the axial compression behaviour of circular FRP-CFST columns. They investigated the parameters affecting the axial compression behaviour of stub columns and a new regression-based formula for ultimate bearing capacity was proposed.

In a broader context, Duong et al. (2023) proposed a machine learning-based approach for the prediction of the ultimate capacity of CFST columns with different cross-sectional shapes: circular, elliptical, square, and rectangular. The training database was gathered from various studies available in the literature, and the results are accessible through a freely available MATLAB-based graphical user interface. The effects of cross-sectional shapes on the axial performance of CFST were also investigated numerically by Ayough et al. (2021) who concluded that hexagonal and octagonal CFST columns

behaved similarly to square columns, whereas circular CFST columns demonstrated superior structural performance.

5.3 Structural Systems

5.3.1 Offshore Aquaculture Platforms

Recent developments in aquaculture fish farms have included a shift towards offshore farming in response to increasing seafood demand and limited space in coastal areas. The size of fish farms is expected to increase, and new designs are being developed to withstand high-energy waves and stronger currents in the open ocean. There is growing interest in combining floating offshore wind turbines with aquaculture cages, creating a new concept called the floating wind-aquaculture platform (FWAP) (Cao et al., 2022). Experimental investigations are being conducted to study the dynamic behaviour and effects of aquaculture nets on the FWAP. Another example is vessel-shaped fish farms (Li *et al.*, 2019b) to improve the longevity of aquaculture systems and the welfare of farmed fish. Furthermore, there is a focus on improving the strength of net structures under the action of flow to ensure the survival and growth of farmed fish. Regulations and standards, such as the Norwegian Standard NS 9415, have been introduced to address technological investments and reduce the number of escaped fish. A study by Chu et al. (2023) presented a review of the most recent developments related to standards and guidelines for the design and analysis of offshore fish farms. Their work covered various crucial aspects for consideration when developing offshore fish farming facilities, such as design criteria, global performance analysis procedures, and decision-making methods. The authors also discussed the limitations and considerations associated with the references used in the review.

A novel BT-FOWT-AC integrated structure designed for a water depth of 100 m was proposed by Zhai et al. (2024). Their study assessed the impact of integrating an aquaculture cage and netting on the structures and responses of three different configurations: Stru1, which included an aquaculture cage and netting; Stru2 without netting; and Stru3 without an aquaculture cage., The study evaluated these configurations under various environmental conditions, including wave and current loads, as well as combined wind, wave, and current forces during both normal operations and shutdown scenarios. Findings revealed that the netting's inherent damping properties significantly diminished structural fluctuations, thereby enhancing the stability and safety of the integrated system.

5.3.2 Offshore Wind Farms

Offshore wind turbines (OWTs) are subjected to various environmental loads such as wind, waves, and currents, which can cause fatigue and ultimate strength failure. Various numerical simulation tools have been developed to predict the dynamic response of OWTs under various loading conditions (Wang et al., 2021). Due to the combined effect of various factors, the support structure may fail and the wind turbine may collapse. Nevertheless, the reliability analysis of OWT trends towards simplified load analysis. The reliability evaluation of these structure is used as a basis for the estimation of safety levels. For example, Ivanhoe et al. (2020) developed a reliability assessment framework

for OWT jacket support structures considering five limit states (including the ULS) using a parameterised finite element model. Wilkie and Galasso (2020) proposed a probabilistic risk modelling framework to assess the structural risk posed by extreme weather conditions to OWTs. Specifically, they formulated a fragility function, which quantified the probability of different damage levels occurring across various wind and wave intensities. Through analysis of two case study sites, they found that the tower generally had a higher probability of failure at the ultimate limit state (ULS) than other structural components, such as the monopile, transition piece, and blades. Notably, the monopile was typically the safest component under these conditions. Moreover, they highlighted that ULS assessment of components is more relevant to sites exposed to hurricane-level conditions (East Coast of the USA), while for milder European conditions fatigue limit states are expected to be more relevant.

Yeter et al. (2019) presented an uncertainty analysis of soil-pile interactions for monopile offshore wind turbine support structures. Their study examined the sensitivity of pile design parameters to variations in soil properties, such as strength, stiffness, and damping. They employed a probabilistic approach in their analysis to assess the uncertainty in the response of the pile, including the ultimate capacity and the natural frequency. Their results suggested that soil properties have a significant impact on pile response, and the level of uncertainty in the design parameters may be relatively high. The authors concluded that a comprehensive understanding of soil properties is essential for the accurate and reliable design of OWT support structures.

In recent years, machine learning has been applied to predict the ultimate strength of offshore structures. For instance, Muhaimin Ishak et al. (2022) developed a machine learning-based tool, IGUSA (Intelligent Global Ultimate Strength Analysis), which was used in a case study to predict the ultimate strength of a fixed offshore jacket platform installed in Malaysian waters. The input parameters for their model included water depth, leg strength, number of risers, number of conductors, and number of legs, as well as response parameters, such as end-on base shear at collapse, broadside base shear at collapse, and diagonal base shear at collapse. They concluded that their model was suitable for rapid assessments of ultimate strength for fixed offshore structures, reducing time and cost in structural integrity management.

Offshore structures are likely to be exposed to corrosive environments, consequently affecting their ultimate strength. Therefore, it is important to investigate the improvement in ultimate load capacity after the application of strengthening and/or repairing methods. George *et al.* (2022a) investigated the flexural response of tubular steel members retrofitted by carbon fibre-reinforced polymer (CFRP) wraps. Two specimen sets underwent a four-point bending test. The ultimate strength of the specimens showed improvement in the range of 18.6 to 22.3% for the "Intact and Strengthened", which were insensitive to the number of CFRP layers, and 14.9 to 32.1% for the "Corroded and Repaired" specimens, which increased as the number of CFRP layers increased. However, the ductility index of the tested specimens fell as the number of CFRP layers increased. They also noted that the ultimate strength of the retrofitted "Intact and Strengthened" specimens was reduced by a maximum of 2.2% after one year of exposure to saline water. Nevertheless, the ultimate strength of "Corroded and Repaired"

specimens was at least 4% higher than the corresponding values of their counterparts before exposure.

George *et al.* (2022b) also investigated the ultimate strength of retrofitted tubular steel members with CFRP, with different retrofitted lengths under axial eccentric compression loading. Their investigation revealed that partial-length CFRP retrofitting did not enhance the ultimate strength of leg specimens, likely due to local yielding that occurred outside the retrofitted zone, resulting in earlier failure compared to non-retrofitted specimens. While leg specimen failure was predominantly due to cross-section yielding, brace specimens—designed to be governed by Euler buckling—showed an average strength improvement of 19.1% due to CFRP retrofitting. Additionally, corroded and subsequently repaired leg and brace specimens demonstrated significant strength gains, with improvements of up to 40.2% and 22.1%, respectively. Full-length CFRP retrofitting of leg specimens led to a substantial increase in ultimate load capacity, reaching up to 53.8% with an increasing number of CFRP layers.

A review of the recent worldwide reports of failure incidents of offshore wind farms highlighted an incident that occurred at the Anholt offshore wind farm in Denmark in April 2022, where a rotor, including three blades, detached from the nacelle of an offshore wind turbine and fell into the sea (Ørsted Media Relations, 2022). This wind farm, commissioned in 2013, comprises 111 S-Gamesa turbines, each with a capacity of 3.6 MW (Rapacka, 2023). Following a thorough investigation, the incident was attributed to a production fault in the affected rotor (Energy Watch, 2023). Although the rotor detachment incident was attributed to a production fault rather than an external load, it highlights the importance of considering manufacturing-induced uncertainties in ULS assessments. Such uncertainties can significantly reduce the actual capacity of structural components and should be incorporated into probabilistic design frameworks.

With the growing number of floating offshore wind turbines, the importance of time-dependent structural assessments has increased due to the unsteady, turbulent wind, and ocean environments that induce a coupled, time-varying structural response. Lee *et al.* (2023a) proposed a time-domain structural analysis method, applied to the substructure of a 15 MW floating offshore wind turbine. This method was tested under two critical load cases: extreme operational conditions and parked states in high wind and wave environments, using two distinct turbulence models. Extreme Von Mises stress values were computed from a failure distribution function, based on three hours of data from the actual structure. The study concluded that the method was computationally efficient and capable of capturing the coupled effects between transient wind loads on the turbine and irregular wave loads on the floating structure.

Xu *et al.* (2021a) conducted a comparative study of the ultimate limit state design of different mooring systems for floating wind turbines in shallow water. Seven mooring concepts designed for a 5 MW semi-submersible floating wind turbine at 50 m water depth (see Fig. 28) were compared to identify solutions that were structurally reliable and economically attractive. This study introduced the concept of mooring system design for further strength assessment.

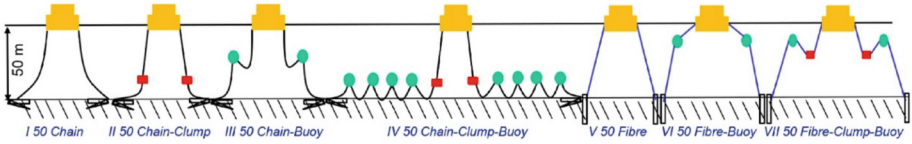

Fig. 28. Seven mooring concepts designed for a 5 MW semi-submersible floating wind turbine at 50 m water depth (Xu *et al.*, 2021a).

An incident involving a ship collision with an offshore wind turbine substructure has raised important considerations for structural resilience (Lewis, 2023). The cargo ship, transporting 1,500 tons of grain from Poland to Belgium, collided with an offshore wind turbine in Germany. Following a post-accident inspection, the turbine was reactivated within 24 h. However, this event highlights the need for further research into the effects of ship collisions on the ultimate load capacity of offshore wind turbine structures. Ladeira et al. (2023) provided a review of structural assessment methods for offshore wind turbines under ship impact. Analytical models, experimental studies, and numerical simulations can play a critical role in predicting the structural response to such collisions.

Jia et al. (2020) conducted an experimental study in China to quantify the effects of ship collision on the structural load of an offshore wind turbine. The collision generated impact forces ranging from 2.4 to 25 kN, and strain measurements were made at the blades of the turbine and tower during the event. The researchers calculated the resulting bending moments in these structural components and observed a slight increase in peak bending moments on both the tower and the blades due to the collision. Despite this increase, the collision did not compromise the structural integrity of either component. Nevertheless, there remains a need for more extensive experimental research on the impact of ship collisions on offshore wind turbine structures, as this area is currently underexplored.

Liu *et al.* (2022a) conducted a three-point bending test and finite element simulation to investigate the effect of impact location, collision angles, and impact velocity on crashing response, see Fig. 29. They designed a down-scaled tubular member of an offshore jacket platform made of DH-36 steel for testing, and modelled plastic deformation using a power law hardening approach. After validating the FE model, they simulated an offshore jacket foundation and considered 27 accident cases with different impact locations, angles, and velocities in the range of 0.5 to 4 m/s applied to the legs and braces. They found that the most severe scenario led to a local indentation of 916 mm on the leg. Additionally, they noted that as the angle of impact increased, the severity of local indentation on the structural members decreased.

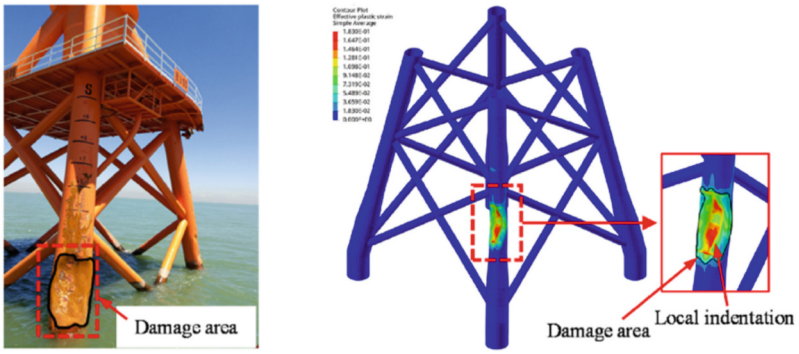

(a) Damage in an actual ship-jacket collision (b) Simulated plastic strain field of the jacket (case ILL3)

Fig. 29. Comparison of actual and simulated damage to the jacket (Liu *et al.*, 2022a).

5.3.3 Other Floating Structures

To address the coupling between hull motion and turbine loading, class societies recommend fully coupled time-domain analyses of floating offshore wind turbines, followed by response-based structural assessments to evaluate structural strength. Recognizing the impracticality of analysing a large number of design load cases with lengthy simulation times using current tools, Moon et al. (2023) proposed an efficient time-domain structural analysis for buckling and ultimate strength assessment. For various design scenarios, they performed time-domain structural analyses by mapping aero-elastic, hydrodynamic, hydrostatic, inertial, and mooring loads onto a FE structural model. To enhance computational efficiency, they introduced a pseudo-spectral stress synthesizer based on "lodal" response analysis, which combines linear frequency-domain loads with non-linear time-domain loads. This lodal response concept enables the method to generate stress component time histories that account for transient wind loading, irregular wave loading, and the resulting motion response of the floating hull.

To address the coupling between hull motion and turbine loading, class societies recommend fully coupled time-domain analyses of floating offshore wind turbines, followed by response-based structural assessments to evaluate structural strength. Recognizing the impracticality of analysing a large number of design load cases with lengthy simulation times using current tools, Moon et al. (2023) proposed an efficient time-domain structural analysis for buckling and ultimate strength assessment. For various design scenarios, they performed time-domain structural analyses by mapping aero-elastic, hydrodynamic, hydrostatic, inertial, and mooring loads onto a FE structural model. To enhance computational efficiency, they introduced a pseudo-spectral stress synthesizer based on "lodal" response analysis, which combines linear frequency-domain loads with non-linear time-domain loads. This lodal response concept enables the method to generate stress component time histories that account for transient wind loading, irregular wave loading, and the resulting motion response of the floating hull.

Mooring system design for floating structures is often governed by ultimate limit state (ULS) conditions. Cai et al. (2024) numerically investigated the ultimate strength of the mooring lines and suspension ropes of a novel semi-spar floating wind turbine

platform under extreme conditions, as well as the relationship between the ropes' tension and the wave direction. Simulation revealed that the lateral suspension ropes parallel to the propagation direction were sensitive to winds and waves.

The FPSO is one of the most common platform types for offshore oil production. Silva et al. (2022) investigated the ultimate strength of FPSO hulls designed with SPS sandwich plates according to the DNV rules. Numerical simulations showed that SPS design provided a reduction of 2.8% of the total weight and a better overall structural performance (an increase of 26% in the magnitude of the ultimate strength of the hull). The authors recommended further research regarding the local ultimate strength and fabrication process of SPS panels.

Fonseca et al. (2024) conducted a mooring analysis of an FPSO in ballast conditions, focusing on horizontal wave drift loads and associated slow drift oscillations. These factors represent the largest contributors to extreme line loads and also carry the greatest uncertainty in numerical predictions. This study highlighted a limitation in state-of-the-art radiation/diffraction potential flow codes, which often underestimate wave drift loads in severe sea states for large floating structures like FPSOs with substantial waterplane areas. To address this, the authors applied empirical quadratic transfer functions (QTFs) of horizontal wave drift loads directly within time-domain simulations for the mooring analysis. The methodology was validated through a case study of an FPSO operating in the North Sea, demonstrating improved accuracy in predicting extreme mooring loads.

Floating photovoltaic (FPV) systems are drawing considerable interest in solar energy generation because of their unique benefits, including space efficiency and cooling effects from water, which improve panel efficiency. A study by Li *et al.* (2023b) assessed the ultimate strength of a modular FPV system designed with ultra-high-performance concrete (UHPC) and fibre-reinforced polymer (FRP). Their study included hydro-elastic and structural analyses focusing on the influence of hinge connections and module configurations on bending capacity under wave loads. Such evaluations are critical for ensuring structural resilience in offshore settings, where wave action can impose significant stresses on the system.

5.4 Rules and Guidelines

Offshore rules and regulations for ultimate strength are essential for ensuring the safety and reliability of offshore structures. These regulations guide the design, construction, and maintenance of offshore structures, ensuring that they can withstand the harsh environmental conditions and extreme loads they are subjected to. Design standards vary depending on the application and are generally divided into two main types: *fixed structures* and *floating production units* (FPUs). Fixed structures, often comprising tubular members and connections, must account for seismic response among other environmental loads, while FPUs, built primarily of plated structures and stiffened panels, face different challenges. Moreover, structural materials and inspection criteria also differ, with tailored standards for each type. International standards organisations also play a significant role in establishing these standards, which are essential for uniformity and reliability across the offshore industry, which are as follows:

- International Organization for Standardization, ISO 19900, Series of standards for offshore structures (ISO, 2019).

- API, Offshore standard, American Petroleum Institute (API, 2021).

Classification societies, which are non-governmental organisations, establish rules, which are typically linked to international standards. The rules and regulations governing the ultimate strength of offshore structures vary across regions. There are also national standardisation organisations that develop standards, such as NORSOK Standards N-series in Norway, the British Standards Institute (BSI) in the UK, Deutsches Institut für Normung (DIN) in Germany, and Danish Standards (DS) in Denmark. Many of these national standards closely relate to, and sometimes incorporate, parts of international standards (such as those of the International Organization for Standardization (ISO)), thus maintaining a level of alignment with global regulations while addressing specific regional needs.

Over the past decade, the offshore industry has increasingly focused on harmonising standards to ensure that offshore structures are designed and maintained to the same standard across different regions. Although there are some differences between standards, such as NORSOK and ISO, these are gradually becoming more aligned. One key difference lies in the frequency of updates. NORSOK standards are typically revised annually to incorporate minor adjustments, whereas ISO standards are updated less frequently, leading to longer intervals between revisions.

Differences in the standards for ultimate strength assessment also vary based on the application. For example, while ISO, NORSOK, and API standards are closely aligned regarding connection requirements, column buckling provisions are very similar in ISO and NORSOK. However, lateral pressure effects differ slightly, resulting in a higher computed capacity in ISO due to a larger safety factor. The use of safety factors also differs across these standards, with ISO applying varied material factors depending on the specific failure modes. NORSOK has recently updated its N-004 standard, adding supplementary material to address topside structures, bolted connections, and corrosion.

Design standards are continuously refined to enhance accuracy and address special cases or innovative designs. There is a growing trend towards advanced methods, such as non-linear finite element (FE) analysis. In support of this, a new Eurocode standard (CEN, 2023) is being developed, which outlines principles and requirements for numerical methods in steel structure design, particularly for ultimate limit state, fatigue, and serviceability limit state verifications. Additionally, classification societies have introduced detailed standards for FE analysis, such as DNV-RP-C208 (DNV, 2022b), a widely recognized guideline covering non-linear FE analyses for ultimate strength, accidental scenarios, and low-cycle fatigue. This guideline provides comprehensive instructions for FE modelling, including aspects such as material properties, mesh configurations, boundary conditions, analysis procedures, and post-processing.

In addition to the requirements mentioned above, offshore operators also have supplementary specifications for offshore structures, which vary depending on the company. The oil industry has a long tradition of cooperation between oil companies in the context of engineering standards, and the industry has recently developed common supplementary specifications for topside structures (IOGP, 2020) and for *Fixed Steel Offshore Structures* (IOGP, 2021). One of the objectives of this undertaking was to limit substantial budget and schedule overruns for oil and gas projects. The oil industry community have implemented an initiative which seeks to drive a reduction in upstream project

costs with a focus on industry-wide, non-competitive collaboration and standardization. It must be noted that these common supplementary specifications are not mandatory, and oil companies in IOGP may still use their own supplementary specifications for specific projects and offshore installations.

DNV provides a set of rules for assessing the strength of offshore structures (DNV-OS-C101, OS-C102, OS-C103, OS-C104, OS-C105, OS-C106, RP-0286, and RP-C208). Buckling assessments are covered in both the load resistance factor design (LRFD) format in OS-C101 and the working stress design (WSD) format in OS-C201; however, the WSD format (OS-C201) was retired in July 2023. Recently, DNV introduced a new voluntary class notation for hull girder strength in OS-C102 (Structural Design of Offshore Ship-Shaped and Cylindrical Units). This addition provides specific hull girder strength capacity checks, addressing the requirements of NORSOK N-004 Annex C that extend beyond the standard's basic requirements.

6 Benchmark Study

The previous benchmark study by the ISSC 2022 Ultimate Strength committee (ISSC, 2022a) highlighted the importance of assessing numerical methods based on the entire end-shortening curve of ship structures, rather than focusing solely on the ultimate capacity point. This is particularly crucial in scenarios where the dissipation of energy in a structure plays a significant role, such as hull girder failure under wave loading (Li and Benson, 2019). The maritime industry's shift towards high-strength steels, though beneficial for reducing hull weight, poses challenges in designing slender structures susceptible to elastic buckling, since while the yield stress is increased, the Young's modulus does not change significantly, complicating the design of such structures. While transverse loads may not be highly intense in ships with longitudinal structures, the low resistance to elastic buckling due to the aspect ratio of plating panels remains a concern. Ongoing international debates focus on the regulatory framework for buckling verification with transverse stress components (IACS, 2023a). A research project funded by Fincantieri in Italy (NBA - Non-linear Buckling Assessment, 2021) produced a full-scale test geometry to assess the structural response of slender steel ship structures to transverse loads. The structure was designed to induce local elastic instability at lower thresholds than its ultimate capacity to provide valuable insights into load redistribution across structural components.

The committee's benchmark study was designed to test researchers' predictive capabilities by having them generate end-shortening curves based on identical information provided to all participants. During the first two phases of the study, no experimental data were made available, allowing researchers to rely solely on theoretical models. In the third and final phase, participants proposed hypotheses to explain any numerical-experimental discrepancies observed.

6.1 Description of the Benchmark Study

The committee-coordinated blind benchmark study evaluated researchers' ability to predict the ultimate strength and non-linear response up to the collapse of a panel structure.

Participants were not provided with experimental results, highlighting the challenge of making accurate predictions based solely on limited data. The study was divided into three phases to assess how additional data and a more in-depth understanding of specific information could affect and potentially improve prediction accuracy. Participants were encouraged to apply their knowledge and expertise, with flexibility in selecting methods, finite element software solvers, numerical damping, element types, formulations, mesh sizes, imperfection modelling, material properties, boundary conditions, and other factors to assess ultimate strength capacity and post-buckling behaviour.

6.1.1 Benchmark Phases

Figure 30 outlines the workflow of the benchmark study, focusing on a full-scale physical model (see Fig. 31) manufactured by Fincantieri and tested at the University of Genoa, Italy. Following the approach of the ISSC 2022 Ultimate Strength committee (ISSC, 2022a), the study was divided into three phases (Phases 1 to 3). Building on the ISSC 2022 Ultimate Strength committee benchmark, the current study incorporated the actual specimen geometry, including imperfections, in the initial phase, with laser scans provided. In Phase 2, more information regarding material properties was disclosed, while in Phase 3, the participants fitted the actual experimental curve using their unique skills.

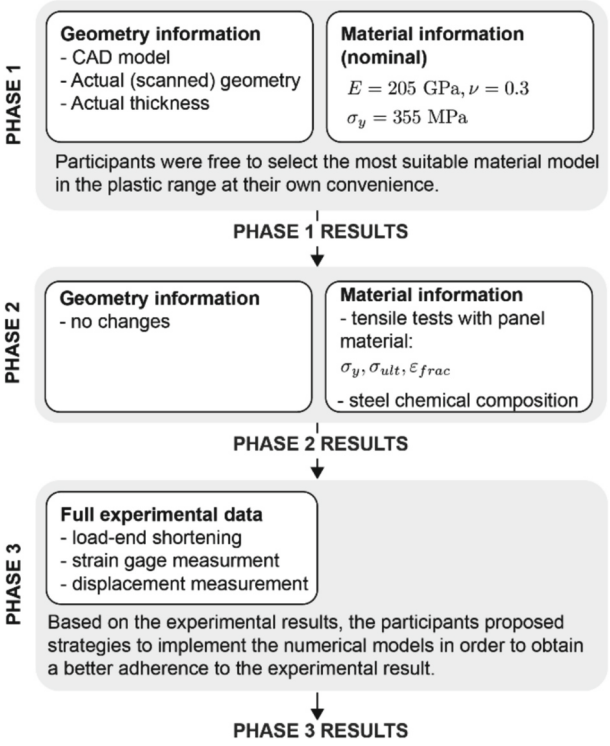

Fig. 30. Benchmark flowchart.

6.2 Description of the Experiment

6.2.1 Setup of the Experiment

Thanks to a collaborative partnership with Fincantieri, the committee was given access to the results of physical experiments on a large-scale structural component. The test structure, depicted in Fig. 31, underwent longitudinal compression until collapse using two 150-ton capacity actuators. These actuators were linked to a shared hydraulic system to ensure uniform internal pressure, with the opposite end of the structure entirely fixed. The setup was designed to ensure equal transmission of external forces to the specimen. Custom jack heads were used to fit precisely within the reinforced structure at the specimen's edge, minimising tolerances and enabling the external edge to withstand concentrated forces. However, machine compliance was not measured, and all results exclude this factor.

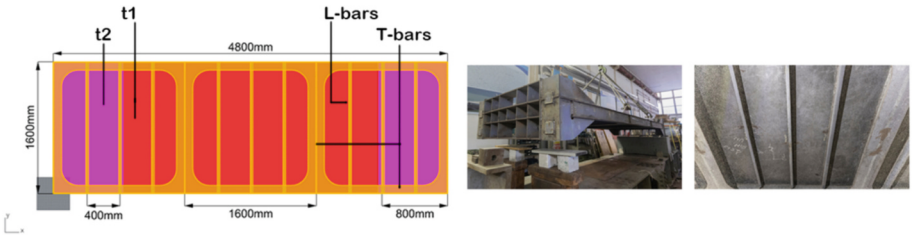

Fig. 31. Panel geometry and detail of the central bay of the as-built panel.

The experimental test, conducted by MaSTeL (Marine Structures Testing Lab) at the University of Genoa, involved several measurements, including:

- Axial displacement of the loaded edge.
- Axial displacement of the fixed edge to evaluate potential deformation of the supporting structure.
- Data collected by four load cells on the fixed edge, providing vertical support to the panel and addressing uncertainties from the friction of supporting elements.
- Active loads applied by the actuators, specifically two on the loaded edge, for comparison with the axial load measured by the load cells.
- 40 measurements of different strain components obtained through 16 strain gauges (12 rosettes and 4 linear gauges).
- Two high-definition videos of the shell plating captured from different angles, featuring markers on the plating suitable for 3D reconstruction.

6.2.2 Panel Geometry

The designed test panel, divided into three bays with transverse stiffening and frames, aimed to induce early local elastic buckling and achieve a substantial post-buckling range before the ultimate load. This design considered both the structural aspects and the dimensions of the laboratory test bench. The panel's slenderness was determined based on Fincantieri's construction geometries, addressing regulatory challenges for

local instability criteria. While these geometries are uncommon in cargo ships, they establish standards for weight-minimising constructions. The dimensions and thicknesses of various structural elements of the panel were as follows:

- Plates: t1 = 4 mm, t2 = 8 mm, where t2 represents the thickness of plating extending longitudinally 850 mm from the ends and t1 the one of the central parts of the panel (see Fig. 31: the red area represents the t1 area which is 4 mm thick).
- L-bars: 60 × 5 × 30 × 5 mm (hw × tw × bf × tf), transverse ordinary stiffeners.
- T-bars: 150 × 6 × 100 × 6 mm, extending longitudinally along the longer edge of the panel and transversally at the end of each bay.

The use of varying plating thicknesses was intentional to prevent collapse at the panel ends, effectively defining a clearer experimental focus area. The panel material was DH36 steel.

6.2.3 Geometrical Imperfections

The shipbuilding standard IACS Rec 47 (IACS, 2021) was considered in the panel fabrication, with a maximum limit of 8 mm for plate imperfections between frames and a standard of 4 mm. The panel manufactured by the shipyard exhibited significant geometric imperfections, with deviations from the average plane of the plating reaching up to 6 mm in the most deformed areas, particularly in the two end intervals where a greater plating thickness was chosen to mitigate edge effects. Hence, the panel exceeded the IACS standard for fairness of plating between frames but still complied with the maximum imperfection limit. Additionally, the common stiffeners displayed a noticeable tilt relative to the welding angle onto the plating. In response to these imperfections, a decision was made to conduct a laser scan of the panel geometry from its flat side to accurately document the deviations of the plating from its mid-plane, see Fig. 32. Furthermore, 3D reconstructions were carried out based on local scans to ascertain the tilt angle of the common beams, as illustrated in Fig. 32. Unfortunately, a complete 3D reconstruction of the full panel specimen was not available as alignment of scans was not maintained during the scanning process.

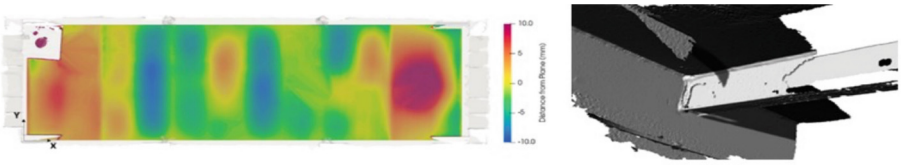

Fig. 32. Deviation from the best-fit plane (left) and example of 3D reconstruction of some details (right).

6.3 Phase 1 Results: Numerical Assumptions

The participants of the benchmark study were provided with the following information:

- An IGES format CAD model of the test specimen.
- Laser scan data file capturing the flat surface of the specimen.

- 3D reconstructions of all connections between common reinforcements and primary beams, along with mid-span areas of individual reinforcements.
- Map of thickness measurements obtained using an ultrasound probe in various areas of the specimen.
- Limited information on material properties: Young's modulus ($E = 205$ GPa), Poisson's ratio ($\upsilon = 0.3$), and yield stress ($\sigma_y = 355$ MPa).
- Fully clamped boundary conditions at the panel's ends.
- No residual stresses were considered.

The participants were encouraged to utilise engineering judgement and expertise when data were not explicitly provided. This included devising strategies for incorporating initial geometrical imperfections and selecting an appropriate non-linear material model. Four FE software packages were used, with ABAQUS being the most popular (9 out of 16 groups). Other software used were LS-Dyna, NX-Nastran and Marc. All participants chose a 4-node shell element, except for one who preferred an 8-node element. The preferred mesh size was 20 × 20 mm, but ranged from 12.5 × 12.5 mm (used by one participant for specific details) to a larger mesh size of 50 × 50 mm for the entire group. Three participants opted for an explicit analysis. The interpretation of initial imperfections is of interest, as seven out of fourteen participants decided to disregard the shape provided through laser scanning, opting for alternative strategies based on their experience.

One participant among the sixteen who submitted results in Phase 1 had significantly different values, and this outlier was excluded from the current analysis. The end-shortening curves from the remaining fifteen participants are shown in Fig. 33 (left). Different modelling strategies for initial imperfections are represented by red for eigenmode imperfections, black for laser scanning-based geometry approximations, and blue for alternative representations. Four teams treated the model as perfectly plastic, while the remaining twelve assumed a work-hardening behaviour, applying a modulus of 1000 MPa with minimal variations. Table 2 presents a summary of the modelling assumptions of each participant and the deviations from the mean values of ultimate strength (K and n are material parameters in the Ramberg-Osgood relationship).

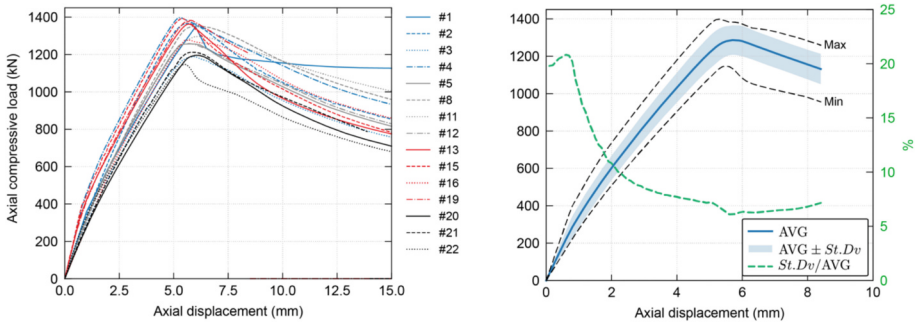

Fig. 33. (Left) The resulting end-shortening curve after Phase 1 of the benchmark study, and (right) average values and dispersion.

Table 2. Salient modelling assumptions of participants and resulting ultimate strength (I: implicit solver; E: explicit solver; E.M. #: eigenmode, # buckling shape number).

Participant	Software	Mesh size	Element: nodes, int. Points, sect. Points	Solver	Imperfection model		Ultimate strength	Deviation from average	Material hardening	Tan. Mod., or (K; n)
					Shape	Amplitude				
		[mm]				[mm]	[kN]	[%]		[MPa]; [-]
#1	NX-Nastran	50 × 50	QUAD4: 4, 4, 6	I	E.M. 1	2.0	1348.3	4.1	Yes	1000
#2	LS-Dyna	20 × 20	Type 16: 4, 4, 5	I	Mapped	6.0	1366.3	5.4	Yes	900
#3	ABAQUS	10 × 10	S4R: 4, 1, 5	E	Mapped	6.0	1188.6	-8.3	Yes (NL)	770; 0.161
#4	LS-Dyna	20 × 20	Type 16: 4, 4, 5	I	E.M. 1	1.5	1398.2	7.9	Yes	1000
#5	ABAQUS	20 × 20	S4R: 4, 1, 5	I	Sinusoidal	6.0	1256.7	-3.0	No	0
#8	ABAQUS	20 × 20	S4R: 4, 1, 5	I	Mapped	6.0	1351.8	4.3	Yes	1000
#11	ABAQUS	20 × 20	S4: 4, 4, 5	I	Mapped	6.0	1296.6	0.1	Yes (NL)	822; 0.164
#12	ABAQUS	19 × 19	S4: 4, 4, 11	I	Mapped	6.0	1258.0	-2.9	Yes (NL)	Swift-Voce model
#13	ABAQUS	12.5 - 50	S4R: 4, 1, 5	E	Only tilt	-	1362.7	5.2	Yes (NL)	790; 0.01
#15	LS-Dyna	20 × 20	ELFORM 2: 4, 1, 5	E	Not used	-	1393.8	7.6	No	0
#16	ABAQUS	25 × 25	S8R: 8, 5, 5	I	Mapped	6.0	1276.7	-1.5	Yes (NL)	606; 0.479
#19	ABAQUS	15 × 15	S4R: 4, 1, 5	I	E.M. 1–5	0.8	1382.6	6.7	Yes (NL)	750; 0.154
#20	LS-Dyna	20 × 20	ELFORM 2: 4, 1, 5	E	Mapped	6.0	1195.6	-7.7	Yes	
#21	Marc	20 × 20	ELEMENT 75: 4, 4, 5	I	Mapped with tilt	6.0	1212.2	-6.4	Yes (NL)	799; 0.171
#22	ABAQUS	20 × 20	S4: 4, 4, 5	I	E.M. 1	2.0	1147.9	-11.4	Yes (NL)	794; 0.11
					Average value		1295.7			
					Standard deviation		80.3			

Averaging and dispersion calculations were applied to the results from different participants, as illustrated in Fig. 33 (right). The average value curve (along with curves derived by adding and subtracting the standard deviation) is presented. The absolute maximum and minimum curves are also depicted, along with a curve representing the ratio of standard deviation over the average value, indicated on the right vertical axis. The maximum relative dispersion occurs in the initial phase of the curve for small applied loads, stabilising at approximately 6% of the average load until reaching the ultimate load. A possible explanation for this phenomenon is discussed in the following paragraph. The increase in dispersion slightly increases again in the post-collapse region after the ultimate load is reached.

6.3.1 Effects of Initial Imperfections

The numerical curves in Fig. 33 reveal a key characteristic of the early stages of the behaviour of the specimen. The elastic buckling load threshold is low, as planned in the design phase of the test, primarily due to local instability in the elementary plating panels. This unique characteristic leads to a sudden change in stiffness and the slope of the end-shortening curve upon reaching the threshold. Initial stiffness varies significantly among different models, with the stiffest showing a pronounced change in stiffness at the first critical load threshold. However, some models with lower initial stiffness do not exhibit a clear transition to post-buckling behaviour due to instability in the plating panels.

The variation in initial stiffness is linked to how geometric imperfections were interpreted. Models without shell plating imperfections (#13 and #15), the one featuring combined eigenmode-type imperfections (#19), and the model incorporating a mode-one eigenmode imperfection with a 1.5 mm amplitude (#4) demonstrate higher initial stiffness and exhibit a noticeable shift due to local elastic instability. Models using a mode-one eigenmode imperfection with a larger amplitude of up to 2.0 mm (#1 and #22) display behaviour closer to models with actual measured imperfections, though they remain slightly stiffer. A comparable response is seen in the model with sinusoidal imperfections (#5), where the amplitude closely matches that observed on the actual specimen. It was noted that in the current study, no significant differences were observed in the results between those who used the stiffeners' tilt and those who ignored it in the imperfection model.

6.3.2 Ultimate Strength and Failure Mode

The average predicted ultimate strength was 1295.7 kN, with a standard deviation of 80.3 kN, equal to 6.20% of the average value. The average axial displacement at which the ultimate response occurred was estimated at 5.77 mm, with a standard deviation of 0.26 mm equal to 4.54% of the average value. Results ±one standard deviation are presented in Fig. 33 (right). The maximum value found exceeds the average ultimate load value by 7.9%, while the minimum value is 11.4% lower. It was difficult to find a certain correlation that links the effect of the salient modelling characteristics with the relative ultimate load value. In the first instance, the effect of the initial imperfections on the value of the ultimate load can be excluded, since the average value between only the results obtained from the curves with eigenmode type imperfection and the average value of the results obtained from the curves with real imperfection modelled according to laser scanning is very close (1255.5 vs. 1251.7 kN). Furthermore, the average curves ± one standard deviation are also very similar in the two cases.

6.3.3 Post Ultimate Response

There seems to be no correlation between predicting material model selection and the predicted peak load of the structure. Figure 34 (left) illustrates that averaging the results of perfectly plastic material models closely matches those incorporating hardening up to ultimate strength, with similar error bars. Most participants considered the work-hardening effect and selected a hardening modulus of around 1000 MPa. Each participant

described an identical collapse scenario, where a plastic hinge forms roughly at the midpoint of the specimen. This hinge corresponds to significant deformations concentrated on the beams' web aligned with the applied load, as shown in Fig. 34 (right). Unlike the observations related to ultimate strength, the behaviour post-ultimate is influenced by the material model, as depicted in Fig. 34 (left). Models assuming perfect plasticity show a converging post-ultimate response with minimal deviation. Conversely, models incorporating hardening exhibit a more dispersed pattern, with the lower error band closely aligning with results from perfect plasticity assumptions.

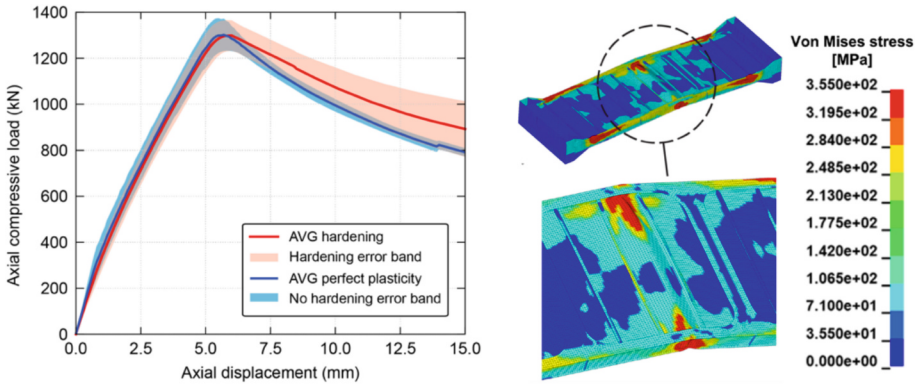

Fig. 34. (Left) Resulting end-shortening curves with and without hardening, and (right) collapse mode, as depicted by all participants with minimum variations.

A key takeaway from Phase 1 is the challenge in linking specific modelling parameters to their influence on predicting the structure's ultimate strength. However, the impact of initial imperfections on local buckling response in the shell plating, as well as the effect of the work hardening model on post-ultimate response, is more evident.

6.4 Phase 2 Results: Material Modelling

Phase 2 involved the sharing of information regarding the characteristics of the material used to construct the test panel. Information was provided about the chemical composition of the alloy used, which was obtained from a hot chemical analysis of samples collected during the production phase. Furthermore, the salient data of tensile tests on specimens extracted from the sheets with which the specimen was built, having different thicknesses, were shared, such as:

- yield strength,
- maximum engineering strength, and
- elongation at break.

The participants were asked to modify their numerical model from Phase 1 taking into account the newly disclosed material properties only, leaving the remaining parameters unaltered. In total, sixteen specimens were tested, the data of which were provided to the participants via the table presented in Table 3. The table also reports the average values

and standard deviations of the specimens derived from plating having thicknesses of 4 and 10 mm, as well as the total average and standard deviation of the whole set. In Phase 2, the participants were also asked to modify only the material properties, leaving all the other input parameters of the numerical model unchanged. In total, fifteen participants completed Phase 2.

In Phase 1, participants uniformly applied the same yield strength, making only minor adjustments to the work-hardening model. However, in Phase 2, with more detailed material information, participants interpreted the plastic behaviour of the material differently. Some tailored the material model to account for the varying sheet thicknesses. Notably, the 4 mm plating model saw substantial diversity in approaches, as illustrated in Fig. 35 (left). Participants adopted various hardening models, including:

- exponential model following the yield stress.
- an initial yield plateau followed by an exponential model.
- bilinear model.
- multi-linear model.

Table 3. Material data for steel DH36 (Young's modulus, $E = 205$ GPa) provided to the participants in Phase 2.

Specimen no	Thickness [mm]	Yield strength [MPa]	Engineering strength [MPa]	Elongation [%]
1	4	417	505	38.2
2	4	394	495	40.2
3	4	416	499	34.1
4	4	382	502	34.7
5	4	385	493	33.5
6	4	412	495	36.9
Average value		401	498	36.3
Standard deviation		15	4	2.4
7	5	398	494	39.4
8	6	387	497	38.3
9	8	399	529	31.8
10	10	395	546	
11	10	406	532	
12	10	397	529	
13	10	396	526	
14	10	389	533	
Average value		397	533	31.3
Standard deviation		6	7	2.9
15	12	425		

(*continued*)

Table 3. (*continued*)

Specimen no	Thickness [mm]	Yield strength [MPa]	Engineering strength [MPa]	Elongation [%]
16	12	392		

Such variations have implications for the structural response near and beyond the ultimate load, with a clear increase in the dispersion of the results in this phase, as highlighted by Fig. 35 (right). The slight deviation in the dispersion in the first section of the curve is not immediately explainable, since the differences compared to the first phase should only concern the structural response once the plasticisation has occurred in the model.

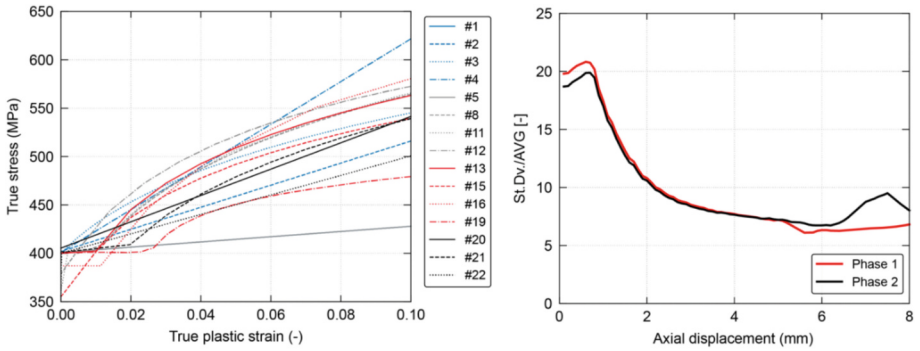

Fig. 35. (Left) True plastic strain vs. true plastic stress as interpreted by different participants in Phase 2, following the material data provided. (Right) Standard deviation of the end shortening curve over the average values observed in Phase 1 and 2.

Figure 36 shows the average of the end shortening curves ± the standard deviation obtained in Phases 1 and 2. The minimum and maximum values for the two phases are also shown. It can be clearly observed that, as expected, the results tend to differ only for high compressive load values capable of inducing a plastic response in the material.

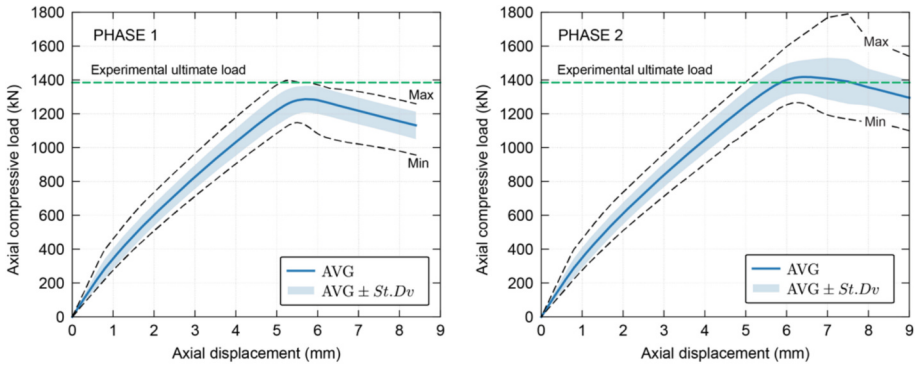

Fig. 36. The resulting average end-shortening curves after Phase 1 and 2, and standard deviation.

At the conclusion of Phase 2, participants received the experimental results, including the measured ultimate compressive force, which is shown on the graph. This additional material data led to numerical results that aligned more closely with the experimental findings, though the flexibility in interpreting the material model contributed to a wider spread in numerical outcomes. Specifically, the average ultimate strength from Phase 1 underestimated the experimental value by 7.47%, whereas in Phase 2, it was overestimated by 1.98%. This progression illustrates how detailed material information can improve accuracy, while also highlighting the impact of varied modelling assumptions on result dispersion.

A key takeaway from Phase 2 is that the additional material data provided to participants generally enhanced the accuracy of the numerical predictions. However, varied interpretations of the plasticity model led to increased result dispersion, underscoring the influence of modelling assumptions on prediction consistency.

6.5 Phase 3 Results: Interpretation of Experimental Results

In Phase 3, after sharing the experimental data, the participants were asked to formulate hypotheses about the modelling parameters to explain the numerical/experimental discrepancies. Following a collegial discussion, it was agreed that the experimental curve shows that boundary conditions changed during the experiment, as shown by the four distinct changes in the experimental curve in Fig. 37. It can also be seen that there is an initial settlement in the experiment followed by 3 drops in load corresponding to support failures. This was not considered in Phase 1 and 2 efforts. It was decided to proceed in separate working groups, each of which with the task of investigating a specific task and its effect on the load-end shortening curve. Three participants focused on the effect of welding residual stresses while two participants investigated constraint conditions that best represented the reality of the experiment without adding residual stresses to their models. Finally, a participant attempted to introduce a different modelling strategy, representing the shell plating through three layers of solid elements, connected by constraint equations to the shell elements still used for the representation of the beams. The solid mesh was created by mapping the actual imperfections of the panel. The participant

observed an increase in the ultimate load of less than 0.5% for Phase 2, with no significant effects observed in the post-ultimate stage. Therefore, for analyses involving thin plating, using solid modelling is generally not recommended due to its complexity and time requirements. Instead, shell or plate elements are often more efficient and sufficient to accurately capture the structural response without the added computational burden of solid modelling.

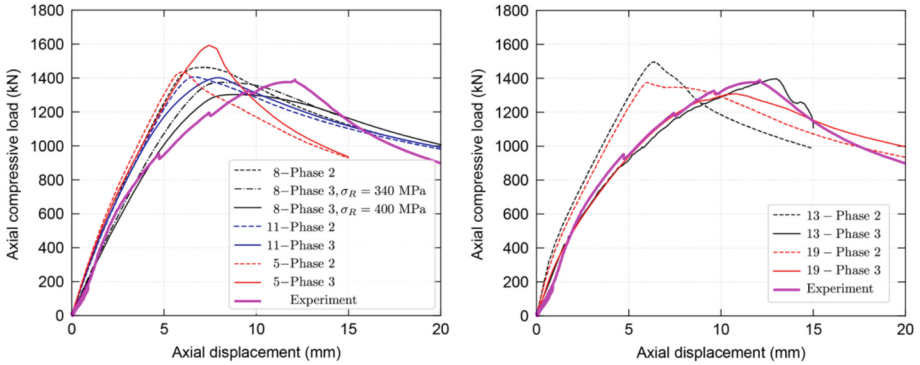

Fig. 37. (Left) Effect of residual stresses. End shortening curve after introducing residual stresses and the Phase 2 curve from the same participants. (Right) The effect of modified boundary conditions.

6.5.1 Effect of Residual Stresses

Three participants incorporated residual stresses due to welding in their models. Participant #8 applied a simplified thermal model targeting residual stress levels of 340 MPa and 400 MPa, as per the Eurocode (CEN, 2023). Participants #5 and #11 followed the approach by Yi et al. (2018), detailed in Paik (2018), directly inputting the stress field and verifying that the residual values matched their target after convergence. Participant #11 maintained a residual-to-yield stress ratio of 0.85 across all materials and thicknesses throughout the structure's welds, yielding a residual stress of 340 MPa in the same areas as Participant #8. Participant #5, however, limited residual stresses to the main parts of the test specimen, excluding the surrounding loading frame.

Participant #8's results indicate a clear effect of residual stresses, showing a reduced ultimate load compared to Phase 2. Participant #11's results also displayed a slight reduction in ultimate load, accompanied by lowered stiffness and greater displacement at peak load. When a residual stress of 400 MPa was simulated, similar to Participant #8, the ultimate load reduction was more pronounced. Interestingly, Participant #5's model showed an increase in ultimate load. A plausible hypothesis is that the residual stress field applied in this model may not be fully self-equilibrated across the shell panel, resulting in residual tensile stress on the beams, which could enhance the ultimate strength of the specimen, as the collapse mode in compression involves beam buckling. Despite these variations, all models demonstrated a stiffness reduction more consistent

with experimental observations. However, residual stresses alone do not fully account for the numerical and experimental discrepancies.

6.5.2 Effect of Modified Boundary Conditions

Further investigation of end conditions was conducted. Using axial displacements evaluated at multiple points, it was possible to develop an estimate of the rotations at the ends of the panel about the transversal *y*-axis. The evaluation is presented in Fig. 38. It is observed that while the rotation is negligible at the loaded edge (actuator side), there is significant edge rotation at the fixed side. After stabilising at 0.1 degrees, the rotation increases dramatically following failure at the end support at 930 kN, after which the rotation increases linearly until the next support failure begins just before 1200 kN.

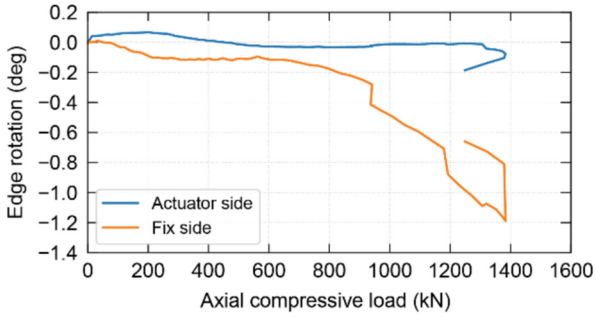

Fig. 38. Evaluation of rotation at edges during the experiment about the transversal *y*-axis.

Motivated by this finding, two Phase 3 participants investigated the role of boundary conditions and machine compliance on the predicted results. Participant #19 analysed the data from the displacement sensors placed at the two ends of the test panel and hypothesised different constraint conditions at the two ends; see Fig. 39. In particular, the absence of rotation was noted at the loaded end, while on the side in contact with the load cells, the boundary conditions were modified according to the following scheme:

- The load cell that consistently indicated a compressive load equal to zero was considered not in contact and consequently the area was left completely free.
- One support was considered perfectly clamped.
- The other two were left free to rotate about an axis transverse to the direction of application of the load.

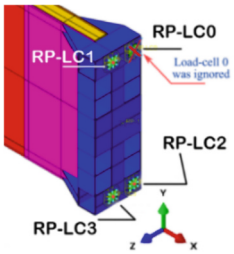

DEGREES OF FREEDOM						
	U-x	U-y	U-z	Ur-x	Ur-y	Ur-z
RP-LC0	free	free	free	free	free	free
RP-LC1	fixed	fixed	fixed	fixed	free	fixed
RP-LC2	fixed	fixed	fixed	fixed	fixed	fixed
RP-LC3	fixed	fixed	fixed	fixed	free	fixed

Fig. 39. Boundary conditions simulated by participant #19.

The correspondence with the experimental curve is excellent up to approximately 1300 kN, as seen in Fig. 37 (Right). However, after this point, the model tends to slightly underestimate the load compared to the experimental curve.

In Phase 3, Participant #13 explored the impact of the loading frame's elastic compliance on structural response, as illustrated in Fig. 37 (right). This analysis employed load pads at the loaded end of the frame to replicate the spring-like behaviour of the elastic compliance system. The load pads were modelled as $100 \times 100 \times 2.5$ mm^3 thin square plates and were positioned at one end of the frame. Normal-hard contact and surface-to-surface contact between the load cell and frame were defined in ABAQUS/Explicit. A reverse-engineering iterative approach determined that a load pad with an elastic modulus of 300 GPa and elastic-perfect plastic behaviour with a yield stress of 355 MPa produced the best fit to the experimental data. Although this setup improved correlation with experimental results, it failed to account for support failures and sharp load drops in the load-shortening curve. This suggests that the observed numerical/experimental discrepancies may stem not only from the elastic compliance system of the load frame but also from complex constraint conditions that are challenging to model accurately.

6.6 Comparison with CSR and UR-S35

One motivation for the experimental test in the benchmark study was to demonstrate that a stiffened plate has reserve strength beyond elastic buckling. In the current formulae for buckling in CSR and UR-S35 (IACS, 2024), local elastic plate buckling is accepted, and the plate can have a reserve above local elastic buckling; however, global elastic buckling is not accepted since this will result in stress redistribution over a larger area, and global elastic buckling is a rather unstable failure mode. In this section, the ultimate load computed by CSR is compared with the non-linear FE analyses calculated for the benchmark study. As mentioned in Sect. 4, these rules are applicable to more than 90% of the ships all over the world.

The computed ultimate stress by CSR for the stiffened plate is equal to 45 MPa, and this corresponds to a force equal to 568 kN which is rather conservative compared to the results obtained by the experimental test and non-linear FE analyses. The reason for the conservative results computed by CSR is that global elastic buckling (i.e., stiffener and plate buckles together out-of-plane) is the critical failure mode and this is a cut-off limit in the rules. This is a sound design principle to prevent very slender stiffeners. It can also be mentioned that the yield strength will not affect the computed strength by

the rules, since global elastic buckling is independent material yield strength as studied in the different phases of the benchmark study.

In some rule frameworks, such as in the DNV Ship Rules (DNV, 2023), the use of non-linear FE analysis is permitted. However, these rules stipulate that global elastic stiffener buckling must be verified separately through eigenvalue analysis to ensure it does not occur. The ultimate capacity is defined as the lower of the global elastic buckling load or the load determined by non-linear FE analysis. In this case, the global eigenmode obtained through FE analysis yields a buckling load of 891 kN, with the associated buckling mode (eigenmode 13) shown in Fig. 40. Thus, within this rule context, global elastic buckling becomes the critical factor since it occurs at a lower load than the maximum achieved in non-linear FE analysis. The computed buckling load from the FE analysis is notably higher than that from the CSR approach. This difference is partially due to boundary conditions: in CSR, the stiffeners are modelled as simply supported, whereas in the FE model, they are welded at the ends, introducing some rotational restraint. This boundary condition significantly influences the global elastic buckling load, making it more sensitive. When plates are simply supported, the results align more closely with those from CSR.

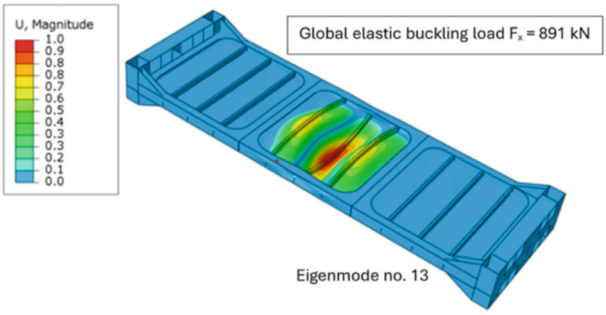

Fig. 40. Global elastic buckling load computed using finite element analysis.

6.7 Concluding Remarks

The results obtained from the committee's benchmark can be summarised as follows.

- Despite all participants using the same input geometry and being given limited modelling parameters in Phase 1, the results displayed considerable variation. This variation underscores the extent to which non-linear FE analysis outcomes are still heavily influenced by user decisions.
- It appears difficult to find a correlation between the effect of the salient modelling characteristics and the relative ultimate load value.
- Variations in the choice of initial imperfection models had a significant impact on the early part of the end-shortening curve, particularly affecting the local buckling response of the shell plating. However, this did not substantially influence the ultimate strength. Nonetheless, differing initial stiffness may lead to varying load redistributions across structural components. It is recommended, therefore, to use real imperfections where possible or to apply an initial imperfection pattern derived from

an eigenvalue analysis with a sufficient amplitude (at least 1.5 mm in this study) to prevent abrupt stiffness changes due to local buckling of the plating.

- Providing data on the yield and engineering ultimate strength of the material is not sufficient to reduce the modelling uncertainties. The participants of this benchmark study formulated different assumptions on the work hardening model, which increased the dispersion of the results.
- Welding-induced residual stresses show a non-negligible, effect on the end-shortening curves. However, the effect on the ultimate strength is still unclear and doubts remain about the correct modelling strategy to introduce this stress field into the model.
- The correct set of experimental boundary conditions appears difficult to deduce. However, the availability of displacement data from multiple measurement points in the experiments enabled the formulation of hypotheses regarding the actual boundary conditions, which were essential to refine the numerical/experimental comparisons. It is therefore recommended that experiments should acquire the axial displacements at intermediate frames as well as panel ends as well as monitor all degrees of freedom at the panel ends to be able to more effectively reconstruct the exact boundary conditions.
- Overall, the Phase 3 simulations and analyses indicate that including welding residual stresses in the model achieves an excellent match with the experimentally measured specimen stiffness, as particularly demonstrated by participant #8 in Fig. 37 (left). However, the numerical model begins to diverge from the experimental data at the first fluctuation in the experimental load, around 950 kN of compressive force. This fluctuation is attributed to the failure of one of the panel supports, leading to a subsequent change in the boundary conditions. To accurately replicate the experimental observations from this point onward, it is necessary to adjust the boundary conditions in the numerical model (see Fig. 37, right).

7 Conclusions, Trends and Recommendations

The committee's report presented a review of published work relevant to the committee's mandate along with results from a benchmark study with submissions from researchers inside and outside the committee. This section summarises the committee's essential findings/trends and offers recommendations for the community to further improve its understanding of the ultimate strength of ships and offshore structures.

7.1 Conclusions and Trends

The committee has identified four areas where the reviewed literature shows important progress during the mandate period: uncertainties/scale effects, numerical methods, multi-scale and multi-physics simulations, and the need for life-cycle management procedures.

Sections 2 and 3 focus on the aspects fundamental to ultimate strength prediction and uncertainties. The influence of scale effects and factors on the material level and the geometry's size (compared to, e.g., sheet thickness) have received much attention during the reporting period. Structures are characterised by load-end-shortening, pressure-displacement, or other similar relationships that are analogous to the stress-strain curve

at the material level. However, the shape and characteristics of these relationships are much more complex due to various uncertainties.

Epistemic and aleatory uncertainties remain a central challenge in determining the ultimate strength of ships and offshore structures. The roles of various factors, such as geometry, imperfections, material properties, residual stresses, boundary conditions, loads, flaws, and their interdependence are best understood through continued physical testing, monitoring of real-world structures, and the development and benchmarking of numerical methods. Furthermore, the role the analyst plays in decisions of what to include in the analysis and how to conduct it remains a significant factor in the outcome of non-linear FE analysis predictions.

The increasing shift from traditional steel structures to lightweight constructions, e.g., aluminium alloys and composite materials is anticipated to continue, and this necessitates continued research. For example, further study is needed regarding initial imperfections of extruded aluminium structures, particularly where friction stir welding or other novel welding techniques are utilised. For composites, major challenges exist in the effective incorporation of material defects, such as delamination, in large-scale structural models. Features, such as welding-induced distortions and corrosion damage, tend to be more realistically simulated in modelling work using the 3D profilometry technique. However, scaling up from the structural element level to the system level remains challenging.

Research efforts focusing on the role of dynamic and cyclic effects are particularly noteworthy, as this area has been under-explored until recently. Recent studies have examined the role of inertia, structural damping, and strain rate effects as well as low-cycle loads in association with crack simulations. Analyses showing that the ultimate strength capacity can be reduced highlight the need for further efforts on these topics, including testing to validate numerical simulations.

Various experimental studies have been conducted since the last report examining the ultimate strength of model and full-scale structures. These efforts provided valuable data but also highlighted the challenge in controlling tests of large-scale objects with regard to control of load application and the boundary conditions. This is particularly noteworthy in the committee's benchmark study where changes in boundary conditions during the experiment were not captured in numerical simulations. Control of the initial stiffness and the boundary conditions, which can greatly affect the collapse sequence and behaviour, and the post ultimate characteristics, is crucial to the value of such efforts.

The effects of various environmental conditions, such as temperature, corrosiveness, or moisture on the material properties in combination with loading effects have been explored via experiments on either a material or component length scale in order to understand the effects of these conditions on ultimate strength. Other experiments have been presented from model to full scale for panels and grillage structures. These have often been conducted to validate numerical simulation procedures.

The committee has seen progress in the development of numerical methods divided into different categories. Fast-running or practical codes such as the Smith method are still used. However, their developments have been minimal due to faster computation resources and easy-to-use CAD and computation tools. Conventional FE methods are the

predominate numerical method, most likely due to the readily available nature of commercial software, whereas other methods, such as the ESL, ISUM and ISFEM, have been reported in the literature as promising alternatives for large-scale and complex structure elements but appear to receive less use. The use of machine learning (ML) and physics-informed neural network (PINN) methods is increasing, especially in studies related to a large number of input parameters with uncertainties, such as structural health monitoring and diagnostics of aged ships and offshore structures where the ultimate strength capacity is reduced due to, e.g., corrosion and accumulated plastic deformation. The most exciting development originates from the aerospace industry, which has developed a framework (the NASMAT software) in which multi-physics, multi-scale materials, and structural analyses are coupled into one seamless modelling package, building on multi-scale structures modelling research.

The ISSC 2022 Ultimate Strength committee (ISSC, 2022a) reported that life-cycle management methodology had become more widely adopted in the literature. This trend has continued during the mandate period of the current committee, and there are examples of studies emphasising the prediction of (residual/effective) ultimate strength capacity. The progress identified by the committee originates from the fact that it is practically impossible to define the ultimate strength capacity at full scale during the lifetime, and thus, computational methods and various level simplifications are needed that affect the sequence of failure from the material to the hull girder level. The development of AI-based tools and methods to create digital twin models, which could include ML-based data or a PINN-based approach, offers the opportunity to more effectively utilise large databases of sensing/inspection records and hence more realistically monitor a structure's structural health as well as the ultimate strength capacity to assist life-cycle management/decision making of the structure.

Section 4 presents the influence of structural configuration, components, and loads on ultimate strength. Compared to previous committee reports, our review notes that dynamic effects and complicated loading scenarios are receiving increasing attention. Recent studies have demonstrated the importance of non-linear wave shapes on wave-induced VBM, which becomes more pronounced in large waves. Traditional linear methods may underestimate the wave-induced VBM because they do not account for the non-linear effects of wave shape. Moreover, incorporating complicated loading scenarios, and non-linear wave shapes, in the design for ultimate strength allows consideration of more realistic loading scenarios (dynamic and non-linear effects) and scenario-based modelling, which should result in higher fidelity ultimate strength analysis. These should also consider dynamic load effects on the ultimate strength from, e.g., whipping and sloshing loads. Another load-related topic is cyclic loading and its accumulation of residual strains and displacements (local and global levels) that affect the ultimate strength capacity in the long term. This effect, together with the influence of corrosion and the possibility of reaching a plastic shakedown response, is recommended to be investigated in more detail.

Empirical formulae are still being developed, particularly to account for different loading conditions and applications. In the shipping industry, there is also a significant focus on harmonising the buckling formulae to obtain one common buckling procedure. For instance, IACS is working on harmonising the procedures for local buckling checks

and the new set of rules will cover 90% of the global fleet. The empirical formulae are also increasingly being replaced by machine learning models that demonstrate better accuracy. Future work may focus on the development of more advanced machine learning models for strength assessment, integrating inspection data into finite element models, and exploring the application of data-driven approaches in ship structural design to reduce reliance on expensive numerical simulations.

The committee found that there is an increasing trend towards accounting for realistic loading scenarios as well as the in-service condition of ships as it relates to ultimate strength analysis. With the increased proliferation of full-field 3D measurement and inspection techniques, inspecting and quantifying distortions during inspection activities or even continuously during operations is possible. This has led to the development of structural digital twins, with inspections, 3D measurements, and sensors providing inputs to model updates. These digital twins can be used as the basis for real-time evaluation of ultimate strength, providing safer ship operations and timely warnings of potentially dangerous combinations of loading and structural conditions.

FE analysis results that account for realistic loading and structural condition inputs are needed to accomplish this goal. These results must then be transitioned to user-friendly reduced-order models, often using ML methods, that are suitable for integration into ship operations. Therefore, the committee recommends continued development of ML-based and other reduced-order models based on high-fidelity computations.

Section 5 presents the recent development of the knowledge and methods on the ultimate strength of various offshore structures and related components. In general, studies on the ultimate strength of oil and gas offshore structures have declined since the committee's last report, which is attributable to the ongoing global green energy transition from fossil fuels to renewables. The global shift towards cleaner and more sustainable energy sources has driven unprecedented growth in offshore structures throughout the reporting period. These structures play a central role in the global energy infrastructure, serving as a cornerstone for the swift advancement of the offshore industry, notably in the renewable energy sector. They play a pivotal role in harnessing the vast potential of offshore wind and tidal energy, ensuring the resilience and durability of these installations in challenging marine environments. The significance of comprehending and enhancing the ultimate strength of these structures cannot be overstated, as it directly correlates with the reliability, safety, and longevity of our offshore energy endeavours, ultimately contributing to a more sustainable and environmentally responsible future.

The rapid expansion of offshore wind energy has introduced new technical challenges, particularly in understanding ultimate strength under extreme operating conditions and unusual load cases. For instance, ship collisions with operational floating wind turbines can severely impact the residual strength of these structures, necessitating detailed research to enhance resilience and safety. Hydrodynamic loads caused by breaking waves can significantly increase the structural demand and may contribute to conditions approaching the ultimate limit state, particularly in shallow water or nearshore environments. The construction of offshore wind turbines in sub-Arctic areas, such as the Baltic Sea and the Bohai Bay, presents a unique challenge, primarily due to sea ice.

Recent trends in the design and longevity assessments of offshore structures emphasise advanced, integrated approaches that enhance safety, reliability, and sustainability

in marine environments. Extensive research on the ultimate strength of structural elements has been conducted over the past decades; however, further advancements could be achieved by leveraging machine learning and digital twin technologies to improve predictions of buckling and post-buckling behaviour. Recent publications have shown that life-extension decisions could significantly benefit from big data analysis using machine learning to establish precise relationships between variables influencing the life-cycle performance of, e.g., offshore wind turbines.

The variety of offshore structures is increasing, expanding to include structures such as oil and gas platforms, floating offshore wind, wave energy converters, photovoltaic platforms, and aquaculture installations. During the reporting period, there has been an increasing interest in mooring designs and ultimate strength assessment of the moorings of these structures. Additional research is essential to ensure safe and reliable mooring designs that account for ultimate strength, particularly for dynamic power cables, which in some structures are suspended freely in the ocean. At a system level, studies on the structural integrity and failure mechanisms of offshore wind farms have also become a key focus area. In addition to conventional research areas, such as system reliability analysis and corrosion-affected components, a few real case failure incidents of offshore wind farms, such as blade breakage from the wind turbines and falling into the sea, highlight new technical challenges in the design of large offshore wind farms and how failure incidents impact ships and other offshore structures or infrastructures. A holistic research approach, which considers technical, economic, societal and environmental aspects, is crucial for the large-scale deployment of offshore wind farms. From a structural perspective, this includes ensuring the reliability and safety of support structures through a comprehensive assessment of ultimate strength, fatigue performance, and degradation mechanisms under long-term environmental exposure.

One evident observation regarding guidelines and regulations is that, while well-established for the oil and gas industry—despite occasional improvements or adjustments—they remain limited for offshore renewable energy exploration. Anticipated guidelines should address specific aspects such as site-specific environmental loading, fatigue and ultimate strength criteria for novel structural configurations, material degradation in marine environments, and design provisions for modularity, maintenance, and decommissioning. These elements are critical to ensure the safety, reliability, and long-term performance of offshore renewable energy structures. Furthermore, many models and methods proposed in academic research hold potential for practical application, though only some have been implemented in the field. Therefore, increased collaboration between academia and industry is needed to ensure that these innovative approaches are effectively implemented in real-world offshore engineering projects. This collaboration can bridge the gap between theoretical advancements and practical applications, ultimately enhancing the safety, reliability, and efficiency of offshore structures.

Section 6 presents the benchmark study coordinated by the committee, involving participants who were internal and external to the committee. As in the benchmark study reported by the committee in the ISSC 2022 report (ISSC, 2022a), the benchmark for this report was divided into three phases. Participants were first furnished identical information related to the modelling task, without access to experimental data in the first two phases. They were then required to propose a series of hypotheses to explain the

observed discrepancies between the numerical and experimental results. Following the recommendation by the Official Discusser in 2022, the current benchmark study aimed to investigate the ability of analysts to predict the end-shortening curve, i.e., the entire load-response path, including post-collapse behaviour. The results obtained from this benchmark can be summarised as follows.

Despite the growing reliability of non-linear numerical models and the availability of increasingly precise experimental data (from multi-point displacement sensors, strain gauges, and digital image correlation, for example), tracing the sources of discrepancies between numerical and experimental approaches has become more complex as data volume and precision increase. This challenge arises partly because, even with ample knowledge, it is easy to focus on detailed analysis rather than the overall system response.

- The results from Phase 1 were rather scattered despite little freedom for an analyst to make assumptions related to the boundary conditions, load, or material modelling; such a varied interpretation of the geometric imperfections by the participants was not foreseen, having been provided by the actual geometric imperfections of the structure. It was not possible to identify a correlation linking the effect of the salient modelling characteristics (such as the FE solver selected, mesh size, and element type) with the relative ultimate load value and post-collapse behaviour. Hence, the results in this phase show, for the case studied, that the skill and overall judgement of analysts are uncertainty factors that are challenging to control or reduce without having strict modelling and simulation guidelines and procedures. This underscores the crucial need for such guidelines in our community. Existing guidelines provide limited practical advice on defining non-linear FE analysis. For example, DNV (2019) highlights the importance of accurately or conservatively representing real conditions, suggesting the use of sensitivity studies when uncertainty exists. ABS (2025) stresses the crucial role of boundary conditions in non-linear FE analysis and cautions against relying on assumptions from linear models. However, no practical examples specifically useful for the analyst are provided. While supplementary materials offer examples, these are often highly idealized.
- The modelling of geometrical imperfections greatly influenced the panel's stiffness in the initial loading phase, affecting load redistribution among the various structural components, as well as the failure sequence and post-collapse behaviour. The participants of the benchmark study compared different alternatives to model geometrical imperfections. The committee recommends modelling the structure using measured structural imperfections, when available, or using an initial imperfection obtained from modal analysis, preferably including the first three modal shapes. Analysts should take particular care in selecting appropriate amplitude magnitudes for these modal shapes, ensuring an adequate amplitude magnitude to correctly represent the initial stiffness (for the current specimen, the threshold identified was 2.0 mm for mode 1).
- Providing the participants with actual material data in Phase 2 did not reduce the scatter in results. The diverse selection of material models (such as yield plateau and work hardening) led to even greater variability than observed in Phase 1. This outcome reinforces the committee's recommendation to develop unified modelling and

simulation guidelines, ideally under IACS leadership with ISSC support. Nonetheless, addressing the dispersions in experimental data remains an open topic for further discussion.

- This committee did not work on defining an acceptable level of deviation in the results. However, it limited the work to photographing the current situation, where significant deviations were observed even when working with a relatively limited number of input parameters. Unfortunately, apart from the clear indications that emerged in the first phase regarding the initial geometric imperfection model, no trends were observed regarding the solver, element, or mesh size.
- Prior to the start of Phase 3, it was identified that the experimental data were significantly influenced by uncertainties related to the intended boundary conditions for the panel. Unfortunately, the designed boundary conditions were not consistently maintained during testing, while numerical models in Phases 1 and 2 adhered to the original boundary conditions as planned. Some participants incorporated the updated information about these shifting boundary conditions into their simulations and successfully achieved a close match with the entire experimental end-shortening curve.
- FE simulations were conducted to investigate the influence of welding-induced residual stresses on the end-shortening curve. The results show that, as expected, they have a non-negligible effect and should preferably be considered.

7.2 Recommendations

The committee presented an extensive literature review in this report and conducted a benchmark study. Several of the committee's members were members of the ISSC 2022 Ultimate Strength committee. Many of the recommendations made in the previous committee's report still apply, since a relatively long time is required to conduct studies and publish findings, develop and implement new methods, and revise guidelines and recommended practices. In addition to the committee's new recommendations, we echo some of the ISSC 2022 committee's recommendations (ISSC, 2022a) to ensure continuity in the development of specific topics and progress in broader research areas:

- Future studies conducted by academia, research institutes, and the industry should focus on developing more advanced machine learning models for strength assessment, integrating traditional inspection as well as LiDAR/3D geospatial data into FE models, and exploring the application of data-driven approaches in ship and offshore structural design to reduce reliance on expensive numerical simulations.
- Distortions resulting from fabrication processes should be incorporated into structural analysis to improve the accuracy of strength predictions. Depending on the stage of the design/assessment, these can be included from actual measurements, idealised distortions, or from modal analysis, where several modes are mapped on the geometry.
- This report emphasises the importance of utilising advanced monitoring and inspection techniques to update FE models and create digital twins that reflect the actual state of the structure. User-friendly practical tools and interfaces need to be developed to minimise uncertainty as a result of the skill level of the analyst.
- Once the failure mode has been validated via a comparison of results from numerical simulation and experiment, any discrepancy in terms of ultimate capacity can

be evaluated by investigating aleatoric and epistemic uncertainties in the numerical model and the experiments.

- Shell elements currently provide a well-balanced approach for modelling large structures. Future advances in computational power could make large-scale models using solid elements more feasible. The development of ESL (Equivalent Single Layer), ISUM (Idealised Structural Unit Method), and ISFEM (Incremental Structural Finite Element Method) should also be pursued for large-scale applications. Reduced-order models are increasingly proposed in the literature but often lack direct comparisons with new or established models. The next committee is advised to include these comparisons in a benchmark study to assess the strengths and limitations of each model.
- Multi-scale and multi-physics frameworks, such as the NASMAT software originally designed for aerospace applications hold significant promise for transforming design methodologies for ships and offshore structures, promoting sustainability throughout their service lives. Although this may extend beyond the current committee's direct focus, it is highly pertinent to the ISSC and aligns with the committee's mandate, as it intersects with ultimate strength, life-cycle management, and life-cycle engineering principles.
- Future research is needed to better predict/quantify the material degradation processes (e.g., corrosion, repeated plastic deformation, development of cracks), especially when new materials are increasingly used for ship and offshore constructions, and to better incorporate the human element (from fabrication to operation) into the analysis.
- The committee did not find any specific studies on the ultimate strength of wind assisted propulsion systems (WAPS), or indeed vessels with WAPS installed. However, the WAPS technology is becoming increasing popular driven by the IMO net zero target set for 2050 in the shipping sector. As these systems, such as Flettner rotors and wingsails, can be quite large (currently up to 50 m tall and 200 tonnes per unit), the structural failure of WAPS or WAPS-ship interface may significantly affect the integrity/ultimate strength of hulls. Therefore, the committee recommends future research into the structural integrity of these systems and their hull-supporting structures.
- Standards and guidelines specifically for offshore renewable energy structures, such as floating wind turbines, should be developed and consolidated, as current regulations are still largely based on oil and gas structures.
- There should be stronger collaboration between research institutions and industry to ensure that innovations in predicting and improving ultimate strength are applied practically in the design and maintenance of offshore structures.
- Continued research into the effects of the corrosive marine environment on the ultimate strength of structures throughout their operational lifespan is essential. Investigating advanced materials, such as composites, along with effective strengthening and retrofitting techniques, will be critical for extending the service life and resilience of these structures. In addition, uncertainties arising from operational conditions, such as variable loading, maintenance practices, and accidental events, should also be considered in the assessment of ultimate strength.

Acknowledgements. The committee extends its gratitude to Dr Beatrice Barsotti for her assistance, coordination, and support in the benchmark study. The committee also thanks Fincantieri (Italy) for financing the experimental test that formed the foundation of the benchmark study and for making the results accessible to all participants.

References

ABS: ABS notations and symbols (2025). https://ww2.eagle.org/content/dam/eagle/rules-and-resources/RuleManager2/class-notations-table.pdf. Accessed 11 July 2025

Alinia, M.M., Saeidpour, A., Amani, M.: The shear buckling and post-buckling behavior of laterally pressured curved panels. Eng. Archive (engrxiv), 1–48 (2019). https://doi.org/10.31224/osf.io/jg27s

Alizadeh, F., Mazruee Sebdani, R., Guedes Soares, C.: Numerical analysis of the residual ultimate strength of composite laminates under uniaxial compressive load. Compos. Struct. **300**, 116161 (2022). https://doi.org/10.1016/j.compstruct.2022.116161

Amaechi, C.V.: Local tailored design of deep water composite risers subjected to burst, collapse and tension loads. Ocean Eng. **250**, 110196 (2022). https://doi.org/10.1016/j.oceaneng.2021.110196

Anyfantis, K.N.: Ultimate strength of stiffened panels subjected to non-uniform thrust. Int. J. Naval Archit. Ocean Eng. **12**, 325–342 (2020). https://doi.org/10.1016/j.ijnaoe.2020.03.003

API: Recommended practice for fitness-for-service, API 579–1/ASME FFS-1. Standard by American Petroleum Institute, Washington, D.C., USA (2021)

Arnold, S.M., Ricks, T., Pineda, E., Bednarcyk, B.: An enabling platform for achieving multiscale multiphysics analysis of multiphase materials. NASA, Glendale Research Center, Cleveland, Ohio, USA (2023). https://ntrs.nasa.gov/citations/20230015286. Accessed 11 July 2025

ASME: BPVC.XI - BPVC Section XI-Rules for inservice inspection of nuclear power plant components. American Society of Mechanical Engineers, New York, NY, USA. ISBN: 9780791871027 (2017)

Attia, A., El Kilani, H.S., El Afandy, M.M., Saad-Eldeen, S.: Numerical simulation of intact and cracked aluminium-alloy stiffened panels: calibration based on experiment. Ocean Eng. **269**, 113474 (2023). https://doi.org/10.1016/j.oceaneng.2022.113474

Augello, R., et al.: Buckling test of stiffened panels: Evaluation of post-buckling and failure by testing and layerwise models. In: Vassilopoulos, A.P., Michaud, V. (eds.), Composites Meet Sustainability; Proceedings of the 20th European Conference on Composite Materials (ECCM 20), Lausanne, Switzerland, 25-30 June 2022. Lausanne: EPFL Lausanne, Composite Construction Laboratory, pp. 459–467 (2022)

Austefjord, H.N., de Hauteclocque, G., Johnson, M.C., Zhu, T.: Update of wave statistics standards for classification rules. In: J.W. Ringsberg & C. Guedes Soares (eds.), Advances in the Analysis and Design of Marine Structures; Proceedings of the 9th International Conference on Marine Structures (MARSTRUCT 2023), Gothenburg, Sweden, 3–5 April 2023. London: CRC Press, pp. 43–52 (2023). https://doi.org/10.1201/9781003399759-5

Ayough, P., Ibrahim, Z., Sulong, N.H.R., Hsiao, P.C.: The effects of cross-sectional shapes on the axial performance of concrete-filled steel tube columns. J. Constr. Steel Res. **176**, 106424 (2021). https://doi.org/10.1016/j.jcsr.2020.106424

Babazadeh, A., Khedmati, M.R.: Progressive collapse analysis of a bulk carrier hull girder under longitudinal vertical bending moment considering cracking damage. Ocean Eng. **242**, 110140 (2021). https://doi.org/10.1016/j.oceaneng.2021.110140

Barooni, M., Nezhad, S.K., Ali, N.A., Ashuri, T., Sogut, D.V.: Numerical study of ice-induced loads and dynamic response analysis for floating offshore wind turbines. Mar. Struct. **86**, 103300 (2022). https://doi.org/10.1016/j.marstruc.2022.103300

Barsotti, B., Gaiotti, M.: Cumulative buckling deformation of stiffened panel under cyclic loading. In: Ergin, S., Guedes Soares, C. (eds.), Sustainable Development and Innovations in Marine Technologies; Proceedings of the 19th International Congress of the International Maritime Association of the Mediterranean (IMAM 2022), Istanbul, Turkey, 26–29 September 2022. London: CRC Press, pp. 109–113 (2022). https://doi.org/10.1201/9781003358961

Barsotti, B., Gaiotti, M.: Evaluation of residual plastic strain on a stiffened panel subjected to compression and tension-compression cyclic load. In: Ringsberg, J.W., Guedes Soares, C. (eds.), Advances in the Analysis and Design of Marine Structures; Proceedings of the 9th International Conference on Marine Structures (MARSTRUCT 2023), Gothenburg, Sweden, 3-5 April 2023. London: CRC Press, pp. 403–409 (2023a). https://doi.org/10.1201/9781003399759-44

Barsotti, B., Gaiotti, M.: FEM numerical strategies for the evaluation of the accumulated plastic strain due to cyclic load condition. In: J.W. Ringsberg & C. Guedes Soares (eds.), Advances in the Analysis and Design of Marine Structures; Proceedings of the 9th International Conference on Marine Structures (MARSTRUCT 2023), Gothenburg, Sweden, 3-5 April 2023. London: CRC Press, pp. 411–417 (2023b). https://doi.org/10.1201/9781003399759-45

Barsotti, B., Gaiotti, M.: Residual plastic strain effects on the ultimate capacity for a HSLA stiffened panel subjected to two different cyclic load conditions. In: Proceedings of the ASME 2024 43rd International Conference on Ocean, Offshore and Arctic Engineering (OMAE 2024), Singapore, 9–14 June 2024. (OMAE2024-126720) (2024)

Barsotti, B., Gaiotti, M., Rizzo, C.M.: Recent industrial developments of marine composites limit states and design approaches on strength. J. Mar. Sci. Appl. **19**, 553–566 (2020). https://doi.org/10.1007/s11804-020-00171-1

Barsotti, B., Battini, C., Gaiotti, M., Rizzo, C.M., Vergassola, G.: Experimental assessment of ultimate strength of a transversally loaded thin-walled structure and comparison with numerical models at different levels of complexity. Mar. Struct. **103**, 103793 (2025). https://doi.org/10.1016/j.marstruc.2025.103793

Bastek, J.H., Kochmann, D.M.: Physics-informed neural networks for shell structures. Eur. J. Mech. A/Solids **97**, 104849 (2023). https://doi.org/10.1016/j.euromechsol.2022.104849

Bonsu, A.O., Mensah, C., Liang, W., Yang, B., Ma, Y.: Mechanical degradation and failure analysis of different glass/basalt hybrid composite configuration in simulated marine condition. Polymers **14**(17), 3480 (2022). https://doi.org/10.3390/polym14173480

Braun, M., et al.: Development of combined load spectra for offshore structures subjected to wind, wave, and ice loading. Energies **15**(2), 559 (2022). https://doi.org/10.3390/en15020559

Brubak, L., Lv, Y., Ishibashi, K., Bollero, A., Bøe, Å.: Rule formulation updates on buckling strength requirements in Common Structural Rules. In: Ringsberg, J.W., Guedes Soares, C. (eds.), Advances in the Analysis and Design of Marine Structures; Proceedings of the 9th International Conference on Marine Structures (MARSTRUCT 2023), Gothenburg, Sweden, 3-5 April 2023. London: CRC Press, pp. 339–346 (2023). https://doi.org/10.1201/9781003399759-37

BV: Rules for the classification of steel ships (2024). https://marine-offshore.bureauveritas.com/nr467-rules-classification-steel-ships. Accessed 11 July 2025

Byklum, E., Amdahl, J.: A simplified method for elastic large deflection analysis of plates and stiffened panels due to local buckling. Thin-Walled Struct. **40**(11), 925–953 (2002). https://doi.org/10.1016/S0263-8231(02)00042-3

Cai, Q., Chen, D., Yang, N., Li, W.: A novel semi-spar floating wind turbine platform applied for intermediate water depth. Sustainability **16**(4), 1663 (2024). https://doi.org/10.3390/su16041663

Cao, S., Cheng, Y., Duan, J., Fan, X.: Experimental investigation on the dynamic response of an innovative semi-submersible floating wind turbine with aquaculture cages. Renew. Energy **200**, 1393–1415 (2022). https://doi.org/10.1016/j.renene.2022.10.072

Carrera, E., Zozulya, V.V.: Carrera unified formulation (CUF) for the micropolar plates and shells. I. High order theory. Mech. Adv. Mater. Struct. **29**(6), 773–795 (2020). https://doi.org/10.1080/15376494.2020.1793241

CCS: Guidelines for direct calculation assessment of hull structure including springing and whipping (2018). https://www.ccs.org.cn. Accessed 11 July 2025

CCS: Rules for structures of container ships (2022). https://www.ccs.org.cn. Accessed 11 July 2025

CEN: Eurocode 3, prEN 1993-1-14: Design of steel structures. Part 1.14: Design assisted by finite element analysis, European Committee for Standardisation, Brussels, 2023 (issued for hearing 2023, planned for publication in April 2025) (2023)

Cerik, B.C., Choung, J.: Progressive collapse analysis of intact and damaged ships under unsymmetrical bending. J. Mar. Sci. Eng. **8**(12), 988 (2020). https://doi.org/10.3390/jmse8120988

Chang, X.P., Qu, C.J., Song, Q., Li, Y.H., Liu, J.: Coupled cross-flow and in-line vibration characteristics of frequency-locking of marine composite riser subjected to gas-liquid multi-phase internal flow. Ocean Eng. **266**, 113019 (2022). https://doi.org/10.1016/j.oceaneng.2022.113019

Chen, B.Q., Guedes Soares, C.: Experimental and numerical investigation on welding simulation of long stiffened steel plate specimen. Mar. Struct. **75**, 102824 (2021). https://doi.org/10.1016/j.marstruc.2020.102824

Chen, X., Chen, Z., Li, D.: Misalignment effect on the ultimate strength of welded stiffened panels under uniaxial compression. Ocean Eng. **284**, 115190 (2023). https://doi.org/10.1016/j.oceaneng.2023.115190

Cheng, J., Liu, Y., Cheng, M., Li, W., Li, T.: Optimum condition-based maintenance policy with dynamic inspections based on reinforcement learning. Ocean Eng. **261**, 112058 (2022). https://doi.org/10.1016/j.oceaneng.2022.112058

Cho, S.J., Ban, I.J., Shin, S.C.: A novel deep learning model to predict ultimate strength of ship plates under compression. Appl. Sci. **12**(5), 2522 (2022). https://doi.org/10.3390/app12052522

Choi, Y.M., et al.: An efficient methodology for the simulation of nonlinear irregular waves in computational fluid dynamics solvers based on the high order spectral method with an application with OpenFOAM. Int. J. Naval Archit. Ocean Eng. **15**, 100510 (2023). https://doi.org/10.1016/j.ijnaoe.2022.100510

Chu, Y.I., et al.: Offshore fish farms: a review of standards and guidelines for design and analysis. J. Mar. Sci. Eng. **11**(4), 762 (2023). https://doi.org/10.3390/jmse11040762

Chujutalli, J.H., Estefen, S.F., Guedes Soares, C.: Indentation parameters influence on the ultimate strength of panels for different stiffeners. J. Constr. Steel Res. **170**, 106097 (2020). https://doi.org/10.1016/j.jcsr.2020.106097

ClassNK: Investigation report on structural safety of large container ships. Investigative panel on large container ship safety (2014). https://www.classnk.or.jp/hp/pdf/news/Investigation_Report_on_Structural_Safety_of_Large_Container_Ships_EN_ClassNK.pdf. Accessed 11 July 2025

Coraddu, A., Oneto, L., Li, S., Kalikatzarakis, M., Karpenko, O.: Surrogate models to unlock the optimal design of stiffened panels accounting for ultimate strength reduction due to welding residual stress. Eng. Struct. **293**, 116645 (2023). https://doi.org/10.1016/j.engstruct.2023.116645

Corigliano, P., Palomba, G., Crupi, V., Garbatov, Y.: Stress-strain assessment of honeycomb sandwich panel subjected to uniaxial compressive load. J. Mar. Sci. Eng. **11**(2), 365 (2023). https://doi.org/10.3390/jmse11020365

Cui, H., Ding, Q.: Ultimate strength and fracture failure of hull stiffened plates based on plastic accumulation under cyclic loading. Ocean Eng. **261**, 112016 (2022). https://doi.org/10.1016/j.oceaneng.2022.112016

Darie, I., Rörup, J.: Hull girder ultimate strength of container ships in oblique sea. In: Guedes Soares, C., Garbatov, Y. (eds.), Progress in the Analysis and Design of Marine Structures; Proceedings of the 6th International Conference on Marine Structures (MARSTRUCT2017), Lisbon, Portugal, 8-10 May 2017. London: CRC Press, pp. 225–233 (2017). https://doi.org/10.1201/9781315157368

Deng, H., Yuan, T., Gan, J., Liu, B., Wu, W.: Experimental and numerical investigations on the collapse behavior of box type hull girder subjected to cyclic ultimate bending moment. Thin-Walled Struct. **175**, 109204 (2022). https://doi.org/10.1016/J.TWS.2022.109204

Ding, H., et al.: Experimental investigation of nonlinear forces on a monopile offshore wind turbine foundation under directionally spread waves. In: Proceedings of the ASME 2024 43rd International Conference on Ocean, Offshore and Arctic Engineering (OMAE 2024), Singapore, 9-14 June 2024. (OMAE2024-125160) (2024)

DNV: Fatigue and ultimate strength assessment of container ships including whipping and springing. Class guideline DNV-CG-0153. DNV AS, Høvik, Norway (2021). www.dnv.com. Accessed 11 July 2025

DNV: Rules for classification: Pt.5 Ch. 2. Class Rules DNVGL-RU-SHIP. DNV AS, Høvik, Norway (2022a). www.dnv.com. Accessed 11 July 2025

DNV: Determination of structural capacity by non-linear FE analysis methods. Recommended practice DNV-RP-C208. DNV AS, Høvik, Norway (2022b). www.dnv.com. Accessed 11 July 2025

DNV: Buckling. Class guideline DNV-CG-0128. DNV AS, Høvik, Norway (2023). www.dnv.com. Accessed 11 July 2025

Do, Q.T., Huynh, V.V., Cho, S.R., Vu, M.T., Vu, Q.T., Thai, D.K.: Residual ultimate strength formulations of locally damaged steel stiffened cylinders under combined loads. Ocean Eng. **225**, 108802 (2021). https://doi.org/10.1016/j.oceaneng.2021.108802

Do, Q.T., Xuan-Phuong, D., Tra, T.H., Tuyen, V.V., Prabowo, A.R., Hung, T.D.: Parametric study of side collision-induced denting failures on the ultimate strength of a handy-size containership under vertical bending. Ocean Eng. **309**, 118534 (2024). https://doi.org/10.1016/j.oceaneng.2024.118534

Duong, T.H., Le, T.T., Le, M.V.: Practical machine learning application for predicting axial capacity of composite concrete-filled steel tube columns considering effect of cross-sectional shapes. Int. J. Steel Struct. **23**, 263–278 (2023). https://doi.org/10.1007/s13296-022-00693-0

Energy Watch: Ørsted CEO says confidence not shaken by malfunction boom in Danish offshore wind (2023). https://energywatch.com/EnergyNews/Renewables/article14304136.ece. Accessed 11 July 2025

Faqih, I., Adiputra, R., Prabowo, A.R., Muhayat, N., Ehlers, S., Braun, M.: Hull girder ultimate strength of bulk carrier (HGUS-BC) evaluation: structural performances subjected to true inclination conditions of stiffened panel members. Results Eng. **18**, 101076 (2023). https://doi.org/10.1016/j.rineng.2023.101076

Faulkner, D.: A review of effective plating for use in the analysis of stiffened plating in bending and compression. J. Ship Res. **19**(1), 1–17 (1975). https://doi.org/10.5957/jsr.1975.19.1.1

Feng, L., Hu, L., Chen, X., Shi, H.: A parametric study on effects of pitting corrosion on stiffened panels' ultimate strength. Int. J. Naval Archit. Ocean Eng. **12**, 699–710 (2020). https://doi.org/10.1016/j.ijnaoe.2020.08.001

Feng, R., Wu, C., Chen, Z., Roy, K., Chen, B., Lim, J.B.P.: Finite element modeling and proposed design rules of stainless steel hybrid tubular joints with square braces and circular chord. J. Construct. Steel Res. **179**, 106557 (2021). https://doi.org/10.1016/j.jcsr.2021.106557

Fonseca, N., Tahchiev, G., Ygre Rogne, O.: Mooring system ULS analysis based on empirical QTFs of wave drift loads. In: Proceedings of the ASME 2024 43rd International Conference on Ocean, Offshore and Arctic Engineering (OMAE 2024), Singapore, 9-14 June 2024. (OMAE2024-127825) (2024)

Fujikubo, M., Alie, M.Z.M., Takemura, K., Iijima, K., Oka, S.: Residual hull girder strength of asymmetrically damaged ships: influence of rotation of neutral axis due to damages. J. Japan Soc. Naval Archit. Ocean Eng. **16**, 131–140 (2012). https://doi.org/10.2534/jjasnaoe.16.131

Gadallah, R., Murakawa, H., Shibahara, M.: Study of various parameters on residual stress relaxation for different welded components. J. Constr. Steel Res. **214**, 108503 (2024). https://doi.org/10.1016/j.jcsr.2024.108503

Garbatov, Y.: Risk-based corrosion allowance of oil tankers. Ocean Eng. **213**, 107753 (2020). https://doi.org/10.1016/j.oceaneng.2020.107753

Garbatov, Y., Palomba, G., Crupi, V.: Risk-based hybrid light-weight ship structural design accounting for carbon footprint. Appl. Sci. **13**(6), 3583 (2023). https://doi.org/10.3390/app13063583

Garbatov, Y., Marchese, S.S., Epasto, G., Grupi, V.: Flexural response of additive-manufactured honeycomb sandwiches for marine structural applications. Ocean Eng. **302**, 117732 (2024). https://doi.org/10.1016/j.oceaneng.2024.117732

George, J.M., Kimiaei, M., Elchalakani, M., Efthymiou, M.: Flexural response of underwater offshore structural members retrofitted with CFRP wraps and their performance after exposure to real marine conditions. Structures **43**, 559–573 (2022). https://doi.org/10.1016/j.istruc.2022.06.075

George, J.M., Kimiaei, M., Elchalakani, M., Fawzia, S.: Underwater strengthening and repairing of tubular offshore structural members using carbon fibre reinforced polymers with different consolidation methods. Thin-Walled Struct. **174**, 109090 (2022). https://doi.org/10.1016/j.tws.2022.109090

Georgiadis, D.G., Samuelides, M.S.: Stochastic geometric imperfections of plate elements and their impact on the probabilistic ultimate strength assessment of plates and hull-girders. Mar. Struct. **76**, 102920 (2021). https://doi.org/10.1016/j.marstruc.2020.102920

Georgiadis, D.G., Samuelides, M.S.: The effect of corrosion spatial randomness and model selection on the ultimate strength of stiffened panels. Ships Offshore Struct. **16**(sup1), 140–152 (2021). https://doi.org/10.1080/17445302.2021.1907063

Georgiadis, D.G., Samuelides, E.S.: A Bayesian approach for the quantification of strength model uncertainty factor in ultimate limit state. In: Ringsberg, J.W., Guedes Soares, C. (eds.), Advances in the Analysis and Design of Marine Structures; Proceedings of the 9th International Conference on Marine Structures (MARSTRUCT 2023), Gothenburg, Sweden, 3-5 April 2023. London: CRC Press, pp. 871–876 (2023a). https://doi.org/10.1201/9781003399759-96

Georgiadis, D.G., Samuelides, M.S., Straub, D.: A Bayesian analysis for the quantification of strength model uncertainty factor of ship structures in ultimate limit state. Mar. Struct. **92**, 103495 (2023). https://doi.org/10.1016/j.marstruc.2023.103495

Ghabezi, P., Harrison, N.M.: Hygrothermal deterioration in carbon/epoxy and glass/epoxy composite laminates aged in marine-based environment (degradation mechanism, mechanical and physicochemical properties). J. Mater. Sci. **57**, 4239–4254 (2022). https://doi.org/10.1007/s10853-022-06917-2

Gong, C., Frangopol, D.M., Cheng, M.: Risk-based decision-making on corrosion delay for ship hull tankers. Eng. Struct. **212**, 110455 (2020). https://doi.org/10.1016/j.engstruct.2020.110455

Graves, W., Nahshon, K., Aminfar, K., Lattanzi, D.: Finite element model updating with quantified uncertainties using point cloud data. Data-Centric Eng. **4**, e16 (2023). https://doi.org/10.1017/dce.2023.7

Gu, Y., Ong, M.C., Janocha, M.J., Blomgren, A.: Review on feasibility of bottom-fixed offshore wind development in the arctic focusing on icing problems. In: Proceedings of the ASME 2023 42nd International Conference on Ocean, Offshore and Arctic Engineering (OMAE 2023), Melbourne, Australia, 11-16 June 2023. (OMAE2023-102822) (2023). https://doi.org/10.1115/OMAE2023-102822

Güneyisi, E.M., Nour, A.I.: Axial compression capacity of circular CFST columns transversely strengthened by FRP. Eng. Struct. **191**, 417–431 (2019). https://doi.org/10.1016/j.engstruct.2019.04.056

Guo, G., Cui, J., Wang, D.: A numerical investigation on collapse modes of stiffened plates under combined dynamic loads. In: Proceedings of the ASME 2024 43rd International Conference on Ocean, Offshore and Arctic Engineering (OMAE 2024), Singapore, 9–14 June 2024. (OMAE2024-126571) (2024)

Guo, Z., Bai, R., Lei, Z., Jiang, H., Zou, J., Yan, C.: Experimental and numerical investigation on ultimate strength of laser-welded stiffened plates considering welding deformation and residual stresses. Ocean Eng. **234**, 109239 (2021). https://doi.org/10.1016/j.oceaneng.2021.109239

Hammer, T.C., Willems, T., Hendrikse, H.: Dynamic ice loads for offshore wind support structure design. Mar. Struct. **87**, 103335 (2023). https://doi.org/10.1016/j.marstruc.2022.103335

Hanif, M.I., Adiputra, R., Prabowo, A.R., Yamada, Y., Firdaus, N.: Assessment of the ultimate strength of stiffened panels of ships considering uncertainties in geometrical aspects: finite element approach and simplified formula. Ocean Eng. **286**, 115522 (2023). https://doi.org/10.1016/j.oceaneng.2023.115522

Hastie, J.C., Guz, I.A., Kashtalyan, M.: Failure analysis of a composite riser pipe under operational and spooling loads. Procedia Struct. Integr. **42**, 614–622 (2022). https://doi.org/10.1016/j.prostr.2022.12.078

Hayama, M., Kikuchi, S., Tsukahara, M., Misaka, Y., Komotori, J.: Estimation of residual stress relaxation in low alloy steel with different hardness during fatigue by in situ X-ray measurement. Int. J. Fatigue **178**, 107989 (2024). https://doi.org/10.1016/j.ijfatigue.2023.107989

He, Y., Vaz, M.A., Caire, M.: Thermoplastic composite pipe failure envelopes under axisymmetric and thermomechanical loading. Eng. Struct. **278**, 115499 (2023). https://doi.org/10.1016/j.engstruct.2022.115499

Heiskari, J., Romanoff, J., Laakso, A., Ringsberg, J.W.: On the thickness determination of rectangular glass panes in insulating glass units considering the load sharing and geometrically nonlinear bending. Thin-Walled Structures **171**, 108774 (2022). https://doi.org/10.1016/j.tws.2021.108774

Heiskari, J., Romanoff, J., Laakso, A., Ringsberg, J.W.: Influence of the design constraints on the thickness optimization of glass panes to achieve lightweight insulating glass units in cruise ships. Mar. Struct. **89**, 103409 (2023). https://doi.org/10.1016/j.marstruc.2023.103409

Hernandez Ramos, M., Zhou, X., Ding, Z.: NSGA-II Enhanced Smith method for evaluation of the ultimate bending strength of damaged ships. In: Proceedings of the 2nd International Conference on the Stability and Safety of Ships and Ocean Vehicles, Wuxi, China, 14-18 October 2024, 895–905 (2024)

Hess, P.E., Bruchman, D., Assakkaf, I.A., Ayyub, B.M.: Uncertainties in material and geometric strength and load variables. Nav. Eng. J. **114**(2), 139–166 (2002). https://doi.org/10.1111/j.1559-3584.2002.tb00128.x

Hosseinabadi, O.F., Khedmati, M.R.: A review on ultimate strength of aluminium structural elements and systems for marine applications. Ocean Eng. **232**, 109153 (2021). https://doi.org/10.1016/j.oceaneng.2021.109153

Hosseinpour, P., Hosseinpour, M., Sharifi, Y.: Artificial neural networks for predicting ultimate strength of steel plates with a single circular opening under axial compression. Ships Offshore Struct. **17**(11), 2454–2469 (2022). https://doi.org/10.1080/17445302.2021.2000265

Houtani, H., Matsui, S., Fujimoto, W.: Numerical investigation of the statistics of vertical bending moments of ships in nonlinearly evolving irregular waves. In: Proceedings of the ASME 2023 42nd International Conference on Ocean, Offshore and Arctic Engineering (OMAE 2023), Melbourne, Australia, 11-16 June 2023. (OMAE2023-104733) (2023). https://doi.org/10.1115/OMAE2023-104733

Hu-Wei, C., Ping, Y.: Ultimate strength of hull plates under monotonic and cyclic uniaxial compression. J. Ship Res. **62**(3), 156–165 (2018). https://doi.org/10.5957/josr.170080

Hu, K., Yang, P., Xia, T.: Ultimate strength prediction of cracked panels under extreme cyclic loads considering crack propagation. Ocean Eng. **266**, 112948 (2022). https://doi.org/10.1016/j.oceaneng.2022.112948

Huang, Y., Wang, J., Taylor, R., Talimi, V., Fuglem, M.: An experimental study of iceberg hydrodynamic interactions with a generic floater on the grand banks NL. In: Proceedings of the 33rd International Ocean and Polar Engineering Conference (ISOPE 2023), Ottawa, Canada, 19–23 June 2023. (ISOPE-I-23-282) (2023)

Huang, Z., Yin, X., Liu, Y.: Physics-guided deep neural network for structural damage identification. Ocean Eng. **260**, 112073 (2022). https://doi.org/10.1016/j.oceaneng.2022.112073

IACS: Evaluation of scantlings of hatch covers and hatch coamings of cargo holds of bulk carriers, ore carriers and combination carriers. Unified Requirements Strength UR-S21 2010. In: International Association of Classification Societies, London, UK (2010)

IACS: Longitudinal strength standard. Unified Requirements Strength UR-S11, June 2015. In: International Association of Classification Societies, London, UK (2015a)

IACS: Evaluation of scantlings of hatch covers and hatch coamings and closing arrangements of cargo holds of ships. Unified requirements strength UR-S21A, May 2015. In: International Association of Classification Societies, London, UK (2015b)

IACS: Requirements concerning strength of ships. Unified Requirement S11A: Longitudinal strength standard for container ships. In: International Association of Classification Societies. London, UK (2020a)

IACS: Technical background for rule change notice for CSR, Pt 1, Ch 8, version 1 (2020). In: International Association of Classification Societies. London, UK (2020b)

IACS: Rec 47 Shipbuilding and repair quality standard, September 2021. In: International Association of Classification Societies, London, England (2021)

IACS: Annual review 2022. In: International Association of Classification Societies. London, UK (2022a). https://iacs.org.uk/about-us/annual-review. Accessed 11 July 2025

IACS: Standard wave data international association of classification societies. London, UK (2022b). https://iacs.org.uk/resolutions/recommendations/21-40. Accessed 11 July 2025

IACS: Common structural rules for bulk carriers and oil tankers (CSR-H). In: International Association of Classification Societies, London, England (2023a)

IACS: Technical background for CSR, 2023. In: International Association of Classification Societies, London, England (2023b)

IACS: Requirements concerning strength of ships. Unified Requirements Strength UR-S35: buckling strength assessment of ship structural elements. In: International Association of Classification Societies, London, England (2024)

Ilman, E.C., Wang, Y., Wharton, J.A., Sobey, A.J.: A hybrid corrosion-structural model for simulating realistic corrosion topography of maritime structures. Thin-Walled Struct. **169**, 108481 (2021). https://doi.org/10.1016/j.tws.2021.10848

IOGP: Supplementary specification for offshore topside structures (S-631–04) 2020. In: The International Association of Oil & Gas Producers (2020)

IOGP: Supplementary specification for fixed steel offshore structures (S-631-11) (2021). In: The International Association of Oil & Gas Producers (2021)

Ishibashi, K., Shiomitsu, D., Tatsumi, A., Fujikubo, M.: Simplified ultimate strength estimation method of rectangular plates under combined loads. Mar. Struct. **95**, 103592 (2024). https://doi.org/10.1016/j.marstruc.2024.103592

ISO: Petroleum and natural gas industries - general requirements for offshore structures, ISO 19900. International Organization for Standardization (2019). https://www.iso.org/standard/69761.html. Accessed 11 July 2025

ISSC: Report of specialist committee IV.2: Ultimate Hull Girder Strength. In H. Ohtsubo & Y. Sumi (eds.), Proceedings of the 14th International Ship and Offshore Structures Congress (ISSC 2000), vol. 2, Nagasaki (Japan), 2-6 October 2000. Elsevier, Oxford, UK, pp. 321–391. ISBN: 0080436021 (2000)

ISSC: Technical committee iii.1: ultimate strength. In: Fricke, W., Bronsart, R. (eds.) Proceedings of the 18th International Ship and Offshore Structures Congress (ISSC 2012), vol. 1, Rostock (Germany), 9–13 September 2012. Schiffbautechnische Gesellschaft, Hamburg, Germany, pp. 285–363 (2012). ISBN: 978-3-87700-131-8

ISSC: Technical Committee III.1: Ultimate Strength. In: Kaminski, M.L., Rigo, P. (eds.), Proceedings of the 20th International Ship and Offshore Structures Congress (ISSC 2018), vol. 1, Liège (Belgium) and Amsterdam (The Netherlands), 9–14 September 2018. IOS Press, Amsterdam, The Netherlands, pp. 335–439 (2018a). https://doi.org/10.3233/978-1-61499-862-4-335

ISSC: Discussion of committee iii.1: ultimate strength. In: Kaminski, M.L., Rigo, P. (eds.), Proceedings of the 20th International Ship and Offshore Structures Congress (ISSC 2018), vol. 3, Liège (Belgium) and Amsterdam (The Netherlands), 9-14 September 2018. IOS Press, Amsterdam, The Netherlands, pp. 61–84 (2018b). https://doi.org/10.3233/PMST200006

ISSC: Technical committee iii.1: ultimate strength. In: Wang, X., Pegg, N., (eds.), Proceedings of the 21st International Ship and Offshore Structures Congress (ISSC 2022), vol. 1, Vancouver, Canada, 11-15 September 2022. The Society of Naval Architects & Marine Engineers, pp. 395–500 (2022a). https://doi.org/10.5957/ISSC-2022-COMMITTEE-III-1

ISSC: Discussion of committee III.1: ultimate strength. In: Wang, X., Pegg, N. (eds.), Proceedings of the 21st International Ship and Offshore Structures Congress (ISSC 2022), vol. 3, Vancouver, Canada, 11-15 September 2022. The Society of Naval Architects & Marine Engineers, pp. 57–72 (2022b). https://doi.org/10.5957/ISSC-2022-DISCUSSION-III-1

Ivanhoe, R.O., Wang, L., Kolios, A.: Generic framework for reliability assessment of offshore wind turbine jacket support structures under stochastic and time dependent variables. Ocean Eng. **216**, 107691 (2020). https://doi.org/10.1016/j.oceaneng.2020.107691

Jafarzadeh, S., Khedmati, M.R.: Progressive collapse analysis of a composite ship hull girder under vertical bending using finite element method. Internal J. Maritime Technol. **14**, 21–32 (2020). http://ijmt.ir/article-1-684-en.html

Jagite, G., Bigot, F.: Numerical investigation of the hull girder ultimate strength under realistic cyclic loading derived from long-term hydroelastic analysis. Ships Offshore Struct. **18**(4), 515–528 (2023). https://doi.org/10.1080/17445302.2022.2035566

Jagite, G., Bigot, F., Malenica, S., Derbanne, Q., Le Sourne, H., Cartraud, P.: Dynamic ultimate strength of a ultra-large container ship subjected to realistic loading scenarios. Mar. Struct. **84**, 103197 (2022). https://doi.org/10.1016/j.marstruc.2022.103197

Jelovica, J., Romanoff, J., Ehlers, S., Varsta, P.: Influence of weld stiffness on buckling strength of laser-welded web-core sandwich plates. J. Constr. Steel Res. **77**, 12–18 (2012). https://doi.org/10.1016/j.jcsr.2012.05.001

Jia, H., Qin, S., Wang, R., Xue, Y., Fu, D., Wang, A.: Ship collision impact on the structural load of an offshore wind turbine. Glob. Energy Interconnect. **3**(1), 43–50 (2020). https://doi.org/10.1016/j.gloei.2020.03.009

Kadry, A.A., Ebid, A.M., Mokhtar, A.S.A., El-Ganzoury, E.N., Haggag, S.A.: Parametric study of unstiffened multi-planar tubular KK-Joints. Results Eng. **14**, 100400 (2022). https://doi.org/10.1016/j.rineng.2022.100400

Kai, Q., Renjun, Y., Mingen, C., Haiyan, Z.: Failure mode shift of sandwich composite L-Joint for ship structures under tension load. Ocean Eng. **214**, 107863 (2020). https://doi.org/10.1016/j.oceaneng.2020.107863

Kang, H., Yang, P., Xia, T.: Ultimate strength prediction of cracked panels under extreme cyclic loads considering crack propagation. Ocean Eng. **266**(3), 112948 (2022). https://doi.org/10.1016/j.oceaneng.2022.112948

Kim, C., Oterkus, S., Oterkus, E., Kim, Y.: Probabilistic ship corrosion wastage model with Bayesian inference. Ocean Eng. **246**, 110571 (2022). https://doi.org/10.1016/j.oceaneng.2022.110571

Kim, D.K., Li, S., Lee, J.R., Poh, B.Y., Benson, S., Cho, N.K.: An empirical formula to assess ultimate strength of initially deflected plate: part 1 - propose the general shape and application to longitudinal compression. Ocean Eng. **252**, 111151 (2022). https://doi.org/10.1016/j.oceaneng.2022.111151

Kim, D.K., Li, S., Yoo, K., Danasakaran, K., Cho, N.K.: An empirical formula to assess ultimate strength of initially deflected plate: part 2 - combined longitudinal compression and lateral pressure. Ocean Eng. **252**, 111112 (2022). https://doi.org/10.1016/j.oceaneng.2022.111112

Kim, J.H., Park, D.H., Kim, S.K., Kim, M.S., Lee, J.M.: Experimental study and development of design formula for estimating the ultimate strength of curved plates. Appl. Sci. **11**(5), 2379 (2021). https://doi.org/10.3390/app11052379

Komoriyama, Y., et al.: Ultimate longitudinal bending strength of damaged box girder in upright and inclined conditions - Model experiment and numerical analysis. In: Le Sourne, H., Guedes Soares, C. (eds.), Advances in the Collision and Grounding of Ships and Offshore Structures, Proceedings of the 9th International Conference on Collision and Grounding of Ship and Offshore Structures (ICCGS 2023), Nantes, France, 11–13 September 2023. London: CRC Press, pp. 377–385 (2024). https://doi.org/10.1201/9781003462170-46

Kong, X., Zhou, H., Zheng, C., Pei, Z., Yuan, T., Wu, W.: Research on the dynamic buckling of a typical deck grillage structure subjected to in-plane impact load. Mar. Struct. **78**, 103003 (2021). https://doi.org/10.1016/j.marstruc.2021.103003

Kõrgesaar, M., Putranto, T., Jelovica, J.: Equivalent single layer approach for predicting ultimate strength of stiffened panel under different load combinations. In: J.W. Ringsberg & C. Guedes Soares (eds.), Advances in the Analysis and Design of Marine Structures; Proceedings of the 9th International Conference on Marine Structures (MARSTRUCT 2023), Gothenburg, Sweden, 3-5 April 2023. London: CRC Press, pp. 347–354. https://doi.org/10.1201/9781003399759-38

KR.: Guidance on strength assessment of container ships considering the whipping effect (2022). https://www.krs.co.kr/KRRules/KRRules2022/KRRulesE.html. Accessed 11 July 2025

Kuznecovs, A., Ringsberg, J.W., Johnson, E., Yamada, Y.: Ultimate limit state analysis of a double-hull tanker subjected to biaxial bending in intact and collision-damaged conditions. Ocean Eng. **209**, 107519 (2020). https://doi.org/10.1016/j.oceaneng.2020.107519

Kuznecovs, A., Ringsberg, J.W., Mallaya Ullal, A., Janardhana Bangera, P., Johnson, E.: Consequence analyses of collision-damaged ships—damage stability, structural adequacy and oil spills. Ships Offshore Struct. **18**, 1–15 (2022). https://doi.org/10.1080/17445302.2022.2071014

Kuznecovs, A., Schreuder, M., Ringsberg, J.W.: Methodology for the simulation of a ship's damage stability and ultimate strength conditions following a collision. Mar. Struct. **79**, 103027 (2021). https://doi.org/10.1016/j.marstruc.2021.103027

Ladeira, I., Márquez, L., Echeverry, S., Le Sourne, H., Rigo, P.: Review of methods to assess the structural response of offshore wind turbines subjected to ship impacts. Ships Offshore Struct. **18**(6), 755–774 (2023). https://doi.org/10.1080/17445302.2022.2072583

Lee, D.H., Paik, J.K.: Ultimate strength characteristics of as-built ultra-large containership hull structures under combined vertical bending and torsion. Ships Offshore Struct. **15**(sup1), S143–S160 (2020). https://doi.org/10.1080/17445302.2020.1747829

Lee, H., et al.: Time-domain response-based structural analysis on a floating offshore wind turbine. J. Mar. Sci. Appl. **22**(1), 75–83 (2023). https://doi.org/10.1007/s11804-023-00322-0

Lee, H.H., Kim, H.J., Paik, J.K.: Use of physical testing data for the accurate prediction of the ultimate compressive strength of steel stiffened panels. Ships Offshore Struct. **18**(4), 609–623 (2023). https://doi.org/10.1080/17445302.2022.2087358

Lewis, M.: In a first, cargo ship strikes an offshore wind turbine (2023). https://electrek.co/2023/06/04/cargo-ship-offshore-wind-turbine/. Accessed 11 July 2025

Li, D., Chen, Z.: Advanced empirical formulae for the ultimate strength assessment of continuous hull plate under combined biaxial compression and lateral pressure. Eng. Struct. **285**, 116041 (2023). https://doi.org/10.1016/j.engstruct.2023.116041

Li, D., Chen, Z.: Progressive collapse analysis and ultimate strength estimation of continuous stiffened panel under longitudinal extreme cyclic load and lateral pressure. Ocean Eng. **285**, 115340 (2023). https://doi.org/10.1016/j.oceaneng.2023.115340

Li, D., Chen, Z., Li, J., Yi, J.: Ultimate strength assessment of ship hull plate with multiple cracks under axial compression using artificial neural networks. Ocean Eng. **263**, 112438 (2022a). https://doi.org/10.1016/j.oceaneng.2022.112438

Li, D., Feng, L., Huang, D., Shi, H., Wang, S.: Residual ultimate strength of stiffened box girder with coupled damage of pitting corrosion and a crack under vertical bending moment. Ocean Eng. **235**, 109341 (2021a). https://doi.org/10.1016/j.oceaneng.2021.109341

Li, F., Suominen, M., Kujala, P., Zhou, L.: A literature survey of probabilistic modelling methods of local ice loads on marine structures. In: Proceedings of the ASME 2024 43rd International Conference on Ocean, Offshore and Arctic Engineering (OMAE 2024), Singapore, 9-14 June 2024. (OMAE2024-127097) (2024a)

Li, H., Li, Y., Li, G., Zhu, Q., Wang, B., Tang, Y.: Transient tower and blade deformations of a Spar-type floating wind turbine in freak waves. Ocean Eng. **294**, 116801 (2024). https://doi.org/10.1016/j.oceaneng.2024.116801

Li, S., Benson, S.D.: A re-evaluation of the hull girder shakedown limit states. Ships Offshore Struct. **14**(sup1), 239–250 (2019). https://doi.org/10.1080/17445302.2019.1573872

Li, S., Kim, D.K.: A comparison of numerical methods for damage index based residual ultimate limit state assessment of grounded ship hulls. Thin-Walled Struct. **172**, 108854 (2022). https://doi.org/10.1016/j.tws.2021.108854

Li, S., Coraddu, A., Oneto, L.: Computationally aware estimation of ultimate strength reduction of stiffened panels caused by welding residual stress: from finite element to data-driven methods. Eng. Struct. **264**, 114423 (2022b). https://doi.org/10.1016/j.engstruct.2022.114423

Li, S., Georgiadis, D.G., Kim, D.K., Samuelides, M.S.: A comparison of geometric imperfection models for collapse analysis of ship-type stiffened plated grillages. Eng. Struct. **250**, 113480 (2022c). https://doi.org/10.1016/j.engstruct.2021.113480

Li, S., Hu, Z., Benson, S.: An analytical method to predict the buckling and collapse behavior of plates and stiffened panels under cyclic load. Eng. Struct. **199**, 109267 (2019). https://doi.org/10.1016/j.engstruct.2019.109627

Li, L., Jiang, Z., Ong, M.C., Hu, W.: Design optimization of mooring system: an application to a vessel-shaped offshore fish farm. Eng. Struct. **197**, 109363 (2019). https://doi.org/10.1016/j.engstruct.2019.109363

Li, S., Kim, D.K., Benson, S.: A probabilistic approach to assess the computational uncertainty of ultimate strength of hull girders. Reliab. Eng. Syst. Saf. **213**, 107688 (2021b). https://doi.org/10.1016/j.ress.2021.107688

Li, S., Kim, D.K., Benson, S.: The influence of residual stress on the ultimate strength of longitudinally compressed stiffened panels. Ocean Eng. **231**, 108839 (2021c). https://doi.org/10.1016/j.oceaneng.2021.108839

Li, W., Bazant, M.Z., Zhu, J.: A physics-guided neural network framework for elastic plates: comparison of governing equations-based and energy-based approaches. Comput. Methods Appl. Mech. Eng. **383**, 113933 (2021d). https://doi.org/10.1016/j.cma.2021.113933

Li, Y., Sakonder, C., Paredes, M.: Plastic collapse analysis in multiaxially loaded defective pipe specimens at different temperatures. J. Pipeline Sci. Eng. **3**(1), 100092 (2023). https://doi.org/10.1016/j.jpse.2022.100092

Li, Z., Chen, D., Feng, X., Chen, J.F.: Hydroelastic analysis and structural design of a modular floating structure applying ultra-high performance fiber-reinforced concrete. Ocean Eng. **277**, 114266 (2023). https://doi.org/10.1016/j.oceaneng.2023.114266

Lima, J.P.S., Evangelista, F., Guedes Soares, C.: Bi-fidelity kriging model for reliability analysis of the ultimate strength of stiffened panels. Mar. Struct. **91**, 103464 (2023). https://doi.org/10.1016/j.marstruc.2023.103464

Lindemann, T., Kaeding, P.: Formulation of idealized structural unit method to perform progressive collapse analyses of welded box girders in bending. In: Proceedings of the ASME 2024 43rd International Conference on Ocean, Offshore and Arctic Engineering (OMAE 2024), Singapore, 9–14 June 2024. (OMAE2024-125828) (2024)

Lindemann, T., La Ferlita, A., Di Nardo, E., Kaeding, P.: Application of different methods to determine the ultimate strength of ships in bending. In: Proceedings of the ASME 2023 42nd International Conference on Ocean, Offshore and Arctic Engineering (OMAE 2023), Melbourne, Australia, 11–16 June 2023. (OMAE2023-103731) (2023). https://doi.org/10.1115/OMAE2023-103731

Lindemann, T., La Ferliata, A., Kaeding, P.: Application of idealized structural unit method to determine the ultimate strength of ship model in bending. In: Proceedings of the ASME 2024 43rd International Conference on Ocean, Offshore and Arctic Engineering (OMAE 2024), Singapore, 9–14 June 2024. (OMAE2024-125843) (2024)

Lindemann, T., Okpeke, B.E., La Ferlita, A., Mühmer, M., Kaeding, P.: Numerical investigations on ultimate strength of a double hull VLCC under combined loads and initial imperfections. In: Proceedings of the ASME 2022 41st International Conference on Ocean, Offshore and Arctic Engineering (OMAE 2022), Hamburg, Germany, 5–10 June 2022. (OMAE2022-80204) (2022). https://doi.org/10.1115/OMAE2022-80204

Liu, B., Guedes Soares, C.: Ultimate strength assessment of ship hull structures subjected to cyclic bending moments. Ocean Eng. **215**, 107685 (2020). https://doi.org/10.1016/j.oceaneng.2020.107685

Liu, B., Doan, Y.T., Garbatov, Y., Wu, W., Guedes Soares, C.: Study on ultimate compressive strength of aluminium-alloy plates and stiffened panels. J. Mar. Sci. Appl. **19**, 534–552 (2020). https://doi.org/10.1007/s11804-020-00170-2

Liu, B., Gao, L., Ao, L., Wu, W.: Experimental and numerical analysis of ultimate compressive strength of stiffened panel with openings. Ocean Eng. **220**, 108453 (2021). https://doi.org/10.1016/j.oceaneng.2020.108453

Liu, B., Liu, K., Villavicencio, R., Dong, A., Guedes Soares, C.: Experimental and numerical analysis of the penetration of welded aluminium alloy panels. Ships Offshore Struct. **16**(5), 492–504 (2020). https://doi.org/10.1080/17445302.2020.1736856

Liu, B., Yao, X., Lin, Y., Wu, W., Guedes Soares, C.: Experimental and numerical analysis of ultimate compressive strength of long-span stiffened panels. Ocean Eng. **237**, 109633 (2021). https://doi.org/10.1016/j.oceaneng.2021.109633

Liu, B., Zhang, X., Garbatov, Y.: Multi-scale analysis for assessing the impact of material composition and weave on the ultimate strength of GFRP stiffened panels. J. Mar. Sci. Eng. **11**(1), 108 (2023). https://doi.org/10.3390/jmse11010108

Liu, L., Yang, D.Y., Frangopol, D.M.: Probabilistic cost-benefit analysis for service life extension of ships. Ocean Eng. **201**, 107084 (2020). https://doi.org/10.1016/j.oceaneng.2020.107094

Liu, L., Yang, D.Y., Frangopol, D.M.: Ship service life extension considering ship condition and remaining design life. Mar. Struct. **78**, 102940 (2021). https://doi.org/10.1016/j.marstruc.2021.102940

Liu, M.: Effect of uniform corrosion on the mechanical behavior of E690 high-strength steel lattice corrugated panel in the marine environment: a finite element analysis. Mater. Res. Express **8**, 066510 (2021). https://doi.org/10.1088/2053-1591/ac0655

Liu, X., Jiang, D., Liufu, K., Fu, J., Liu, Q., Li, Q.: Numerical investigation into impact responses of an offshore wind turbine jacket foundation subjected to ship collision. Ocean Eng. **248**, 110825 (2022). https://doi.org/10.1016/j.oceaneng.2022.110825

Liu, Y., Lei, Z., Zhu, R., Shang, Y., Bai, R.: Artificial neural network prediction of residual compressive strength of composite stiffened panels with open crack. Ocean Eng. **266**, 112771 (2022). https://doi.org/10.1016/j.oceaneng.2022.112771

Lowde, M.J., Peters, H.G.A., Geraghty, R., Graham-Jones, J., Pemberton, R., Summerscales, J.: The 100 m composite ship? J. Mar. Sci. Eng. **10**(3), 408 (2022). https://doi.org/10.3390/jmse10030408

LR: Global Design Loads of Container Ships and Other Ships Prone to Whipping and Springing. Lloyd's Register, London (2022)

Ma, H., Wang, D.: Lateral pressure effect on the ultimate strength of the stiffened plate subjected to combined loads. Ocean Eng. **239**, 109926 (2021). https://doi.org/10.1016/j.oceaneng.2021.109926

Ma, H., Xiong, Q., Wang, D.: Experimental and numerical study on the ultimate strength of stiffened plates subjected to combined biaxial compression and lateral loads. Ocean Eng. **228**, 108928 (2021). https://doi.org/10.1016/j.oceaneng.2021.108928

Ma, H., Yang, Y., He, Z., Jia, Z., Zhang, Y.: Experimental study on constitutive relation of the high performance marine structural steel under extreme cyclic loads. Ocean Eng. **168**, 204–215 (2018). https://doi.org/10.1016/j.oceaneng.2018.09.003

Ma, Z., Pei, Z., Wu, W.: Dynamic ultimate strength analysis of stiffened plate based on Idealized Structural Unit Method. Mar. Struct. **84**, 103203 (2022). https://doi.org/10.1016/j.marstruc.2022.103203

Ma., H., Kawamura, Y., Okada, T., Wang, D., Hayakawa, G.: A general scaled model design method of stiffened plate subjected to combined longitudinal compression and lateral pressure considering the ultimate strength and collapse modes. Marine Struct. **90**, 103435 (2023). https://doi.org/10.1016/j.marstruc.2023.103435

Martin, M.B., Harris, J.C., Renaud, P., Hulin, F., Filipot, J.F.: Numerical investigation of slamming loads on floating offshore wind turbines. In: Proceedings of the 32nd International Ocean and Polar Engineering Conference (ISOPE 2022), Shanghai, China, 5–10 June 2022. (ISOPE-I-22-031) (2022)

Mohd, M.H., et al.: The effect of corrosion depth on the ultimate strength of an aging fixed offshore structure. In: Ismail, A., Dahalan, W.M., Öchsner, A. (eds.), Design in Maritime Engineering, Proceedings of the 2nd International Conference on Marine and Advanced Technologies (ICMAT 2021), Kuala Lumpur, Malaysia, 24 August 2021. Springer, pp. 271–286 (2022). https://doi.org/10.1007/978-3-030-89988-2_21

Mokhtari, M., Wang, X., Amdahl, J.: Buckling and post-buckling behaviour of extruded aluminium panels subject to the combined effects of welding and pitting corrosion. In: Proceedings of the ASME 2023 42nd International Conference on Ocean, Offshore and Arctic Engineering (OMAE 2023), Melbourne, Australia, 11–16 June 2023. (OMAE2023-105048) (2023). https://doi.org/10.1115/OMAE2023-105048

Moon, W., et al.: Time-domain response-based structural assessment of a FOWT – buckling and ultimate strength assessment. In: ASME 2022 4th International Offshore Wind Technical Conference (IOWTC 2022), Boston, Massachusetts, USA, 7–8 December 2022. (IOWTC2022-96497) (2023). https://doi.org/10.1115/IOWTC2022-96497

Muhaimin Ishak, M.I., et al.: IGUSA: prediction of ultimate strength of fixed offshore structures in Malaysian waters using machine learning techniques. In: Proceedings of the Offshore Technology Conference Asia (OTC 2022), Virtual and Kuala Lumpur, Malaysia, 22–25 March 2022. (OTC-31493-MS) (2022). https://doi.org/10.4043/31493-MS

Mun, J.S., Ri, Y.H.: Study on ultimate strength estimation of intermittently welded stiffened plates under uniaxial compression. Mar. Struct. **84**, 103163 (2022). https://doi.org/10.1016/j.marstruc.2022.103163

Mursid, O., et al.: Effect of pitting corrosion position to the strength of ship bottom plate in a grounding incident. Curved Layered Struct. **10**, 20220199 (2023). https://doi.org/10.1515/cls-2022-0199

Musial, W., et al.: Offshore wind market report: 2023 edition. U.S. Department of Energy (2023). https://www.energy.gov/eere/wind/articles/offshore-wind-market-report-2023-edition. Accessed 11 July 2025

Nahshon, K., Rynolds, N., Shields, M.D.: Efficient uncertainty propagation for high-fidelity simulations with large parameter spaces: application to stiffened plate buckling. J. Verification, Validation and Uncertainty Quant. **3**(1), 011003 (16 pages) (2018). https://doi.org/10.1115/1.4039836

Nassiraei, H., Yara, A.: Numerical analysis of local joint flexibility of K-joints with external plates under axial loads in offshore tubular structures. J. Mar. Sci. Appl. **21**(4), 134–144 (2023). https://doi.org/10.1007/s11804-022-00302-w

NSIA: Marine casualty involving the cruise ship "Viking Polaris" south-east of Cape Horn, 29 November 2022. Report MARINE 2023/06. Norwegian Safety Investigation Authority, Lillestrøm, Norway (2023)

Othman, N.A., Mohd, M.H., Rahman, M.A.A., Musa, M.A., Fitriadhy, A.: Investigation of the corrosion factor to the global strength of aging offshore jacket platforms under different marine zones. Int. J. Naval Archit. Ocean Eng. **15**, 100496 (2023). https://doi.org/10.1016/j.ijnaoe.2022.100496

Paik, J.K.: Ultimate Limit State Analysis and Design of Plated Structures (2nd edn.) Wiley, Hoboken (2018). https://doi.org/10.1002/9781119367758

Paik, J.K., Thayamballi, A.K.: An empirical formulation for predicting the ultimate compressive strength of stiffened panels. In: Proceedings of the 7th International Ocean and Polar Engineering Conference (ISOPE 1997), Honolulu, Hawaii, USA, 25–30 May 1997. (ISOPE-I-97-444) (1997)

Paik, J.K., Andrieu, C., Cojeen, H.P.: Mechanical collapse testing on aluminum stiffened plate structures for marine applications. Marine Technol. SNAME News **45**(4), 228–240 (2008). https://doi.org/10.5957/mt1.2008.45.4.228

Pan, J., Xu, R.J., Song, Z.J., Wan, Q., Li, X.B.: Study on the load-end shortening formulae of structural elements including hard corner element considering collapse modes based on test and numerical modeling. Thin-Walled Struct. **185**, 110624 (2023). https://doi.org/10.1016/j.tws.2023.110624

Pandey, M., Young, B.: Ultimate resistances of member-rotated cold-formed high strength steel tubular T-joints under compression loads. Eng. Struct. **244**, 112601 (2021). https://doi.org/10.1016/j.engstruct.2021.112601

Papanikolaou, N., Anyfantis, K.: Construction of surrogate models for predicting the buckling strength of stiffened panels through DoE and RSM methods. Eng. Comput. **39**(4), 1374–1406 (2022). https://doi.org/10.1108/EC-03-2021-0176

Paredes, M., Grolleau, V., Wierzbicki, T.: On ductile fracture of 316L stainless steels at room and cryogenic temperature level: an engineering approach to determine material parameters. Materialia **10**, 100624 (2020). https://doi.org/10.1016/j.mtla.2020.100624

Park, J.S., Ha, Y.C., Seo, J.K.: Estimation of buckling and ultimate collapse behavior of stiffened curved plates under compressive load. J. Ocean Eng. Technol. **34**(1), 37–45 (2020). https://doi.org/10.26748/ksoe.2019.108

Park, Y.I., Kim, J.H.: Artificial neural network based prediction of ultimate buckling strength of liquid natural gas cargo containment system under sloshing loads considering onboard boundary conditions. Ocean Eng. **249**, 110981 (2022). https://doi.org/10.1016/j.oceaneng.2022.110981

Peeters, D.M.J., et al.: Buckling test of stiffened panels: Modeling and vibrational correlation testing. In: Vassilopoulos, A.P., Michaud, V., (eds.), Composites Meet Sustainability; Proceedings of the 20th European Conference on Composite Materials (ECCM 20), Lausanne, Switzerland, 25-30 June 2022. Lausanne: EPFL Lausanne, Composite Construction Laboratory, pp. 763–770 (2022)

Peng, R.X., Qiu, W.L., Teng, F.: Investigation on seawater freeze-thaw damage deterioration of marine concrete structures in cold regions from multi-scale. Ocean Eng. **248**, 110867 (2022). https://doi.org/10.1016/j.oceaneng.2022.110867

Petrolo, M., Carrera, E.: Best theory diagram for multi-layered structures via shell finite elements. Adv. Model. Simul. Eng. Sci. **6**, 4 (2019). https://doi.org/10.1186/s40323-019-0129-8

Petrolo, M., Carrera, E.: Selection of element-wise shell kinematics using neural networks. Comput. Struct. **244**, 106425 (2021). https://doi.org/10.1016/j.compstruc.2020.106425

Petrolo, M., Iannotti, P.: Best theory diagrams for laminated composite shells based on failure indexes. Aerotecn. Missili Spazio **102**, 199–218 (2023). https://doi.org/10.1007/s42496-023-00158-5

Piscopo, V., Scamardella, A.: Incidence of pitting corrosion wastage on the hull girder ultimate strength. J. Mar. Sci. Appl. **20**, 477–490 (2021). https://doi.org/10.1007/s11804-021-00218-x

Piscopo, V., Scamardella, A.: Ultimate strength assessment of simply supported pitted platings: a new stochastic approach based on Monte Carlo simulation. Mar. Struct. **87**, 103312 (2023). https://doi.org/10.1016/j.marstruc.2022.103312

Preventas, M., Fanourgakis, S., Samuelides, M.S.: Effect of low cycle/high amplitude loads on the moment carrying capacity of a ship's hull. In: Amdahl, J., Guedes Soares, C. (eds.), Developments in the Analysis and Design of Marine Structures; Proceedings of the 8th International Conference on Marine Structures (MARSTRUCT 2021), Trondheim, Norway, 7-9 June 2021. London: CRC Press, pp. 137–146 (2021). https://doi.org/10.1201/9781003230373-16

Putranto, T., Kõrgesaar, M.: Numerical investigation on the buckling response of stiffened panel subjected to biaxial compression with non-linear equivalent single layer approach. In: Proceedings of the 31st International Ocean and Polar Engineering Conference (ISOPE 2021), Rhodes, Greece, 20–25 June 2022 (2021). (ISOPE-I-21-4206)

Putranto, T., Kõrgesaar, M., Jelovica, J.: Ultimate strength assessment of stiffened panels using equivalent single layer approach under combined in-plane compression and shear. Thin-Walled Struct. **180**, 109943 (2022). https://doi.org/10.1016/j.tws.2022.109943

Putranto, T., Kõrgesaar, M., Tabri, K.: Application of equivalent single layer approach for ultimate strength analyses of ship hull girder. J. Mar. Sci. Eng. **10**(10), 1530 (2022). https://doi.org/10.3390/jmse10101530

Putranto, T., Kõrgesaar, M., Jelovica, J., Tabri, K., Naar, H.: Ultimate strength assessment of stiffened panel under uni-axial compression with non-linear equivalent single layer approach. Mar. Struct. **78**, 103004 (2021). https://doi.org/10.1016/j.marstruc.2021.103004

Quispe, J.P., et al.: Numerical and experimental analyses of the ultimate strength of a small-scale hull box girder. Marine Struct. **85**, 103273 (2022). https://doi.org/10.1016/j.marstruc.2022.103273

Rapacka, P.: Anholt wind farm incident. Developer asks to establish 'no sail zones' (2023). https://balticwind.eu/anholt-wind-farm-incident-developer-asks-to-establish-no-sail-zones/. Accessed 11 July 2025

Ren, Y., Shi, W., Venugopal, V., Zhang, L., Li, X.: Experimental study of tendon failure analysis for a TLP floating offshore wind turbine. Appl. Energy **358**, 122633 (2024). https://doi.org/10.1016/j.apenergy.2024.122633

Ringsberg, J.W., et al.: The ISSC 2022 committee III.1-Ultimate strength benchmark study on the ultimate limit state analysis of a stiffened plate structure subjected to uniaxial compressive loads. Marine Struct. **79**, 103026 (2021). https://doi.org/10.1016/j.marstruc.2021.103026

Romanoff, J., Karttunen, A., Varsta, P.: Design space for bifurcation buckling of laser-welded web-core sandwich plates as predicted by classical and micropolar plate theories. Ann. Solid Struct. Mech. **12**, 73–87 (2020). https://doi.org/10.1007/s12356-020-00064-6

Saberi, S., Fantuzzi, N.: Analysis of unreinforced and reinforced tubular T-joints structures with open source finite element software. Mech. Adv. Mater. Struct. **30**(4), 912–922 (2022). https://doi.org/10.1080/15376494.2022.2028043

Seyffert, H.C., Troesch, A.W., Collette, M.D.: Combined stochastic lateral and in-plane loading of a stiffened ship panel leading to collapse. Mar. Struct. **67**, 102620 (2019). https://doi.org/10.1016/j.marstruc.2019.04.008

Shen, Q., Wang, J., Wang, J., Ding, Z.: Axial compressive performance of circular CFST columns partially wrapped by carbon FRP. J. Constr. Steel Res. **155**, 90–106 (2019). https://doi.org/10.1016/j.jcsr.2018.12.017

Shi, G., Wang, M., Wang, Y., Wang, F.: Cyclic behavior of 460 MPa high strength structural steel and welded connection under earthquake loading. Adv. Struct. Eng. **16**(3), 451–466 (2013). https://doi.org/10.1260/1369-4332.16.3.451

Shi, G.J., Gao, D.W.: Reliability analysis of hull girder ultimate strength for large container ships under whipping loads. Struct. Infrastruct. Eng. **17**(3), 319–330 (2020). https://doi.org/10.1080/15732479.2020.1744023

Shi, G.J., Gao, D.W.: Model experiment of large superstructures' influence on hull girder ultimate strength for cruise ships. Ocean Eng. **222**, 108626 (2021). https://doi.org/10.1016/j.oceaneng.2021.108626

Shi, G.J., Wang, D.Y., Wang, F.H., Cai, S.J.: Analysis of dynamic response and ultimate strength for box girder under bending moment. J. Mar. Sci. Eng. **11**(2), 373 (2023). https://doi.org/10.3390/jmse11020373

Shi, W., Zhang, L., Karimirad, M., Michailides, C., Jiang, Z., Li, X.: Combined effects of aerodynamic and second-order hydrodynamic loads for floating wind turbines at different water depths. Appl. Ocean Res. **130**, 103416 (2023). https://doi.org/10.1016/j.apor.2022.103416

Shi, X.H., Shen, H., Zhang, J., Guedes Soares, C.: Uncertainty of ultimate strength of ship hull with pits. In: Guedes Soares, C. (ed.), Maritime Technology and Engineering 5 Volume 1; Proceedings of the 5th International Conference on Maritime Technology and Engineering (MARTECH 2020), Lisbon, Portugal, 16-19 November 2020. London: CRC Press, pp. 583–590 (2021). https://doi.org/10.1201/9781003216582-65

Shiomitsu, D., Ishibashi, K., Yanagimoto, F., Fujikubo, M.: A simple estimation method for ultimate strength of curved plates under axial compression. In: Proceedings of the ASME 2023 42nd International Conference on Ocean, Offshore and Arctic Engineering (OMAE 2023), Melbourne, Australia, 11-16 June 2023. (OMAE2023-102688) (2023). https://doi.org/10.1115/OMAE2023-102688

Shokrieh, M., Poon, C., Lessard, L.: Three-dimensional progressive failure analysis of pin/bolt loaded composite laminates. In: Proceedings of the 83rd Meeting of the AGARD Structures and Materials Panel (AGARD CP-590), Florence, Italy, 2-3 September 1996 (1996)

Silva, J.P., Chen, B.Q., Videiro, P.M.: FPSO hull structures with sandwich plate system in cargo tanks. Appl. Sci. **12**(19), 9628 (2022). https://doi.org/10.3390/app12199628

Smith, C.S.: Influence of local compressive failure on ultimate longitudinal strength of ship's hull. In: Proceedings of the International Symposium on Practical Design in Shipbuilding (PRADS), Tokyo, Japan, 17-21 October 1977, pp. 73–79 (1977)

Smith, C.S., Davidson, P., Chapman, J.C.: Strength and stiffness of ship's plating under in-plane compression and tension. Royal Inst. Naval Archit. Trans. **130** (1987). https://api.semanticscholar.org/CorpusID:134846745

Soleimani, E., Tabeshpour, M.R., Seif, M.S.: Parametric study of buckling and post-buckling behavior for an aluminium hull structure of a high-aspect-ratio twin hull vessel. Proc. IMechE Part M, J. Eng. Maritime Environ. **234**(1), 15–25 (2020). https://doi.org/10.1177/1475090219868635

Song, Y., Yang, P., Peng, Z., Xia, T.: Residual ultimate strength of ship cracked plates considering fatigue crack propagation under cyclic loads. Ships Offshore Struct. **17**(6), 1403–1412 (2022). https://doi.org/10.1080/17445302.2021.1926143

Storheim, M., Alsos, H.S., Amdahl, J.: Evaluation of nonlinear material behavior for offshore structures subjected to accidental actions. J. Offshore Mech. Arctic Eng. **140**(4), 041401 (7 pages) (2018). https://doi.org/10.1115/1.4038585

Sun, H., Wang, Y., Jia, L., Lin, Z., Yu, H.: Theoretical and numerical methods for predicting the structural stiffness of unbonded flexible riser for deep-sea mining under axial tension and internal pressure. Ocean Eng. **310**, 118672 (2024). https://doi.org/10.1016/j.oceaneng.2024.118672

Sun, K., et al.: Experimental study on ultimate strength of novel aluminum alloy stiffened panel with floating girder. In: Proceedings of the ASME 2021 40th International Conference on Ocean, Offshore and Arctic Engineering (OMAE 2021), Virtual, Online, 21-30 June 2021. (OMAE2021-63761) (2021a). https://doi.org/10.1115/OMAE2021-63761

Sun, Z., Lei, Z., Zou, J., Bai, R., Jiang, H., Yan, C.: Prediction of failure behavior of composite hat-stiffened panels under in-plane shear using artificial neural network. Compos. Struct. **272**, 114238 (2021). https://doi.org/10.1016/j.compstruct.2021.114238

Sundarraja, M.C., Prabhu, G.G.: Investigation on strengthening of CFST members under compression using CFRP composites. J. Reinf. Plast. Compos. **30**(15), 1251–1264 (2011). https://doi.org/10.1177/0731684411418018

Tabri, K., Tõns, T., Suominen, M., Kõrgesaar, M.: Ice-induced loads on offshore wind turbines in the Baltic Sea. In: Proceedings of the ASME 2022 41st International Conference on Ocean, Offshore and Arctic Engineering (OMAE 2022), Hamburg, Germany, 5-10 June 2022. (OMAE2022-79035) (2022). https://doi.org/10.1115/OMAE2022-79035

Takami, T., Fujimoto, W., Houtani, H., Matsui, S.: Extreme wave and vertical bending moment predictions by higher order spectrum method and FORM. In: Proceedings of the ASME 2023 42nd International Conference on Ocean, Offshore and Arctic Engineering (OMAE 2023), Melbourne, Australia, 11-16 June 2023. (OMAE2023-101876) (2023). https://doi.org/10.1115/OMAE2023-101876

Tatsumi, A., Fujikubo, M.: Ultimate strength of container ships subjected to combined hogging moment and bottom local loads, part 1: nonlinear finite element analysis. Mar. Struct. **69**, 102683 (2020). https://doi.org/10.1016/j.marstruc.2019.102683

Tatsumi, A., Ko, H.H.H., Fujikubo, M.: Ultimate strength of container ships subjected to combined hogging moment and bottom local loads, part 2: an extension of Smith's method. Mar. Struct. **71**, 102738 (2020). https://doi.org/10.1016/j.marstruc.2020.102738

Tekgoz, M., Garbatov, Y., Guedes Soares, C.: Review of ultimate strength assessment of ageing and damaged ship structures. J. Mar. Sci. Appl. **19**, 512–533 (2020). https://doi.org/10.1007/s11804-020-00179-7

Tran, H., Gao, Y.F., Chew, H.B.: Numerical and experimental crack-tip cohesive zone laws with physics-informed neural networks. J. Mech. Phys. Solids **193**, 105866 (2024). https://doi.org/10.1016/j.jmps.2024.105866

Truong, D.D., Jang, B.S.: Estimation of ice loads on offshore structures using simulations of level ice-structure collisions with an influence coefficient method. Appl. Ocean Res. **125**, 103235 (2022). https://doi.org/10.1016/j.apor.2022.103235

Vizentin, G., Vukelic, G.: Failure analysis of FRP composites exposed to real marine environment. Procedia Struct. Integr. **37**, 233–240 (2022). https://doi.org/10.1016/j.prostr.2022.01.079

Wang, B., Luo, L., Nie, X., Duan, S., Wang, L.: Post-buckling reliability and sensitivity analysis of composite stiffened plates based on adaptive Kriging method. Acta Mech. Solida Sin. **36**, 340–348 (2023). https://doi.org/10.1007/s10338-022-00366-9

Wang, J.T., Liu, X.H., Sun, Q., Li, Y.W.: Analytical behavior and bearing capacity research on out-of-code tapered CFDST members under pure torsion and compression-torsion combination. Ocean Eng. **284**, 115324 (2023). https://doi.org/10.1016/j.oceaneng.2023.115324

Wang, M., Wang, C., Hnydiuk-Stefan, A., Feng, S., Atilla, I., Li, Z.: Recent progress on reliability analysis of offshore wind turbine support structures considering digital twin solutions. Ocean Eng. **232**, 109168 (2021). https://doi.org/10.1016/j.oceaneng.2021.109168

Wang, Q., Liu, K., Zhang, M.: Numerical studies on the performance of the circular fibre reinforced plastics-concrete filled steel tubes stub column under axial compression. J. Reinf. Plast. Compos. **41**(9–10), 383–398 (2022). https://doi.org/10.1177/07316844211051707

Wang, S., Moan, T.: Methodology of load effect analysis and ultimate limit state de-sign of semi-submersible hulls of floating wind turbines: with a focus on floater column design. Mar. Struct. **93**, 103526 (2024). https://doi.org/10.1016/j.marstruc.2023.103526

Wang, X., Amdahl, J., Egeland, O.: Numerical study on buckling of aluminum extruded panels considering welding effects. Mar. Struct. **84**, 103230 (2022). https://doi.org/10.1016/j.marstruc.2022.103230

Wang, X., Jia, P., Wang, B.: Progressive failure model of high strength glass fiber composite structure in hygrothermal environment. Compos. Struct. **280**, 114932 (2022). https://doi.org/10.1016/j.compstruct.2021.114932

Wang, Z., et al.: Structural fire behavior of aluminium alloy structures: review and outlook. Eng. Struct. **268**, 114746 (2022). https://doi.org/10.1016/j.engstruct.2022.114746

Wang, X., Yu, Z., Amdahl, J.: Ultimate strength of welded aluminium stiffened panels under combined biaxial and lateral loads: a numerical investigation. Mar. Struct. **97**, 103654 (2024). https://doi.org/10.1016/j.marstruc.2024.103654

Wilkie, D., Galasso, C.: Site-specific ultimate limit state fragility of offshore wind turbines on monopile substructures. Eng. Struct. **204**, 109903 (2020). https://doi.org/10.1016/j.engstruct.2019.109903

Woloszyk, K., Bielski, P.W., Garbatov, Y., Mikulski, T.: Photogrammetry image-based approach for imperfect structure modeling and FE analysis. Ocean Eng. **223**, 108665 (2021). https://doi.org/10.1016/j.oceaneng.2021.108665

Woloszyk, K., Garbatov, Y., Kowalski, J., Samson, L.: Numerical and experimental study on effect of boundary conditions during testing of stiffened plates subjected to compressive loads. Eng. Struct. **235**, 112027 (2021). https://doi.org/10.1016/j.engstruct.2021.112027

Wong, W.J., Walters, C.L.: Effect of strain hardening on the bending capacity of high-strength welded I-section beams. Ships Offshore Struct., 1–16 (2023).https://doi.org/10.1080/17445302.2023.2195727

Wu, Q., Hu, S., Tang, X., Liu, X., Chen, Z., Xiong, J.: Compressive buckling and post-buckling behaviors of J-type composite stiffened panel before and after impact load. Compos. Struct. **304**, 116339 (2023). https://doi.org/10.1016/j.compstruct.2022.116339

Xiong, Y., Li, C., Cai, S., Wang, D.: The dynamic ultimate strength of stiffened panels under axial impact loading. Ships Offshore Struct. **18**(5), 707–720 (2023). https://doi.org/10.1080/17445302.2022.2067417

Xu, G., Qin, K., Yan, R., Dong, Q.: Research on failure modes and ultimate strength behavior of typical sandwich composite joints for ship structures. Int. J. Naval Archit. Ocean Eng. **14**, 100428 (2022). https://doi.org/10.1016/j.ijnaoe.2021.100428

Xu, K., Larsen, K., Shao, Y., Zhang, M., Gao, Z., Moan, T.: Design and comparative analysis of alternative mooring systems for floating wind turbines in shallow water with emphasis on ultimate limit state design. Ocean Eng. **219**, 108377 (2021). https://doi.org/10.1016/j.oceaneng.2020.108377

Xu, M.C., Guedes Soares, C.: Experimental evaluation of the ultimate strength of stiffened panels under longitudinal compression. Ocean Eng. **220**, 108496 (2021). https://doi.org/10.1016/j.oceaneng.2020.108496

Xu, M.C., Song, Z.J., Pan, J.: Study on the similarity methods for the assessment of ultimate strength of stiffened panels under axial load based on tests and numerical simulations. Ocean Eng. **219**, 108294 (2021). https://doi.org/10.1016/j.oceaneng.2020.108294

Xu, M.C., Song, Z.J., Wang, T., Zhang, W.Z., Pan, J.: Empirical formulae assessment of ultimate strength for perforated stiffened panels under longitudinal compression. Ocean Eng. **264**, 112445 (2022). https://doi.org/10.1016/j.oceaneng.2022.112445

Xu, W., Zhou, X., Li, C., Ren, H.: Post-ultimate strength behavior and collapse severity of ship hull girder under extreme wave load by an analytical method. Ships Offshore Struct. **17**(2), 410–424 (2022). https://doi.org/10.1080/17445302.2020.1834753

Yan, C., Vescovini, R., Dozio, L.: A framework based on physics-informed neural networks and extreme learning for the analysis of composite structures. Comput. Struct. **265**, 106761 (2022). https://doi.org/10.1016/j.compstruc.2022.106761

Yeon, S.M., et al.: Development and verification of modeling practice for numerical estimation of wind loads on offshore floating structures. Int. J. Naval Archit. Ocean Eng. **14**, 100434 (2022). https://doi.org/10.1016/j.ijnaoe.2021.100434

Yeter, B., Garbatov, Y., Guedes Soares, C.: Uncertainty analysis of soil-pile interactions of monopile offshore wind turbine support structures. Appl. Ocean Res. **82**, 74–88 (2019). https://doi.org/10.1016/j.apor.2018.10.014

Yeter, B., Garbatov, Y., Guedes Soares, C.: Life-extension classification of offshore wind assets using unsupervised machine learning. Reliab. Eng. Syst. Saf. **219**, 108229 (2022). https://doi.org/10.1016/j.ress.2021.108229

Yeter, B., Garbatov, Y., Guedes Soares, C.: Review on artificial intelligence-aided life extension assessment of offshore wind support structures. J. Mar. Sci. Appl. **21**, 26–54 (2022). https://doi.org/10.1007/s11804-022-00298-3

Yi, M.S., Hyun, C.M., Paik, J.K.: Three-dimensional thermo-elastic-plastic finite element method modeling for predicting weld-induced residual stresses and distortions in steel stiffened-plate structures. World J. Eng. Technol. **6**(1), 176–200 (2018). https://doi.org/10.4236/wjet.2018.61010

Yu, Z., Amdahl, J., Rypestøl, M., Cheng, Z.: Numerical modeling and dynamic response analysis of a 10 MW semi-submersible floating offshore wind turbine subjected to ship collision loads. Renew. Energy **184**, 677–699 (2022). https://doi.org/10.1016/j.renene.2021.12.002

Yuan, L., Liu, Z., Chen, N.: On the buckling of mechanically lined pipes under combined tension and bending. Ocean Eng. **262**, 111991 (2022). https://doi.org/10.1016/j.oceaneng.2022.111991

Zavvar, E., Abdelwahab, H.S., Uzunoglu, E., Chen, B.Q., Guedes Soares, C.: Numerical study of the wave induced motions and loads on the CENTEC-TLP floating wind turbine. In: Guedes Soares, C. (ed.), Trends in Renewable Energies Offshore; Proceedings of the 5th International Conference on Renewable Energies Offshore (RENEW 2022), Lisbon, Portugal, 8-10 November 2022. London: CRC Press, pp. 567–573 (2022). https://doi.org/10.1201/9781003360773-65

Zavvar, E., Henneberg, J., Guedes Soares, C.: Stress concentration factors in FRP-reinforced tubular DKT joints under axial loads. Mar. Struct. **90**, 103429 (2023). https://doi.org/10.1016/j.marstruc.2023.103429

Zhai, Y., Zhao, H., Li, X., Feng, M., Zhou, Y.: Effects of aquaculture cage and netting on dynamic responses of novel 10 MW barge-type floating offshore wind turbine. Ocean Eng. **295**, 116896 (2024). https://doi.org/10.1016/j.oceaneng.2024.116896

Zhang, J., Shi, X.H., Guedes Soares, C., Liu, J.: Ultimate strength of stiffened panels with a crack and pits under uni-axial longitudinal compression. Ships Offshore Struct. **17**(2), 319–338 (2022). https://doi.org/10.1080/17445302.2020.1827805

Zhang, Q., Yang, H., Wu, S., Cheng, W., Liang, Y., Huang, Y.: A study on the ultimate strength and failure mode of stiffened panels. J. Marine Sci. Eng. **11**(6), 1214 (2023). https://doi.org/10.3390/jmse11061214

Zhang, T., Zaghi, A.E.: Estimation of the residual bearing strength of corroded bridge deck girders using 3D scan data. Thin-Walled Struct. **188**, 110798 (2023). https://doi.org/10.1016/j.tws.2023.110798

Zhang, X., Wang, Y., Chemori, A.: Structural reliability based energy-efficient arctic position mooring control of moored offshore structures under ice loads. Ocean Eng. **268**, 113435 (2023). https://doi.org/10.1016/j.oceaneng.2022.113435

Zhang, Y., Hu, Z.: An aero-hydro coupled method for investigating ship collision against a floating offshore wind turbine. Mar. Struct. **83**, 103177 (2022). https://doi.org/10.1016/j.marstruc.2022.103177

Zhang, Y., et al.: Seismic performance evaluation and numerical analysis of CFDST long columns with local corrosion under eccentric compression. Ocean Eng. **306**, 118006 (2024). https://doi.org/10.1016/j.oceaneng.2024.118006

Zhao, N., Chen, B.Q., Zhou, Y.Q., Li, Z.J., Hu, J.J., Guedes Soares, C.: Experimental and numerical investigation on the ultimate strength of a ship hull girder model with deck openings. Mar. Struct. **83**, 103175 (2022). https://doi.org/10.1016/j.marstruc.2022.103175

Zhong, Q., Wang, D.Y.: Ultimate strength behavior of laser-welded web-core sandwich plates under in-plane compression. Ocean Eng. **238**, 109685 (2021). https://doi.org/10.1016/j.oceaneng.2021.109685

Zhong, Q., Wang, D.Y.: Dynamic ultimate strength characteristics of stiffened plates subjected to the in-plane impact load and lateral pressure. In: Proceedings of the ASME 2021 40th International Conference on Ocean, Offshore and Arctic Engineering (OMAE 2021), Virtual, Online, 21-30 June 2021. (OMAE2021-62663) (2021b). https://doi.org/10.1115/OMAE2021-62663

Zhong, Q., Wang, D.: Numerical investigation on ultimate strength of sandwich box girders under vertical bending and torsion. Ocean Eng. **254**, 111338 (2022). https://doi.org/10.1016/j.oceaneng.2022.111338

Zhou, J., Pei, Z., Wu, W., Ding, J.: Progressive collapse behavior of ship structures considering fluid-structure interaction effect. In: Proceedings of the ASME 2023 42nd International Conference on Ocean, Offshore and Arctic Engineering (OMAE 2023), Melbourne, Australia, 11-16 June 2023. (OMAE2023-102755) (2023). https://doi.org/10.1115/OMAE2023-102755

Zhu, Y., Zhang, Y., Du, F.: Ultimate strength of hull structural stiffened plate with grooving corrosion damage under uniaxial compression. J. Ship Res. **65**(4), 309–319 (2021). https://doi.org/10.5957/JOSR.03200014

Zhuang, X., Guo, H., Alajlan, N., Zhu, H., Rabczuk, T.: Deep autoencoder based energy method for the bending, vibration, and buckling analysis of Kirchhoff plates with transfer learning. Eur. J. Mech. A/Solids **87**, 104225 (2021). https://doi.org/10.1016/j.euromechsol.2021.104225

Økland, O.D., Lian, G., Vestbøstad, T.: Experimental investigation of slamming loads on vertical column exposed to short and long crested waves. In: Proceedings of the ASME 2022 41st

International Conference on Ocean, Offshore and Arctic Engineering (OMAE 2022), Hamburg, Germany, 5–10 June 2022. (OMAE2022–79076) (2022). https://doi.org/10.1115/OMAE2022-79076

Ørsted Media Relations: Incident at Anholt offshore wind farm (2022). https://orsted.com/en/media/newsroom/news/2022/04/incident-at-anholt-offshore-wind-farm. Accessed 11 July 2025